TU Delft

DOC and Ammonium Removal Processes in Slow Sand Filters - Influence of Grain Size and Flow Rate

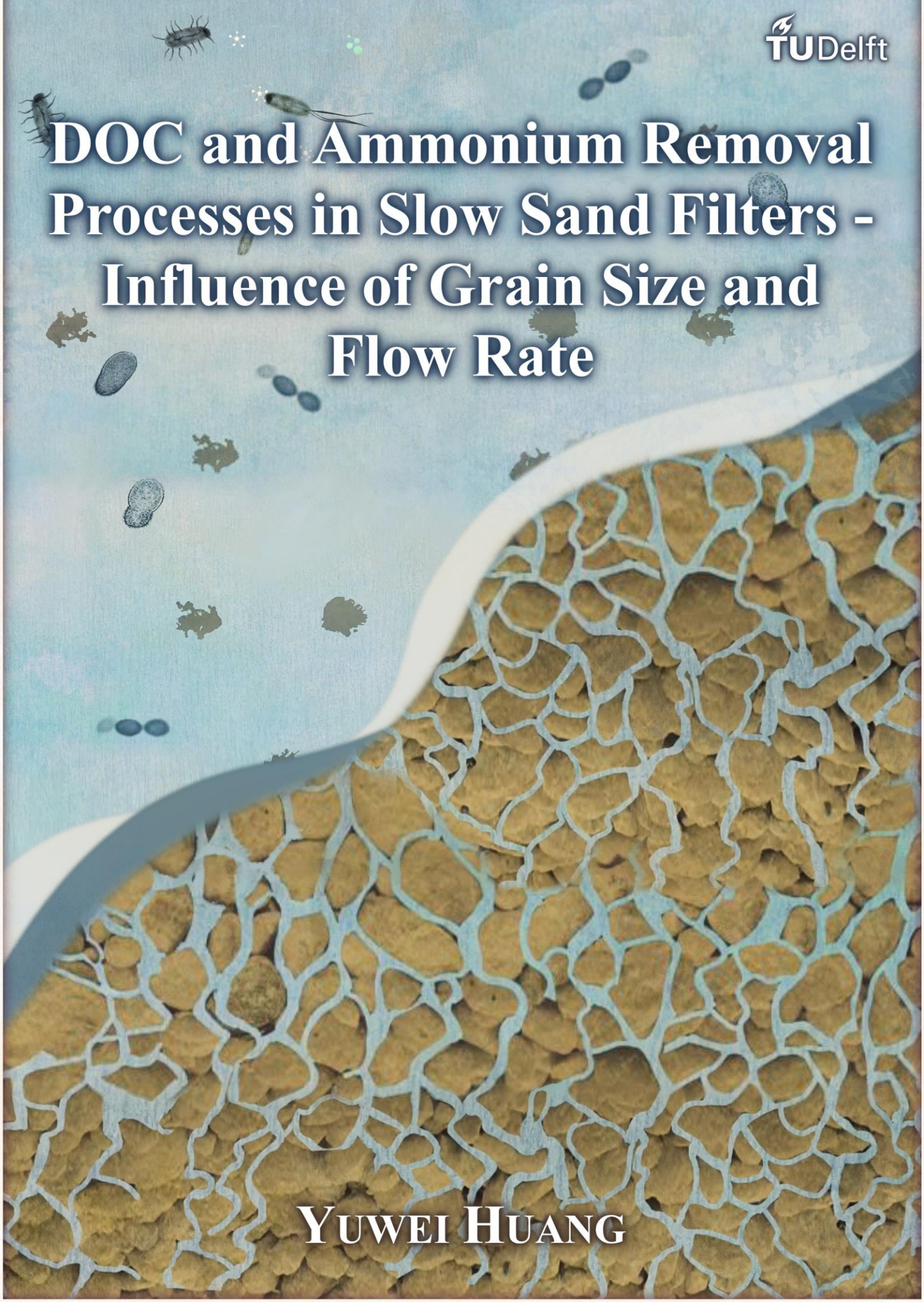

YUWEI HUANG

DOC and Ammonium Removal Processes in Slow Sand Filters – Influence of Grain Size and Flow Rate

by

Yuwei Huang (5555566)

29 September 2023

in partial fulfilment of the requirements for the degree of

Master of Science in Applied Earth Sciences

Track: Environmental Engineering

at the Delft University of Technology

Thesis committee:

Prof. Dr. Ir. Jan Peter van der Hoek	Delft University of Technology
Prof. Dr. Ir. Doris van Halem	Delft University of Technology
Prof. Dr. Ir. Merle de Kreuk	Delft University of Technology
Ir. Shreya Trikannad	Delft University of Technology

Faculty of Civil Engineering and Geosciences · Delft University of Technology

Acknowledgements

In the blink of an eye, my master journey in Delft is drawing to a close. I must express my heartfelt thanks to my supervisor, Shreya Trikannad. Without her unwavering guidance, it would have been a thorny task. She provided invaluable experimental support and critical feedback throughout the entire research journey. Our relationship has evolved into a cherished friendship, and I'm profoundly grateful for that. My mentors, Doirs van Halem and Jan Peter van der Hoek, also deserve special mention. They've been constant sources of support and wisdom. Whether engaging in in-person discussions or providing prompt responses online, they've deepened my understanding. Additionally, their support during my PhD application process, particularly Doris's unwavering belief in me, was vital in my decision to pursue further studies. Congratulations once more to Doris on her inaugural ceremony! Many thanks to Merle de Kreuk for providing valuable feedback. Further, I also want to thank Emiel Kruisdijk and Javier Pavez Jara for their assistance with my project.

I am deeply grateful for the assistance of the water lab staff. Thank you Armand Middeldorp for your all-encompassing support, Bright Namata for your guidence in white lab, Jane Erkemeij for teaching me the Discrete Analyzer, Bokuretsion Estifanos for your instruction on portable meters, and Jasper Krijn for material procurement.

To my friends and senior students I met in the Netherlands, you've been a source of unwavering support in both my academic and personal life, with whom I've shared countless emotions, sincere research discussions, excited outings, and delectable feasts. I genuinely look forward to all of us having a better life and achieving exceptional outcomes in our future studies and work.

Lastly, but most importantly, I want to express my deepest gratitude to my parents and grandparents. Your sacrifice and support made it possible for me to pursue my master's degree in the Netherlands. I'm profoundly thankful for your understanding during my two-year absence and for the encouragement that fuels my pursuit of personal and academic goals.

To everyone who has touched my life during my two years in the Netherlands, I extend my heartfelt thanks. Your presence has not only enriched my experience but has also contributed significantly to my growth as an individual.

Abstract

Slow sand filters (SSFs) are essential for ensuring microbial quality and biological stability of drinking water in the Netherlands. However, gaps exist in understanding of removal processes of dissolved organic carbon (DOC) and ammonium (NH_4^+-N) and the effects of grain size, loading rate, and backwashing on removal in SSFs.

Four lab-scale SSF columns filled with fine (0.4-0.6 mm) and coarse (0.85-1.25 mm) sand were constructed and operated in two phases with a total of 165 days. In phase I, SSFs operated at a flow rate of 0.5 m/h to investigate the influence of grain size. After stabilization, higher loading rate of 2 m/h and backwashing procedure (20% expansion for 5 min) was applied during the phase II experiment. Various physicochemical and biological parameters, including DOC, NH_4^+-N, phosphate (PO_4^{3-}-P), and ATP were analyzed in water along the filter depth. Additionally, biomass development on sand was quantified suing ATP measurement.

Results showed the stable SSF operation after 90-100 days, removing 100% of dosed 1.5 mg/L of DOC and 1.0 mg/L of NH_4^+-N. Compared with fine sand, coarse sand had similar removal performance but better backwashing effectiveness and lower clogging risk. Increased loading rate led to faster microbial growth, reducing operational lifespan, and poor removal performance. Backwashing showed minimal impact on DOC and NH_4^+ removal capacity and microbial activity, which were recovered after backwashing within 7-14 days, indicating the potential for backwashing to prolong SSF's operational lifespan.

This research investigated the DOC and NH_4^+ removal processes and the influence of grain size, loading rate, and backwashing on filter performance. Providing insights for optimized SSF design and operation. Future studies could delve into mechanisms using isotope analysis or metagenomics, along with more comprehensive sand sample analysis.

List of figures

Figures in Appendix

List of tables

Tables in Appendix

Symbols and abbreviations

AOA	Ammonia-oxidizing archaea
AOB	Ammonia-oxidizing bacteria
AOC	Assimilable organic carbon
BOD_5	Five-day biochemical oxygen demand
BTC	Breakthrough curve
cATP	Cellular ATP
CDOC	Chromatographic dissolved organic carbon
DIN	Dissolved inorganic nitrogen
DO	Dissolved oxygen
DOC	Dissolved organic carbon
DON	Dissolved organic nitrogen
EC	Electric conductivity
EPS	Extracellular polymetric substance
HMW	High molecular weight
HOC	Hydrophobic organic carbon
IC	Ion chromatography
LC-OCD	Liquid chromatography organic carbon detection
LMW	Low molecular weight
LRV	Log reduction value
MSA	Modified Scholten's Agar
MSB	Modified Scholten's Broth
NOB	Nitrite-oxidizing bacteria
OD	Optical density
PCR	Polymerase chain reaction
POC	Particulate organic carbon
PV	Pore volume
RLU	Relative light units
RSF	Rapid sand filter
SSF	Slow sand filter
ssMSA	Semi-solid Modified Scholten's Agar
SUVA	Specific UV absorbance
TOC	Total organic carbon

Table of Contents

1. Introduction

1.1 Background

Urbanization has increased the microbiological risk of drinking water, due to contamination with human and/or animal feces, resulting in thousands of deaths every day (WHO. 2004). Water disinfection is now an indispensable step to ensure water safety. In addition to microbial concerns, surface and ground water sources often contain pollutants like organic matter, ammonium, and others from industrial discharges, agricultural runoff, and sewage effluents from urbanized areas. Among these contaminants, assimilable organic carbon (AOC) and ammonium are easily biodegradable, promoting microbial growth and biological instability of produced drinking water (Chien et al. 2008, Chu and Lu 2004). Ammonium in the distribution system can cause corrosion, aesthetic issues, pH fluctuations, oxygen depletion, (Lee et al. 2014), and potential nitrite accumulation (Wilczak et al. 1996). Therefore, the removal of AOC and ammonium during treatment is essential to prevent microbial regrowth in the distribution network. Pathogenic microorganisms, including bacteria, viruses, and (oo)cysts of *Cryptosporidium* and *Giardia*, must be effectively removed to meet quantitative microbial risk assessment requirements in the Dutch Drinking Water Act, aiming for an annual infection risk below 10^{-4} per person (Hijnen et al. 2004, WHO. 2004). The Dutch drinking water quality criterion for nitrogen compounds is 0.2 mg/L NH_4^+, 0.1 mg/L NO_2^-, and 50 mg/L NO_3^- (Ahmad et al. 2020).

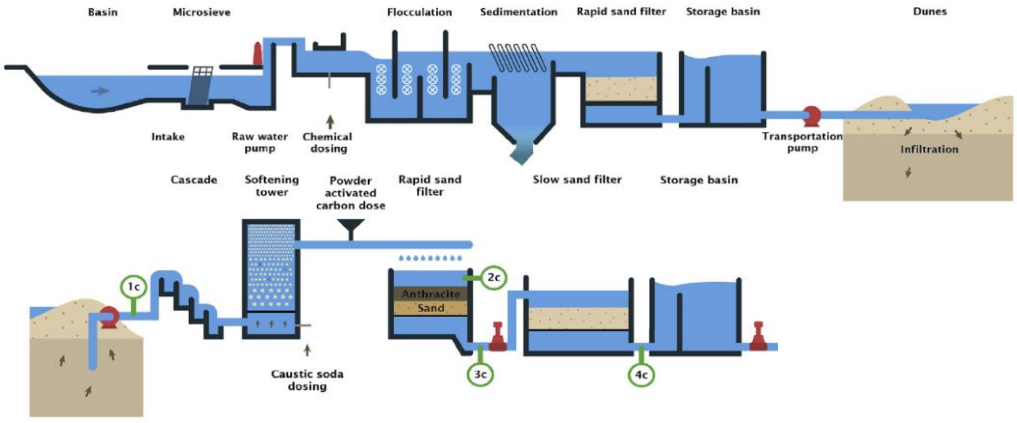

Fig. 1. Process schemes of drinking water treatment at Katwijk, the Netherlands (Ahmad et al. 2020).

SSFs have been widely applied for decades in drinking water treatment. In the Netherlands, drinking water is produced using a multi-barrier approach to produce hygienically safe and biologically stable drinking water. Water utilities in the

Netherlands employ a combination of physicochemical and biological processes to remove a wide range of contaminants. SSFs are the final stage in this prolonged treatment scheme (Fig. 1), ensuring microbial water quality and eliminating nutrients that promote microbial growth. SSFs can remove organic matter, nitrogen, phosphorus, and other contaminants in addition to pathogens (Ahmad et al. 2020, Hijnen et al. 2004, Lee et al. 2014, Pfannes et al. 2015). The removal processes are driven by a diverse range of microbial communities, including heterotrophic bacteria, nitrifiers, denitrifiers, and other predators. However, it's important to recognize that despite their widespread use in water treatment even with very extended pre-treatment applied nowadays, SSFs can encounter certain operational challenges.

The widespread adoption of SSFs faces challenges, mainly due to their large land requirements and low flow rates typically ranging from 0.1 to 0.4 m/h (Verma et al. 2017). Furthermore, the use of fine sands with a grain size of 0.15-0.45 mm (Guchi 2015) presents issues related to bioclogging. Given that SSFs are likely to become a part of new treatment facilities in the Netherlands to meet expanding production needs in the coming decade, there’s a growing demand for efficient SSF designs to meet the increasing population. Therefore, understanding how design and operational parameters affect pollutant removal processes is crucial for developing efficient treatment systems.

SSFs are influenced by design and operational parameters, impacting removal. Factors like temperature (van der Aa et al. 2002), oxygen levels (Dong et al. 2009, Lytle et al. 2013), grain size, loading rate (product of concentration and flow rate), and cleaning techniques (Lopato et al. 2013, Nakhla and Farooq 2003, Perujo et al. 2017) can affect the removal of organic matter, ammonium, and pathogenic microorganisms. Grain size affects the removal of pollutants within the filters. Previous studies have shown that fine sand enhanced retention of suspended solids and microorganisms (Freitas et al. 2022, Jenkins et al. 2011), due to its larger specific surface area and lower porosity, resulting in higher adsorption and interception ability. But it also increases the risk of clogging (Huang et al. 2013). On the other hand, coarse sand offers higher hydraulic conductivity (Perujo et al. 2017), associated with high biogeochemical rates and high transfer of nutrients in depth, which may be advantageous to nitrification (Liu et al. 2023). High flow rates can increase production rates but may compromise effluent quality due to short hydraulic detention times, leading to incomplete pollutant removal (Anderson et al. 2009, Nakhla and Farooq 2003). Additionally, proper cleaning methods

like backwashing and biofilm scraping are essential for SSF performance, but their effects on the removal efficiency of organic matter, ammonium, and microorganisms remain unclear (de Souza et al. 2021a, Freitas et al. 2022, Guchi 2015).

Currently, there is still a lack of research regarding the removal and stratification of DOC and NH_4^+ in SSFs. To further optimize the process, it is essential to gain a comprehensive understanding of the pollutant removal mechanisms in SSFs, considering the impact of grain size, loading rate, and backwashing. Addressing these research gaps is crucial to enhance the efficiency of SSF systems and change the operation of SSFs from high loaded with limited pretreatment to low loaded with extend pretreatment, to meet the rising water needs in the Netherlands. This study investigated the removal of DOC and NH_4^+ along the filter height and investigate how grain size, loading rate (different flow rate with same influent concentration), and backwashing influences removal effect of grain size on pollutant removal and bioactivity at various depths within the SSF and explored the impact of backwashing and loading rate adjustments by elucidating the mechanisms involved in pollutant removal and their transformation processes. Through this research, we aim to optimize SSF design and operation for more effective and sustainable drinking water treatment.

1.2 Research objectives and questions

1.2.1 Research objectives

1. Investigate DOC and NH_4^+ removal processes along the filter height.
2. Evaluate the influence of grain size, loading rate, and backwashing on stratification of DOC and NH_4^+ removal and overall removal efficiency.

1.2.2 Research questions

1. How is the removal of DOC and NH_4^+ stratified within the SSFs?
2. How does grain size, loading rate, and backwashing affect stratification of DOC and NH_4^+ removal?
3. How does grain size, loading rate, and backwashing affect biomass development?
4. What is the optimal range of grain sizes and loading rates that balance the pollutant removal efficiency, cost, robustness, and longevity of SSFs' performance?

2. Literature review

2.1 Design and operation of slow sand filters

Table 1. Recommended design parameters of SSF.

Bed depth (m)	Effective medium size (mm)	Flow rate (m/h)	Support bed depth (m)	Supernatant depth (m)	Source
1.2	0.15-0.35	0.1-0.4		1-1.5	(WHO. 2014)
0.9	0.15-0.3	0.1-0.2	0.3-0.5	1	(Visscher et al. 1987)
0.8	0.3-0.45	0.08-0.24	0.4-0.6	0.9	(Guchi 2015)
0.6-1	0.1-0.3	0.1-0.3			(Castro-Castellon et al. 2014)

The history of slow sand filters (SSFs) date back to 1928 in Paisley, Scotland, when John Gibbs used them to supply water to the city (Baker and Taras 1948). The modern SSF design, which originated in 1852 with James Simpson for the Chelsea water company in London, became a legal requirement for Thames River water extraction in 1892 due to concerns about waterborne diseases (Hendricks et al. 1991). While rapid sand filters (RSFs) emerged in the late 19th century, SSFs have remained a primary water treatment method. Currently, the USEPA recognizes SSFs as a safe water treatment technology for human consumption (USEPA 2001).

The basic components of SSFs are supernatant water layer, sand bed, gravel, and outlet hose (Verma et al. 2017). The sand medium is commonly used for filtration due to its low cost and availability, while the gravel supports the filter bed and provides an unobstructed passage for treat water. SSF purifies water through physical, chemical, and biological processes occurring along and on the sand filter medium, effectively removing organic and inorganic substances, as well as microorganisms like bacteria, viruses, and (oo)cysts of Giardia and Cryptosporidium (Jenkins et al. 2011, Mahlangu et al. 2012). While some design parameters for SSF are well-established in the literature (Table 1), further research is needed on variable parameters like grain size, loading rate, and filtration layer depth (Freitas et al. 2022).

2.2 Mechanisms in slow sand filters

The SSF utilizes a combination of physical, chemical, and biological processes to purify water. Within the same filter bed, biological filtration, driven by various biological activities, operates alongside physical filtration. However, the intricate interplay of

biogeochemical dynamics is influenced by multiple factors, which complicates the comprehension of the physical, chemical, and biological interactions responsible for potential nutrient, pathogen, and particulate matter removal from water.

2.2.1 Biological processes

Water purification in SSF involves biological activities that take place within the Schmutzdecke and along the filter bed. The Schmutzdecke is a biological layer that develops on the surface of the sand bed (Young-Rojanschi and Madramootoo 2014), and where most of the contaminant removal is considered to occur.

Biological processes, such as natural die-off, predation, toxin excretion, and food competition are responsible for pathogen removal in SSFs (Huisman and Wood 1974, Ranjan and Prem 2018). Previous studies reported that combined biological processes with the physicochemical processes, SSFs could achieve the removal efficiency of bacteria, protozoa, and viruses of 3-5 $\log_{10}$ (Adeyemo et al. 2015).

Besides, the main biological processes involved in nutrient utilization are heterotrophic bacteria, nitrifying bacteria, and denitrifying bacteria. Organic matter degradation begins with extracellular enzymatic hydrolysis of macromolecules into smaller substrates, which are transported into the biofilm. Subsequently, a diverse microbial biofilm community utilizes specific enzymes to further degrade the organic carbon, converting it to CO_2 with the utilization of electron acceptors like oxygen or sulfate (Larsen and Harremoës 1994). Nitrification is a two-step biological process carried out by autotrophic bacteria and archaea including ammonia-oxidizing bacteria (AOB), archaea (AOA), and nitrite-oxidizing bacteria (NOB) using oxygen as the electron acceptor (Lee et al. 2014).

2.2.2 Physicochemical processes

Physicochemical filtration dominates particle removal and water quality improvement in the maturing SSF (Freitas et al. 2022). These processes can be categorized into two groups: transport mechanisms, including straining, sedimentation, diffusion, interception, and inertial effects, and attachment mechanisms, involving electrostatic attraction, Van der Waals force, and adherence (Guchi 2015).

Straining or screening is one of the key transport processes in SSF that physically removes particles bigger than the pore size of the medium (Guchi 2015). Sedimentation occurs when the mass density of a particle is substantially larger than that of water (over

4 um) and its settling velocity leads the particle to divert from the flow path and settle on the medium surface (Maiyo et al. 2023). Interception happens when deposited particles aggregate on the media surface, gradually reducing pore size and serving as additional collectors for passing particles (Guchi 2015). Attachment mechanisms effectively capture particles carried to the filter medium, leading to successful collisions. Mass attraction (Van der Waals force) and electrostatic attraction between oppositely charged particles are examples of such processes, particularly crucial for smaller particles (Ellis and Aydin 1995). Adsorption generally refers to the attachment of dissolved chemicals to the medium.

Smaller particles, including bacteria (0.1-10 um), viruses (0.01-0.1 um), and colloidal particles (0.001-1 um), cannot be removed by straining alone. Consequently, they penetrate deeper into the bed, where inertia, sedimentation, interception, hydrodynamic action, and diffusion become crucial (Guchi 2015). Particulate organic carbon and nitrogen are removed through a combination of mechanical exclusion, physical adsorption, and microbial bio-degradation (Bar-Zeev et al. 2012).

2.3 Performance of slow sand filters

2.3.1 Pollutants removal

Table 2. Typical removal efficiencies for SSF.

Parameter	Removal efficiency	Source
Turbidity	59-90%	(Guchi 2015)
Coliforms	> 99%	(Guchi 2015)
Viruses	0.2-2.2 $\log_{10}$	(Anderson et al. 2009, Hijnen et al. 2004)
TOC	2-30%	(Freitas et al. 2022)
DOC	5-40%	(Guchi 2015)
AOC	14-40%	(Guchi 2015)
NH_4^+	100%	(Lee et al. 2014)
Nitrogen compounds	45-67.5%	(Nakhla and Farooq 2003)

SSF creates turbidity-low, impurity-free effluent that is nearly devoid of bacteria, viruses, and protozoa (Guchi 2015), made it popular in the Netherlands that phased out chlorine disinfection. The removal values may differ under other experimental conditions, and the typical removal efficiencies for SSF as shown in Table 2.

The reported total organic carbon (TOC) displays average removals between 2% and 30% (Freitas et al. 2022, Guchi 2015). But SSFs are reported not as efficient for removing organic matter due to its low capacity to remove dissolved compounds which

are not readily biodegradable, such as humic substances (Zheng et al. 2010). The best results were sometimes associated with lower filtration rates. Nitrate removal rates in SSFs vary between <5% to 53% (Freitas et al. 2022) As the most oxidized form of nitrogen, nitrate is likely to be removed by biofilms that have microanoxic environments, wherein the diffusion of molecular oxygen is limited and denitrification can occur, forming N_2. However, some studies have also shown an increase in the concentration of nitrate and nitrite in SSF effluent (Freitas et al. 2022, Nakhla and Farooq 2003), which was reported as a result of a dynamic nitrogen cycling (i.e., nitrification and denitrification) that can occur within the filter media. However, it should be careful about the concentrations of nitrite and nitrate in treated water, which is an undesirable result given the consequences of their ingestion of human health (Freitas et al. 2022). Moreover, although nitrification in biological filters is a commonly used treatment technology for removing ammonium, the process can experience problems (Lee et al. 2014). Incomplete ammonium or nitrite removal can be caused by several factors including temperature (van der Aa et al. 2002), insufficient oxygen (Lytle et al. 2013), phosphate (nutrient) limitations (De Vet et al. 2012), and improper design and operation of filters (Lopato et al. 2013).

E.coli bacteria and PhiX 174 have been used in many studies as the comparable to bacteria and viruses (Attinti et al. 2010, Trikannad et al. 2023, Wielen et al. 2008). Bacteria and viruses removal by SSFs show an average reduction of 1-2 $\log_{10}$ and 0.2-2.2 $\log_{10}$, respectively (Guchi 2015, Hijnen et al. 2004), but they are influenced by several factors (Hussain et al. 2015), such as temperature, source water quality (Hussain et al. 2015), grain size (Pfannes et al. 2015), biological maturity (Trikannad et al. 2023).

2.3.2 Stratification in slow sand filter

According to previous studies, SSFs and RSFs with regular backwashing have heterogeneous flow patterns (Lopato et al. 2013), stratified biomass distributions (Albers et al. 2015, de Souza et al. 2021a), bioactivity (Perujo et al. 2019), and biokinetics (Tatari et al. 2016). Bacterial activity is most prominent in the upper filter layer, and declining trends in biomass and biofilm activity in depth have been commonly reported in porous media (Perujo et al. 2019, Yan et al. 2017), mainly attributed to trapped materials by sieving (Weber-Shirk and Dick 1997) and a decrease in the availability of nutrients in depth, thus limiting microbial growth (Perujo et al. 2019). Moreover, it has been found that both ammonium removal and AOB density

were strongly stratified in sand filters, with the highest values at the top layer. However, the relative abundance of AOB to AOA gradually decreased with depth (Lee et al. 2014). Similar stratifications in RSFs (Tatari et al. 2013, 2016), granular activated carbon filters (van der Aa et al. 2002), and nitrifying trickling filters (van Den Akker et al. 2008) were also been reported.

2.3.3 Clogging

Clogging is a surface phenomenon mainly occurring in finer sand systems, which was most likely caused by a build-up of organic matter, due to the loading of humic acid with high suspended solids, and biomass accumulation (Grace et al. 2016b). When clogging occurs, head loss through the filter increases and beyond a certain point maintenance of flow rate becomes so difficult that the filter run is aborted (Nogaro et al. 2010, Perujo et al. 2019). Therefore, maintenance and operation of SSFs basically consist periodic cleaning. Once flow is reduced, the top of the filtration layer must be cleaned usually by removing the Schmutzdecke and the top 5 cm of sand from the filter, which is called scraping (Freitas et al. 2022, Guchi 2015). Except scraping, backwashing of SSFs is also been applied and investigated (de Souza et al. 2021b). The cleaning methods are shown in Section 2.4.3.

2.4 Operation and construction parameters of slow sand filter

2.4.1 Grain size

Table 3. Advantages and disadvantages of grain size on SSF application.

Find sand	Coarse sand
· Potentially better retention of suspended solids and microorganisms. · Larger specific surface area, potentially higher adsorbing capacity. · Potentially greater bacterial density near the surface. · Potentially greater bacterial activity variety near the surface.	· Potentially lower clogging risk. · Potentially higher nutrient loads at greater depth. · Potentially higher overall bacterial biomass concentration. · Potentially greater bacterial activity in depth.

The grain size of the porous medium is an essential feature of filtration systems (Brix et al. 2001, Nogaro et al. 2010). It is primarily associated with pore size distribution and connectivity, regulates the distribution and movement of terminal election acceptors, nutrients, and organic matter in depth (Nogaro et al. 2010), and functions as a driver of biogeochemical processes and rates (Baker and Vervier 2004). The

recommend grain size is the fine sand with d_{10} between 0.15 and 0.30 mm (Guchi 2015), uniformity coefficient between 1.5 and 2.5, and a percentage of fines lower than 4% (Freitas et al. 2022, Jenkins et al. 2011) to increase the retention of suspended solids and microorganisms (Jenkins et al. 2011).

Coarse sand suggests high permeability values, which result in high DO concentrations in depth, favoring aerobic processes such as nitrification while suppressing anaerobic reactions, which are critical for dissolved nitrogen removal (Mueller et al. 2013, Perujo et al. 2017). Furthermore, coarse sand increases nutrient and organic matter loads at greater depth, which are linked with high biogeochemical rates but short advection periods (Perujo et al. 2017). Fine SSF has larger specific surface area (Huang et al. 2013) but lower permeability, which increase the adsorbing capacity but also the risk of substrate clogging (Wu et al. 2015). Grain size also influences biomass and bio-activity, with fine sediments having the greatest bacterial density and EPS values near the surface, while coarse sediments having higher overall bacterial biomass concentrations (Grace et al. 2016b). But low water residence time in coarse sediments leads to a low fraction of live bacteria in depth and a significant reduction in functional activity variety, resulting in less digested organic matter (Perujo et al. 2017).

As for the influence on SSFs' performance, the biological properties of the fine (0.075-0.25 mm) and coarse (0.9-1.2 mm) SSFs were equivalent in terms of biofilm colonization because both systems attained equal total biomass densities in the top layer (Perujo et al. 2019). Coarse grain size results in lower nitrification and total nitrogen removal (Nakhla and Farooq 2003, Perujo et al. 2017) due to less attached biomass. However, there are different reports on the effects of sand size on organic matter removal that biochemical oxygen demand removal decreases with larger sand size (Nakhla and Farooq 2003), but dissolved organic carbon (DOC) removal shows no difference (Perujo et al. 2017). Considering all this, it is difficult to assess which substrate size is better to use as both grain sizes display benefits and drawbacks.

2.4.2 Loading rate

Loading rate refers to the product of influent concentration and flow rate (Nakhla and Farooq 2003). Over a decade, flow rate of 0.008-0.38 m/h and even up to 1.5 m/h had been applied for the SSFs (Baig et al. 2011, Guchi 2015), and the biosand filter construction manual states a maximum filtration rate of 0.40 m/h (Freitas et al. 2022). A higher flow rate means water flows through the system more quickly, resulting in a

shorter average detention time. Detention time is critical for the initial creation and maintenance of Schmutzdecke because it permits particles suspended in water to settle and come into contact with the filter medium top (Huisman and Wood 1974), and is integrated into it by mass attraction or electrical forces (Freitas et al. 2022). Therefore, the flow rate is reported to be inversely proportional to the head loss in the column (Verma et al. 2017). Under normal conditions, a higher flow rate favors a higher production rate, but a lower effluent quality. Poor organic matter, nitrogen compounds (Nakhla and Farooq 2003), and bacteriophage (Anderson et al. 2009) removal in SSFs with high flow rate is most likely owing to increased shear and short hydraulic detention times. However, the higher oxygen transfer into the sand bed with increasing flow rate (Nakhla and Farooq 2003) and lower external mass transfer resistance with increasing loading rate (van Den Akker et al. 2008) can theoretically enhance nitrification.

2.4.3 Cleaning strategy

Periodic maintenance (cleaning) the filter medium is required as clogging results in insufficient water production. Typically, SSFs are operated for days, months, or years based on the influent water quality (de Souza et al. 2021b). And some studies reported the household SSFs were used for periods of up to 8 years (Freitas et al. 2022). The clogging is resolved by scraping the Schmutzdecke layer and backwash (de Souza et al. 2021a, Freitas et al. 2022, Guchi 2015). While backwashing is not typically employed in full-scale SSFs, it has garnered increased attention in recent years.

Backwash is an unusual alternative for SSF cleaning as uniform backwash does not occur in filters with large dimensions (de Souza et al. 2021a). However, considering backwash requires less expensive equipment, less energy consumption, and less labor than scarping and other methods, its application on small scale filters (such as community or household-scale) can be recommended. Previous studies show that backwashing did not significantly disturb biomass while scraping changed its surface sand layers, and this process preserved more biomass within the filters with less stratified bacterial community (de Souza et al. 2021a). With ~ 4 min backwash, the contaminants such as turbidity (< 1 NTU effluent), coliforms (> 80%), and protozoa cysts (> 2 $\log_{10}$) were removed with no significant differences from scraped filters (de Souza et al. 2021a, de Souza et al. 2021b, Pizzolatti et al. 2015), indicating that backwashing can be a good alternative for small-scale systems. However, its effect on the removal performance of DOC and ammonuim is still unclear.

3. Materials and methods

3.1 Lab-scale slow sand filters

Fig. 2. Experimental set-up of lab-scale slow sand filters.

Table 4. Characteristics of used quartz sand.

Sand sample	Particle size (mm)	Bulk density (g/cm^3)	Particle density (g/cm^3)	Calculated porosity	Specific surface area (m^2/g)
Fine	0.4-0.6	1.59 ± 0.03	2.6	0.39 ± 0.01	2.71×10^{-3}
Coarse	0.85-1.25	1.54 ± 0.01	2.6	0.41 ± 0.01	2.14×10^{-3}

Four lab-scale columns of 2.1 m height and 4 cm diameter were constructed as shown in Fig. 2. The set-up consisted of two fine sand (F1 and F2) and two coarse sand (C1 and C2) columns with a bed height of 85 cm followed by 5 cm of supporting gravel layer. The fine and coarse columns had sand grain sizes of 0.4-0.6 mm and 0.85-1.25 mm, respectively. The grain sizes were determined by sieving of the dry filter material through corresponding sieves, and the characteristics of sand are shown in Table 4.

The cylindrical columns were covered with aluminum foil to prevent light from entering the columns. The columns were provided with eight sampling ports installed on the side wall at depths 0, 5, 20, 30, 45, 55, 65, and 90 cm to collect water and sand

samples from the top to the bottom.

3.2 Slow sand filters operation

Table 5. Compounds and spiked concentrations.

Parameter	Spiked concentration (mg/L)	Compound	Chemical concentration (mg/L)
AOC	1.5	Sodium acetate ($NaC_2H_3O_2$)	2.83
		Sodium formate ($NaCHO_2$)	2.83
		Sodium oxalate ($Na_2C_2O_4$)	2.79
NH_4^+-N	1	Ammonia chloride (NH_4Cl)	3.82
PO_4^{3-}-P	0.015	Potassium dihydrogen phosphate (KH_2PO_4)	0.02

Table 6. Raw and synthetic tap water quality.

Parameter	Unit	Tap water	Synthetic tap water
pH	-	7.89 ± 0.03	7.90 ± 0.05
Temperature	℃	18.94 ± 1.97	18.94 ± 1.97
DO	mg/L	8.83 ± 0.58	9.12 ± 0.68
DOC	mg/L	2.80 ± 0.49	4.37 ± 0.82
NH_4^+-N	mg/L	0	0.90 ± 0.36
NO_2^--N	mg/L	0	0
NO_3^--N	mg/L	2.14 ± 0.10	2.11 ± 0.10
PO_4^{3-}-P	mg/L	0	0.012 ± 0.005
cATP	pg/mL	76.71 ± 42.10	137.46 ± 71.61
E.coli WR1	cfu/mL	< 1	$(3.21 \pm 1.40)\times10^5$
PhiX 174	pfu/mL	< 1	$(4.99 \pm 0.74)\times10^5$

The filters were operated under continuous flow condition. Tap water dosed with 1.5 mg/L AOC, 1 mg/L NH_4^+-N, and 0.015 mg/L PO_4^{3-}-P according to the C:N:P molecular ratio of bacteria and biomass (100:10:1) was used as the influent. The nutrient concentration employed in this experiment is referred to previous researches (Tatari et al. 2016, Zhou et al. 2022). Although it exceeds the typical influent water quality of SSFs, this deliberate elevation improved sensitivity by ensuing measurements were above detection limits and allowed readily observation and recording of the changes in pollutants levels. The concentrations of dosed compounds and tap water quality are shown in Table 5 and 6, respectively. All chemicals were provided by Sigma-Aldrich.

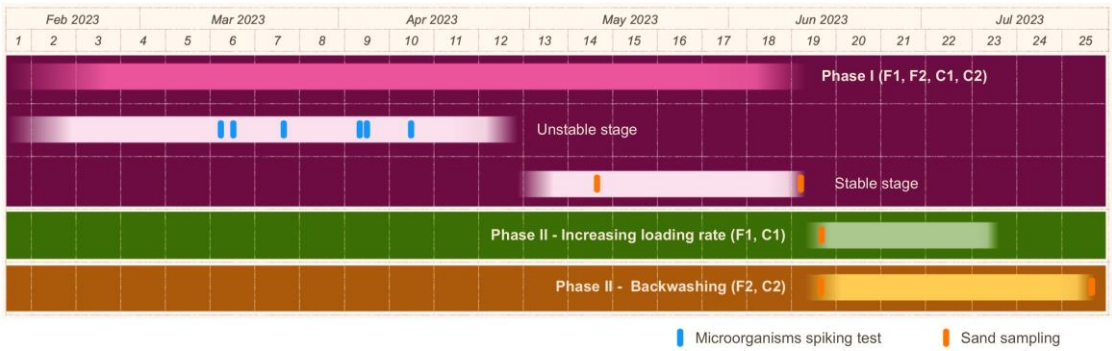

Fig. 3. Gantt chart of experiment phases and operation conditions.

The filters were operated in two phases with a total of 170 days from February to July. In phase I was studied the effect of grain size. During phase I experiment, both fine and coarse sand columns were operated at same flow rate of 0.5 m/h. The phase II experiment aimed to study the influence of loading rate and backwash, which was conducted after day 125. The phase II (increasing loading rate) experiment increased the flow rate from 0.5 m/h to 2 m/h with same influent concentration, and phase II (backwashing) experiment conducted backwashing (20% expansion for 5 min) on day 125 and kept the flow rate of 0.5m/h afterwards. The operating condition of each filter columns and timeline are shown in Fig. 3.

3.3 Water and sediment sampling

Water was sampled once a week in duplicate from eight sampling ports along the depth of the filter. The collected water samples were filtered with 0.45 um filter and used for DOC, NH_4^+, NO_2^-, NO_3^-, and PO_4^{3-} analysis. The samples were stored at 4 °C and analyses were initiated within 1 h of sampling.

Sand was sampled through the sampling ports by inserting a long spatula. 1.5-2 g (wet weight) of sand was collected from depths 5, 20, and 55 cm. Due to the limited amount of sand available in the columns, sampling was performed in the middle (day 93) and end (day 125) of phase I and at the start (day 132) and end (day 170) of phase II.

3.4 Analyses

3.4.1 Physiochemical analyses

Water samples for both DOC and ion measurement were filtered through a 0.45 um filter. After adding 1.6 mL of 2 M HCl solution into 30 mL filtered samples, DOC was measured using a total organic carbon analyzer (TOC; Shimadzu). Nitrite (NO_2^-), nitrate (NO_3^-), ammonium (NH_4^+), and phosphate (PO_4^{3-}) ions were measured by Ion Chromatography (IC; Metrohm). DO, pH, electrical conductivity (EC) and water

temperature were measured with WTW electrodes (SenTix 940, TerraCon925 and FDO925, respectively).

Table 7. The fractions and derived indices obtained from LC-OCD (Huber et al. 2011).

		Description
Fraction	Biopolymers	Organic matter with high molecular weight, including polysaccharides, proteins, and amino sugars
	Humics	Mixture of acids containing carboxyl and phenolate groups produced by the biodegradation of dead organic matter
	Building blocks	Molecular chains of polyphenolics/polyaromatic acids that have disaggregated, due to breakage of hydrogen bonding and electrostatic interactions
	LMW acids	Representing protic organic acids
	LMW neutrals	Uncharged small organics, including LMW alcohols, aldehydes, ketones, sugars, and LMW amino acids
	HOC	Fraction of DOC remaining in the column, implying a strong hydrophobic interaction with the column material, comprising longer chain aliphatic and polycyclic aromatic material
Index	Molecular weight	A derived value of average molecular mass of the humic fraction
	SUVA	An additional parameter derived from the ratio of DOC and spectral adsorption coefficient UVA_{254}

The organic matter was characterized by Liquid Chromatography Organic Carbon Detection (LC-OCD) analysis by Het Waterlabertorium. The LC-OCD is an automated size-exclusion chromatography system coupled to three detectors, for organic carbon, dissolved organic nitrogen (DON), and UV absorbance, respectively. Details of the measurement procedure have been reported by previous research (Huber et al. 2011). The chromatography subdivides TOC into hydrophobic organic carbon (HOC) and chromatographic dissolved organic carbon (CDOC), of which CDOC can be further divided into 5 components, including biopolymers, humics, building blocks, low molecular weight (LMW) acids, an LMW neutrals. The fractions and derived indices obtained from LC-OCD are shown below.

3.4.2 ATP analyses

ATP measurements were used to evaluate the microbial biomass within biofilters due to its capacity for precise and consistent assessment of microbial activity in complex aquatic systems (Lautenschlager et al. 2014). The cellular ATP (cATP) indicated the total living biomass quantity. The standard cATP was done by adding 100 uL of UltraCheck 1 and 100 uL of Luminase to a test tube with the same calibration procedure

as above, recorded the RLU value as RLU_{std}. The water sample was by filtering 50 mL sample with 0.45 um filter at a rate of 3-5 mL/s. Then added 1 mL of UltraLyse 7 into the syringe barrel and passed the UltraLyse 7 through the filter to dryness and collect in a 9 mL Ultralute tube. After thoroughly mixed, added 100 uL of the mixture and 100 uL of Luminase into the test tube to measure RLU_{cATP}.

The calculation to convert the RLU values to cATP in water sample is given below:

$$cATP\ (\text{pg ATP/mL}) = \frac{RLU_{cATP}}{RLU_{std}} \times \frac{10{,}000\ (\text{pg ATP})}{V_{Sample}\ (\text{mL})}$$

For sand samples, 1 g of the solids is weighted and added into a 15 mL sampling vial contained 5 mL of UltraLyse 7. Allowed at least 5 min for incubation and then transferred 1 mL of the mixture into a 9 mL UltraLute (Dilution) Tube. For the assay, 100 uL of mixture from UltraLute (Dilution) Tube and 100 uL of Luminase were added into a test tube and inserted into luminometer to obtain the RLU_{tATP} value. The calculation to convert the RLU values to tATP on sand samples is given below:

$$tATP\ (\text{pg ATP/g}) = \frac{RLU_{tATP}}{RLU_{std}} \times \frac{50{,}000\ (\text{pg ATP})}{m_{Sample}\ (\text{g})}$$

3.5 Tracer test

The conservative tracer test is commonly used in column experiments to investigate the characteristics of porous media. Sodium chloride (NaCl) was chosen as a conservative tracer. 1 g/L NaCl solution was injected into the columns by lowering the supernatant slightly above the sand bed. The tracer was continuously dosed for 85 mins using a peristaltic pump. The EC of the effluent was recorded every 5 min, and NaCl concentration was determined by a calibration curve measured at the same temperature. The calibration curve is shown in Fig. A1 in Appendix.

3.6 *E.coli* WR1 and PhiX 174 preparation and enumeration

3.6.1 Microbiological cultures preparation

The experiments were carried out with *E.coli* WR1 (NCTC 13,167) and bacteriophage PhiX 174 (ATCC 13,706-B1). *E.coli* WR1 is widely used as an indicator of enteric bacteria in drinking water studies (Eisfeld et al. 2022, Trikannad et al. 2023) and is used here as a surrogate for pathogenic bacterial.

A highly concentrated suspension of *E.coli* WR1 (~10^9 cfu/mL) was prepared by

growing in buffered peptone water for 18 h at 37 ℃, harvested by centrifugation at 3000 g for 5 min and washing in sterile water as per ISO 9308-1. PhiX 174 is an icosahedral, single-stranded DNA-phage with a diameter of 26 nm and an isoelectric point of 4.4 (Soliman et al. 2020). PhiX 174 is generally seen as a good viral surrogate due to its size and shape resemblance to several human enteroviruses such as poliovirus, norovirus, etc., as well as its low hydrophobicity and stability (Oudega et al. 2021). Although PhiX 174 may not be an ideal conservative colloidal tracer, somatic caliphates have gained special importance due to their high prevalence in sewage and persistence in the environment (Oudega et al. 2021). Moreover, for PhiX 174, it shows more conservation than bacteriophage MS2 due to its higher isoelectric point and lower contact angle (Attinti et al. 2010, Wielen et al. 2008). A highly concentrated suspension of PhiX (~10^{11} pfu/mL) was prepared as described in ISO-10,705.

Measurement of PhiX 174 requires pre-culture of its host bacteria. 100 mL of Modified Scholten's Broth (MSB) was added in a conical flask and placed on a shaker in the incubator to warm up. One vial of *E.coli* WG5 culture, which used as the reference host culture of PhiX 174, was removed from the -80 ℃ freezer and being thawed at room temperature. Once defrosted, transferred 1 mL of *E.coli* WG5 into the MSB in the nephelometric flask, and incubated WG5 culture in the incubator at 37 ℃ and 100 rpm. The growth of *E.coli* WG5 will be reflected by the increasing optical density of the broth. Measure the optical density at a wavelength of 600 um (OD_{600}) by spectrophotometer (DR3900, HACH, USA) every 30 min until OD_{600} increased to 0.5-0.6. Once the required OD_{600} was reached, immediately placed the flask in melting ice, and host bacteria must be used within 8 h.

3.6.2 Microbiological assays

Samples were diluted before assays to get a suitable number of colonies per plate. The dilution factor was varied according to spiking time, bed depth, and spiked microbe. By adding 0.5 mL water sample and 4.5 mL phosphate-buffered saline, the dilution was carried out in a gradient of 10 times dilution factor.

E.coli WR1 assay was performed by the spread plate method. 0.1-0.3 mL diluted/undiluted samples were added to the chromocult coliform agar, then spread in the same direction by a sterile spreader until the liquid was entirely absorbed by agar. Inoculated plates were placed upside down in the incubator with a constant temperature of 37 ℃ for 24 h.

As for PhiX 174 assay, semi-solid Modified Scholten's Agar (ssMSA) was melted in the water bath at 99 ℃, and then decreased the water bath temperature at 50 ℃. After cooling down, added 150 uL calcium chloride ($CaCl_2$) solution into each 25 mL ssMSA and mixed thoroughly. Distributed 2.5 mL ssMSA into sterile glass tubes and place in the water bath. Gently transferred 1 mL of *E.coli* WG5 host suspension and 1 mL of water sample into ssMSA, mixed the solution gently and poured on the surface of the Modified Scholten's Agar (MSA) plate. Incubated the plates at 37 ℃ for 24 h.

3.7 *E.coli* WR1 and PhiX 174 spiking tests

The spiking water was prepared by dosing *E.coli* WR1 or PhiX 174 stock solution to the tap water without nutrient dosage at a concentration of 10^5-10^6 cfu/mL and 10^5-10^6 pfu/mL, respectively. *E.coli* WR1 spiking solution was stirred (150 rpm) to prevent settling. The *E.coli* WR1 spiking tests of columns F1, F2, C1, and C2 were conducted on day 34, 64, 57, and 64, respectively. PhiX spiking tests were conducted on day 36, 56, 44, and 56, respectively. Spiking was done by lowering the supernatant slightly above the sand bed and dosing the spiking water using a peristaltic pump. After 5 h (~14 pore volumes (PVs)) spiking, influent water free of *E.coli* WR1 or PhiX 174 was dosed for the next 25 h (~70 PVs). Supernatant and effluent samples were collected in 250 mL sterile bottles every 15 min for the first 30 min (~1.5 PVs) and every 1 h for the next 7-8 h. After 24 h operation, the sampling interval time increased to 2-3 h. The microbial removal performance along the filter depth was detected by taking samples at 5, 20, 30, and 55 cm depths after 2 h and 4 h operation. The collected samples were refrigerated and further analyzed on the same day to yield breakthrough curves.

3.8 Data analysis

The overall efficiency of the SSFs in relation to the various water quality parameters was determined as the difference in values at the influent and effluent sampling locations. The efficiency of the parameter within the filter was estimated as the difference of the concentrations per unit depth (cm^{-1}) between intermediate horizontal layers. Each sampling depth was taken to represent the endpoint of a depth layer.

SPSS Statistics 22.0 was used for all static analysis. OriginPro 2020 was used for drawing figures. The differences were regarded as significant at $p < 0.05$ based on *t*-test. The relations between factors were analyzed by Pearson correlation-coefficient. The error bars were the mean ±1 standard deviation of duplicate measurements.

4. Results

4.1 Tracer test

Table 8. Results of tracer test.

Sand sample	Particle size (mm)	Breakthrough time (min)	Porosity
Fine	0.4-0.6	42.11 ± 0.19	0.39 ± 0.00
Coarse	0.85-1.25	43.16 ± 2.85	0.40 ± 0.03

The tracer breakthrough curves (BTCs) for SSFs are presented in Fig. A2 in Appendix and results are shown in Table 8. The values are in close agreement with the theoretical porosity calculated from the bulk and particle densities (Table 4). The higher porosity of the coarse column could be attributed to factors like grain size, effective size, and uniformity coefficient (Brix et al. 2001, Nogaro et al. 2010) , although these parameters were not directly investigated.

4.2 Variation of DO and pH

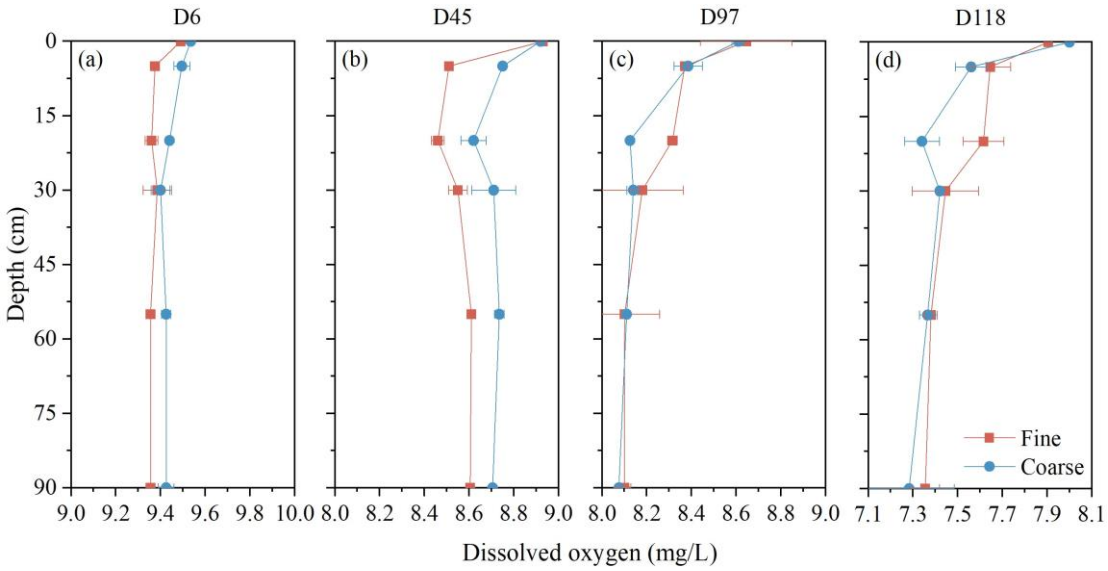

Fig. 4. Depth profile of DO concentration within the SSFs on day 6 (a), 45 (b), 97(c), and 118 (d).

The temperature, DO, and pH in water was measured along the filter depth. The temperature increased from 17.11 ℃ to 22.91 ℃ from February to August (Fig. A8). The vertical DO and pH distributions stabilized as filtration progressed as seen in Fig 4 and 5. SSFs remained aerobic and weakly alkaline (pH 7-8) throughout the experiment. Increasing water temperature lowered DO content in tap water (Fig. 4) from 9.51 ± 0.03 mg/L to 7.90 ± 0.07 mg/L. DO distribution in fine and coarse columns remained the same during operation ($p > 0.05$). The surface 5 cm had the highest DO

consumption, while fine column DO decreased rapidly starting about day 45. The top 5 cm of all columns consumed 42.1%-61.4% of total DO (0.23-0.44 mg/L) intake after 97 days. The coarse column had a lower DO concentration at 5-30 cm than the fine column, but below 30 cm it was similar. After stable operation, all filter columns used 0.54-0.72 mg/L DO.

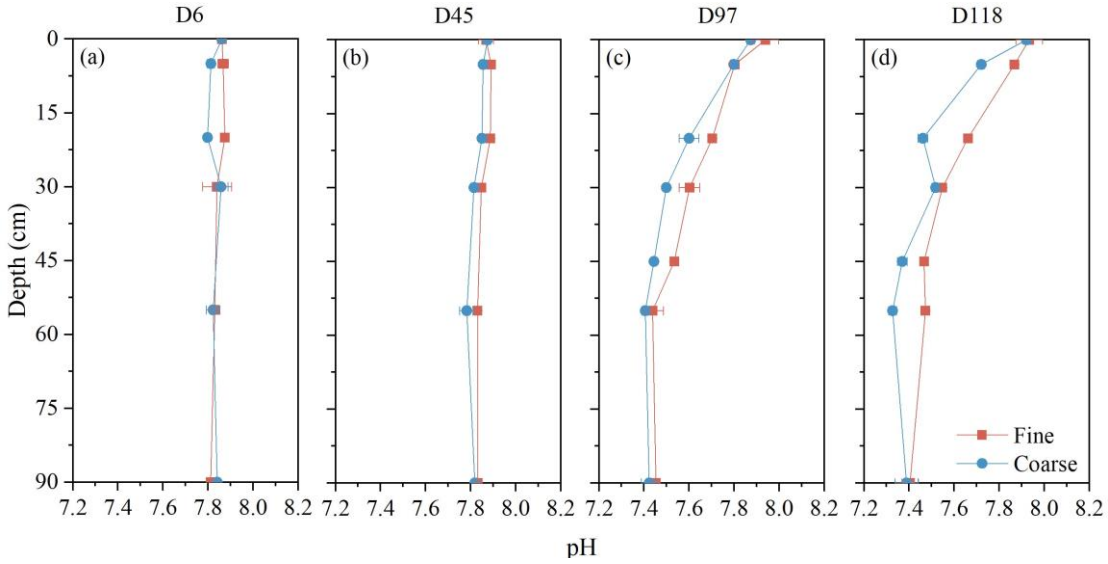

Fig. 5. Depth profile of pH within the SSFs on day 6 (a), 45 (b), 97(c), and 118 (d).

pH decreased significantly after day 97, that the effluent pH of fine and coarse column decreased by 0.49 and 0.45, respectively. And approximately 0.53 on day 118 (Fig. 5). Similar to the DO distribution, the fasted pH drop occurred at the surface 5 cm layer. The observation indicated an influence of grain size on pH variation in SSFs ($p < 0.01$).

4.3 Removal of DOC

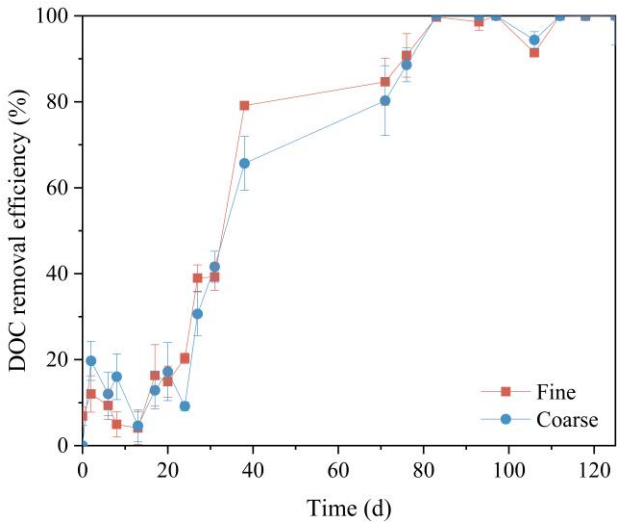

Fig. 6. Temporal changes in DOC removal efficiency in fine and coarse columns during phase I.

The DOC removal efficiency ranged from 11.3% before day 25 and rapidly increased in both columns (Fig. 6). Following 93 days of operation, both fine and coarse columns achieved 100% removal of the additional DOC (1.23 ± 0.39 mg/L). This increase in removal as filtration progressed indicates the function of biological processes in removal. There was no significant difference in DOC removal efficiency between fine and coarse columns ($p > 0.05$). However, as fine sand possesses a larger specific surface area, the DOC removal load per unit specific surface area was greater for coarse sand. Specifically, DOC could be removed at a value of 0.019 g/h/m^2 for fine sand and 0.025 g/h/m^2 for coarse sand on day 125.

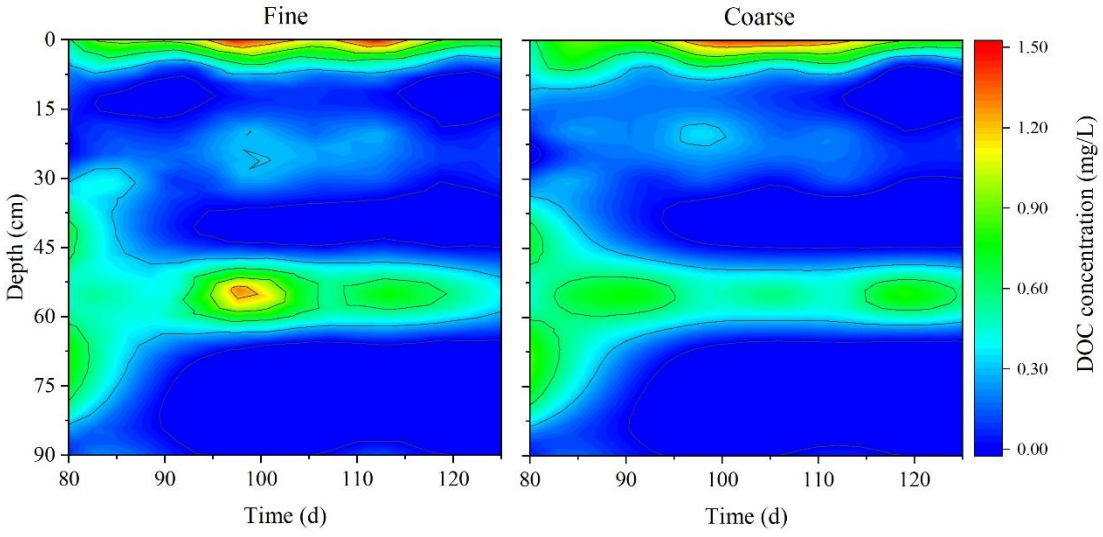

Fig. 7. Depth profiles of DOC in fine and coarse columns operating at 0.5 m/h. The DOC measurements were normalized by removing background concentrations of tap water.

The depth profiles show a decrease in DOC with depth (Fig. 7). DOC was majorly removed in the top 5 cm layer, resulting in removal efficiencies of 73.2% ± 15.6% and 69.8% ± 20.2% in the fine and coarse columns, respectively. It is interesting to observe that, DOC increased in the deeper layers between 45-65 cm (Fig. A9). over time, the peak concentration in fine and coarse sand increased by 0.94 ± 0.32 mg/L and 0.72 ± 0.36 mg/L, respectively, specifically at 55 cm depth. The DOC concentration rapidly declined below 55 cm, indicating a complete removal of additional DOC in the influent.

4.4 Characterization of DOC

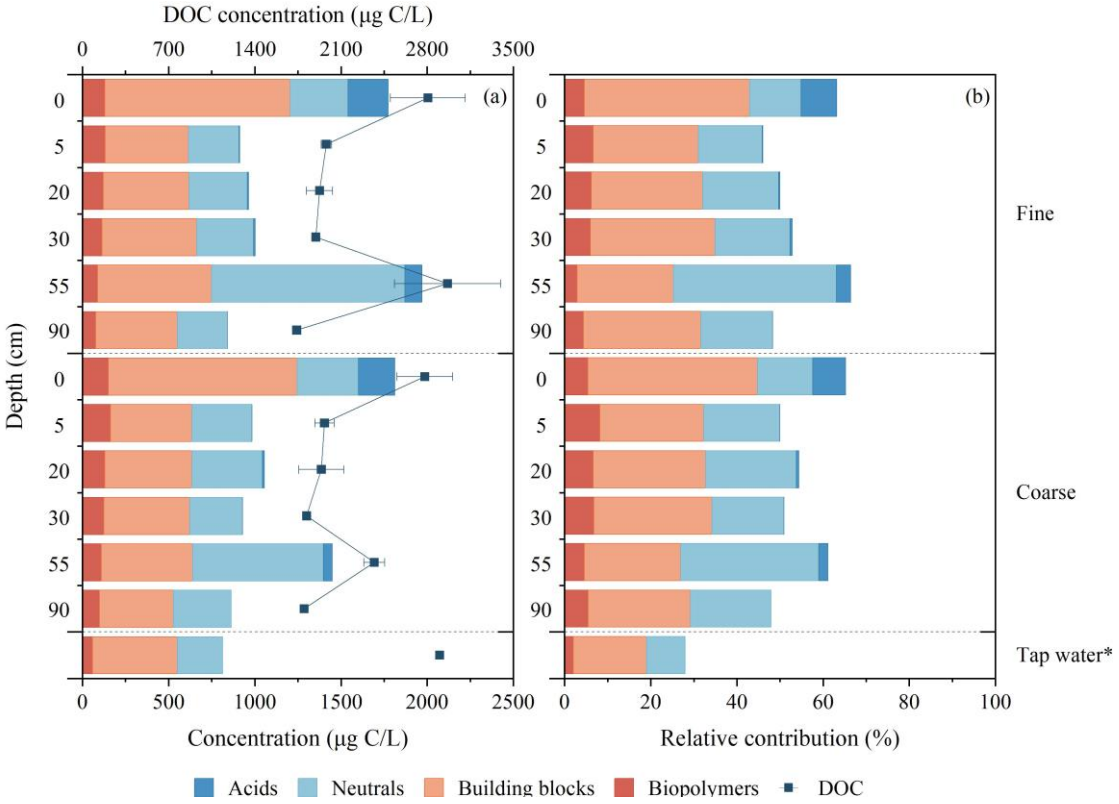

Fig. 8. Vertical concentrations (a) and relative distributions (b) of the DOC fractions within the SSFs on day 106. * The data for tap water referred to (Baghoth et al. 2008).

After the filters stabilized (day 106), LC-OCD analysis was performed on water samples from various depths to determine the increase of DOC in the deeper layers (Fig. A10). The water from the two stage drinking water treatment train of Amsterdam Water Supply operated by Waternet (Baghoth et al. 2008), served as a reference of tap water.

The TOC contains POC and DOC. The relative proportion of POC remained consistent in both fine and coarse columns below 1%. DOC can be divided into HOC and CDOC, with the latter consisting of humic substances, biopolymers, building blocks, LMW

neutrals, and LMW acids. HOC was completely removed in the influent of both columns. The humics was not removed in the filter, indicating its recalcitrant nature. Because the study focus on evaluating the removal of easily biodegradable organic carbon, Fig. 8 illustrates the data of the DOC fractions excluding HOC and humics.

The additional AOC in the tap water corresponds to an increase of 222.38 ug/L building blocks and 634.50 ug/L LMW acid in the influent. These fractions were rapidly removed by 593.00-621.50 ug/L and 211.67-230.51 ug/L in the top 5 cm for acids and building blocks, respectively in both columns. Below 5 cm, the concentrations of building blocks and LMW acids remained stable indicating that apart from the dosed AOC, the SSFs exhibited limited removal of LMW substances (building blocks, LMW neutrals, and LMW acids) in tap water (Chen et al. 2016). The proportion of biopolymers remained less than 10%. The biopolymers at 5 cm depth of fine and coarse sand initially increased by 3.4% and 7.4%, respectively, before subsequently declining and achieved a removal efficiency of 40%. The relatively high percentage of biopolymers removal can be attributed to the fact that biopolymers have been reported as substrates that can facilitate biofilm formation, even at low concentration levels in drinking water (Chen et al. 2016).

In contrast to typical SSF findings (Grace et al. 2016a, Zheng et al. 2010), DOC in SSF increased at a 55 cm depth in both fine and coarse columns. This surge was due to LMW neutrals, with concentrations of 791.50 ug/L and 453.30 ug/L in the fine and coarse columns, followed by building blocks at 113.00 ug/L and 30.50 ug/L, and LMW acids at 89.24 ug/L and 50.67 ug/L in fine and coarse columns, respectively.

Fig. A13 shows the specific UV absorbance (SUVA) profile within the filters. SUVA increased with depth, except at 55 cm. Fine and coarse filters raised SUVA by approximately 0.89 L/(m·mg) and 0.82 L/(m·mg), reaching 2.24 ± 0.018 L/(m·mg) and 2.26 ± 0.018 L/(m·mg), respectively, indicating increasing proportion of humic substances in DOC post-SSF. However, at 55 cm, due to increased DOC, SUVA dropped to1.34 L/(m·mg) and 1.69 L/(m·mg) in fine and coarse column, respectively.

4.5 Removal of ammonium

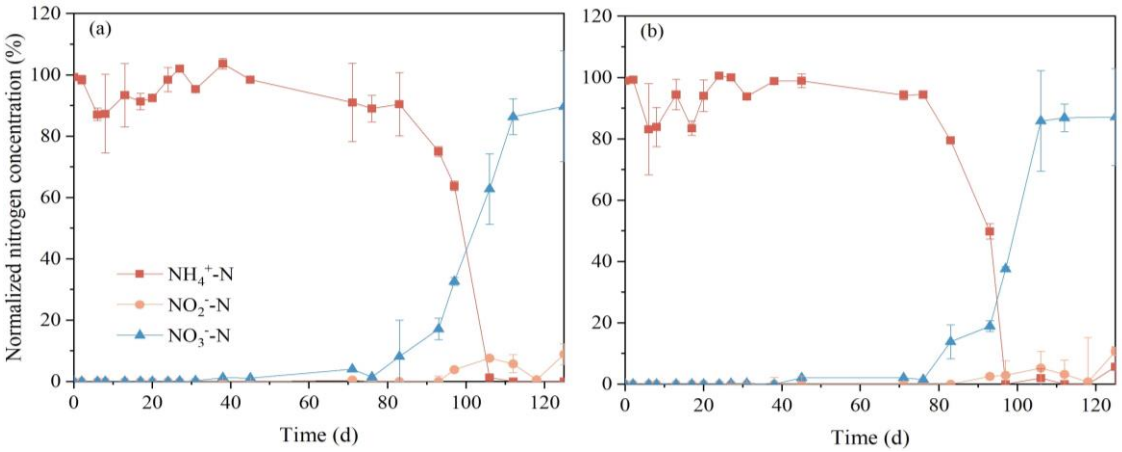

Fig. 9. Nitrogen conversion profile between NH_4^+-N, NO_2^--N, and NO_3^--N within fine (a) and coarse (b) columns during the phase I. The concentrations are normalized by dividing the influent NH_4^+-N.

The main nitrogen source for microbes in SSFs was the dosed NH_4^+-N. To understand the transformation and conversion of ammonium into different nitrogen species, the nitrogen oxides (NO_x^-) were measured during the experiment (Fig. 9).

A significant negative correlation was observed between the concentrations of NH_4^+-N and NO_3^--N in the effluent, that the effluent concentration of ammonium began to decrease at day 40, and simultaneously, the concentration of nitrate started to increase. Subsequently, after 80 days of operation, nitrite and nitrate rapidly increased as ammonium decreased, consistent with the results shown in Fig. 9. By day 100, the dosed NH_4^+ was completely consumed, with approximately 88.0% ± 2.4% and 86.6% ± 0.7% converted to NO_3^-, and 7.3% ± 2.2% and 6.3% ± 3.8% converted to NO_2^- in fine and coarse column, respectively. This suggests that an estimated 4.6 ± 4.6% of ammonium in the fine column and 7.0% ± 2.2% in the coarse column might have been removed through mechanisms such as volatilization and accumulation within the biomass and sediments (Perujo et al. 2018).

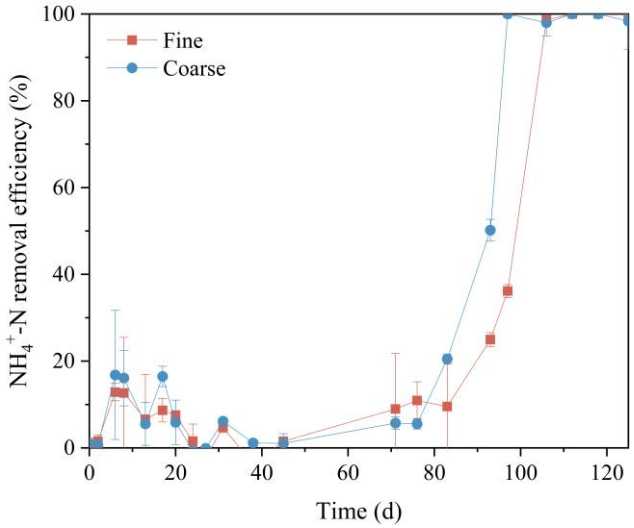

Fig. 10. Temporal changes in NH_4^+-N removal efficiency in fine and coarse columns during phase I.

As depicted in Fig. 10, the removal efficiencies of NH_4^+-N showed initial fluctuations for the first 20 days, likely due to variations in influent water quality. The NH_4^+ removal efficiency increased significantly in both fine and coarse columns from day 80 and reached 100% on day 97 in coarse columns and day 112 in fine columns. After normalized by specific surface area, fine sand removed 0.019 g/h/m^2 of NH_4^+-N and coarse sand removed 0.023 g/h/m^2 on day 125. The grain size had no significant effect on NH_4^+ removal efficiency based on *t*-test analysis.

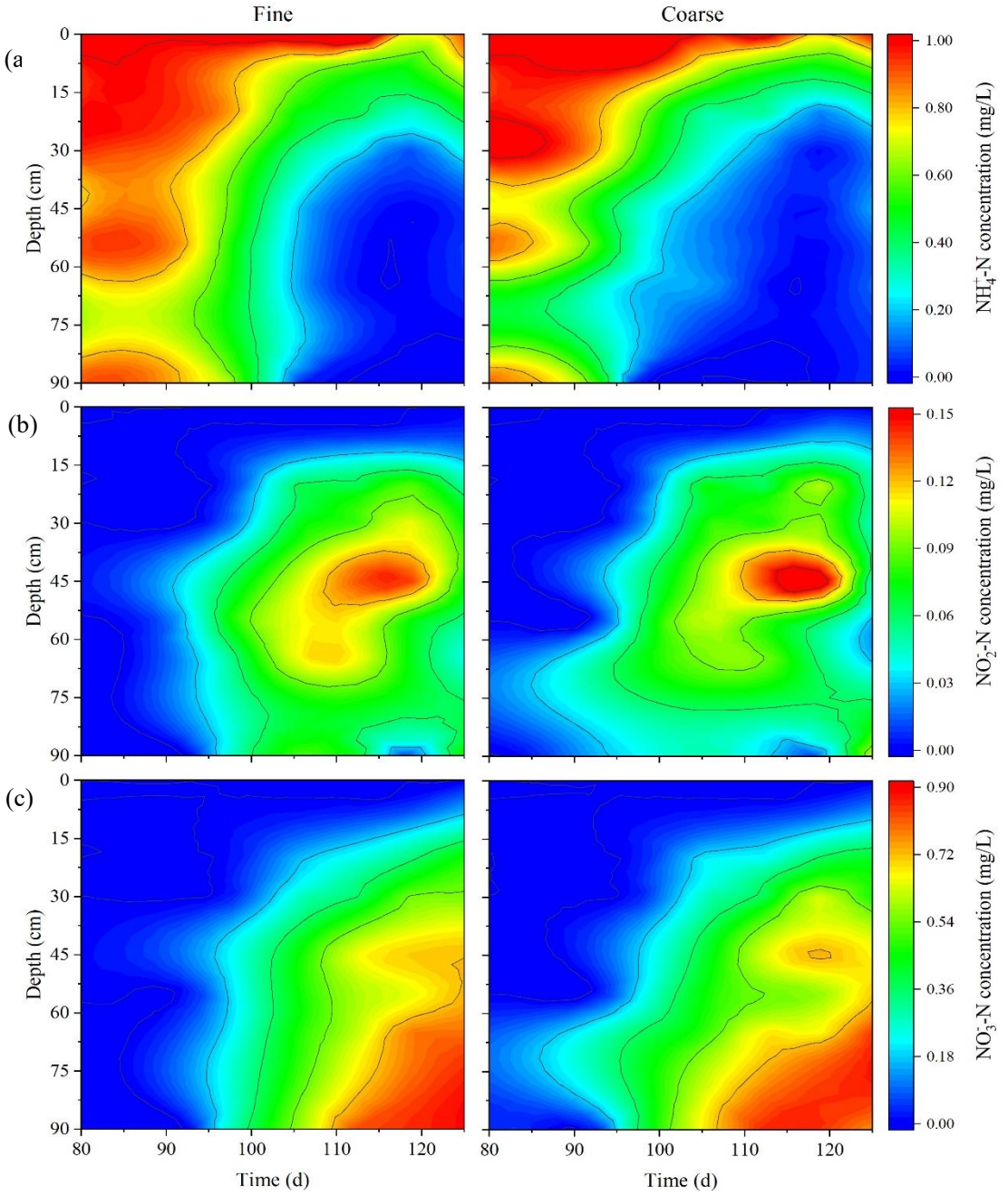

Fig. 11. Depth profiles of NH_4^+-N (a), NO_2^--N (b), and NO_3^--N (c) in fine and coarse columns operating at 0.5 m/h during phase I. The measurements were normalized by removing background concentrations of tap water.

Fig. 11 shows depth profiles of NH_4^+-N, NO_2^--N, and NO_3^--N in the filter column. NH_4^+ removal initially occurred in the deep layer of the coarse sand filter columns, about 10 days earlier than in the fine columns on approximately day 85. Over time, the concentration gradient of NH_4^+ moved upward, reaching about 30 cm in the fine column and 20 cm in the coarse column by day 120 (Fig. 11(a)).

A strong correlation was observed between ammonium decrease and increased NO_x^- in

both fine (r^2 = - 0.94, $p < 0.01$) and coarse (r^2 = -0.91, $p < 0.01$) columns. However, in the top 5 cm, the decrease in ammonium did not correspond with NO_x^-, indicating the removal path other than nitrification. After day 118, the NH_4^+ was completely removed in the top 45 cm. The highest NO_2^- concentration was observed on days 112-118 in the 45 cm depth (Fig. 11(b)), reaching approximately 0.15 ± 0.03 mg/L in fine column and 0.18 ± 0.02 mg/L in coarse column. NO_3^- increased with the depth with effluent concentration of 0.89 ± 0.01 mg/L and 0.76 ± 0.01 mg/L in fine and coarse columns, respectively (Fig. 11(c)). According to *t*-test, the grain size showed a significant effect (t = 1.836, $p < 0.05$) on the distribution of NH_4^+ distribution within the SSFs However, the effect was not significant in relation to the distribution of NO_2^- and NO_3^-.

4.6 Mass balance

Table 9. The spatial changes in removal flux of DOC, nitrogen, phosphate, and DO within intermediate horizontal layers of the filters. The data is derived from the average values recorded between days 97 and 125. A negative value indicates substance reduction through the layer, while a positive value indicates substance increase.

Depth (cm)	DOC (ug/L/cm)	DIN	NH_4^--N	NO_2^--N	NO_3^--N	PO_4^{3-}-P	DO
Fine column							
0-5	-166.59	-62.44	-62.44	0.00	0.00	0.12	-62.00
5-45	-99.36	21.19	-106.92	105.71	22.40	-0.67	-6.75
45-55	183.13	-18.09	-6.32	-8.11	-3.66	0.00	1.00
55-65	-179.86	6.28	-1.89	9.36	-1.19	0.08	-1.43
65-90	-8.71	18.11	1.30	23.94	-7.13	-0.06	0.00
Coarse column							
0-5	-165.01	-37.09	-38.83	0.89	0.89	0.05	-56.00
5-45	-111.55	-7.42	-134.23	104.43	22.39	-0.46	-8.75
45-55	143.91	-17.97	-2.38	-7.70	-7.90	0.01	-1.00
55-65	-130.24	23.55	-5.01	28.09	0.46	-0.07	0.00
65-90	-7.34	-2.67	-17.71	24.58	-9.53	-0.13	0.00

The filter bed is divided into sections: 0-5, 5-45, 45-55, 55-65, 65-90 cm based on Fig. A9. Table 9 and A1 assess the changes in DOC, nitrogen, phosphorus, and DO concentrations per cm, to determine substance conversion and reaction rates. A negative and positive flux in the filter bed indicates concentration decrease and increase, respectively.

A negative DOC flux was observed in the top 45 cm and 55-90 cm depth in all columns, however, a positive flux occurred in 45-55 cm depth. Given the absence of detected

DON concentration, dissolved inorganic nitrogen (DIN) was determined through a comprehensive calculation involving NH_4^+, NO_2^-, and NO_3^-. NH_4^+ showed a decrease at 5-45 cm layer, with values of -106.92 ug/L/cm in fine column and -134.23 ug/L/cm in coarse column. And maximum increments of NO_2^- and NO_3^- were similarly situated within this layer. NO_3^- displayed an overall positive flux within the filter columns, apart from the 45-55 cm depth, where the flux became -8.11 ug/L/cm and -7.70 ug/L/cm in fine and coarse column, respectively. Correspondingly, NO_2^- flux shifted predominantly to negative below the 45 cm depth. DO significantly declined in the 0-5 cm layer, measuring -60.20 ug/L/cm in fine column and -56.00 ug/L/cm in coarse column. Flux values tapered progressively below 5 cm, almost ceasing beneath 45 cm.

4.7 Microbial water quality

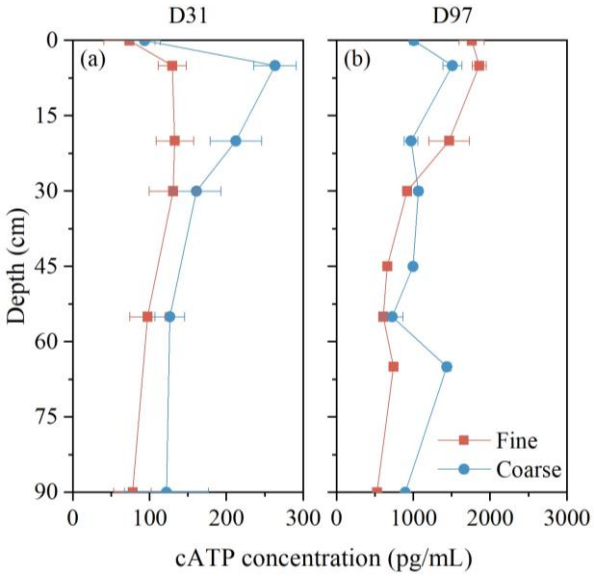

Fig. 12. Depth profile of cATP concentration in water on day 31 (a) and 97 (b).

Fig. 12 shows cATP concentration in water duirng mid (day 31) and later (day 97) stage of the phase I experiment. cATP at 5 cm depth was higher than in the supernatant, with a concentration of 129.30 ± 18.02 pg/mL and 263.13 ± 27.58 pg/mL in fine and coarse column, respectively. cATP further decreased with depth, however, effluent concentration was still higher than the supernatant. After 97 days, cATP significantly increased throughout the columns, especially in the top 5 cm. In fine column, the peak at 5 cm depth was 1857.32 ± 91.26 pg/mL and decreased to 524.45 ± 1.26 pg/mL in the effluent. In the coarse column, cATP at 5 cm (1506.85 ± 120.73 pg/mL) was lower compared to the fine column but remained higher than the fine column below 30 cm, showing a relatively uniform vertical distribution.

Comparing cATP concentrations on days 31 and 97, significant increases occurred in all columns. The most substantial increase was within the surface 5 cm layer, where cATP increased by 18 times in fine column and 7 times in coarse column. Below 5 cm, concentrations increased on average by 8 times in fine sand and 6 times in coarse sand. Similar to observations in RSF (Bar-Zeev et al. 2012), cATP in filtrate water also increased at 65 cm depth on day 97. The vertical distribution of cATP in filtrate water was comparable in both fine and coarse columns ($p > 0.05$).

4.8 Biomass development on sand

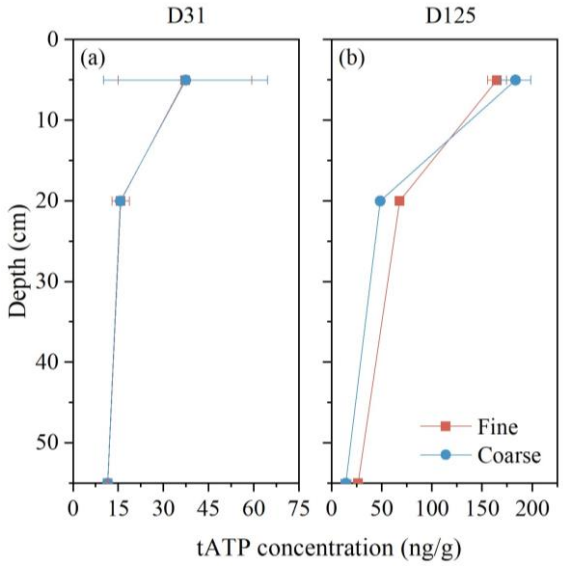

Fig. 13. Depth profile of deposit tATP concentration normalized to the mass of sand on day 31(a) and 125 (b).

Fig. 13 shows the attached tATP concentrations per unit mass of sand. Biomass on sand increased with time. On day 31, the highest concentration of 37.14 ± 22.22 ng/g and 37.36 ± 27.23 ng/g was observed in the top 5 cm of fine and coarse columns, respectively. The concentration decreased with depth with 11.43-15.76 ng/g at 20 cm in all columns. On day 125, 5 cm depth contained highest tATP concentration of 164.78 ± 9.34 ng/g in fine column and 183.27 ± 15.07 ng/g in coarse column. Compared to day 31, the increase occurred in the deeper layers with 32.68-51.97 ng/g and 2.65-14.88 ng/g at 20 cm and 55 cm, respectively. However, the concentrations in the deeper layers were much lower than the surface.

The stratification of attached tATP with depth became more prominent due to the excessive biomass growth in the top layer. Moreover, similar to cATP concentrations in the water, grain size had no obvious impact on attached tATP ($p > 0.05$), as indicated

by the *t*-test results.

4.9 Influence of loading rate

The effect of loading rate on DOC and NH_4^+ removal and biomass were examined by increasing the flow rate to 2 m/h with same influent concentrations. It is important to note that fine column experienced clogging issues on day 139, leading to a noticeable reduction in the effluent flow rate. This problem occurred in the coarse column on day 140. To maintain the loading rate of 2 m/h, a hydraulic cleaning of the surface layer was performed on day 152. This involved applying high-velocity horizontal water flow, approximately 1-2 cm just below the sand surface while simultaneously extracting rinsed water from 2-3 cm above the sand surface. This process suspended surface sand particles and dirt without affecting the lower sand layers (Fig. A17). The rinsed water produced during cleaning contained a significant amount of brown floc (Fig. A18).

4.9.1 Removal of DOC

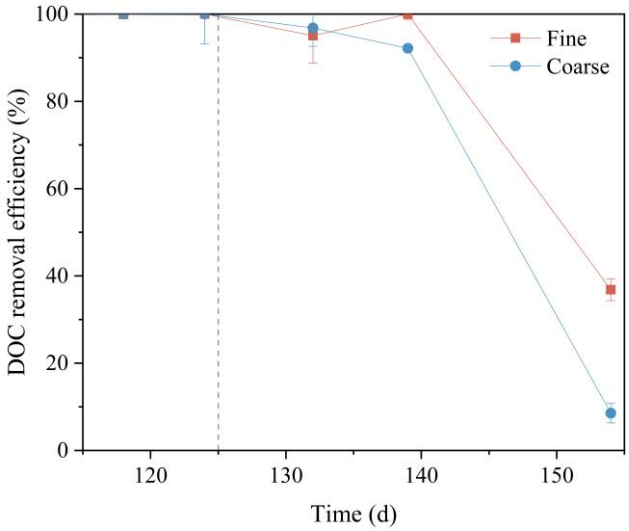

Fig. 14. Temporal changes in DOC removal efficiency in fine and coarse columns during phase II. The dashed line indicates the start of the phase II – increasing loading rate.

As shown in Fig. 14, the DOC removal efficiency remained relatively stable until the conduction of surface cleaning (after day 152). Before the cleaning, the increase in loading rate from 0.5 m/h to 2 m/h slightly decreased the filters' ability to treat DOC, with the removal efficiency reduced to 95.0% and 92.2% for fine and coarse column, respectively. Considering the increasing load and specific surface area, the DOC removal ability per unit surface area increased to 0.152 g/h/m^2 for fine sand and 0.182 g/h/m^2 for coarse sand on day 139. This represented a 8-fold increase for fine column

and 7-fold increase for coarse column compared to the values on day 125, before the loading rate was increased.

Significantly, the surface cleaning process substantially reduced DOC removal from 100% and 92.2% ± 0.3% to only 36.8% ± 2.5% and 8.5% ± 2.2% in the fine and coarse column on day 154, respectively. Attributed to the influent pipe of surface cleaning process in coarse column was positioned at a lower depth compared to that in fine column, the coarse column experienced a greater cleaning depth and consequently a more pronounced reduction in DOC removal ability. Moreover, this highlights the important role of the Schmutzdecke and surface sand layer in DOC removal within SSFs, accounting for a substantial 63.2% to 83.7% of the reduction in DOC.

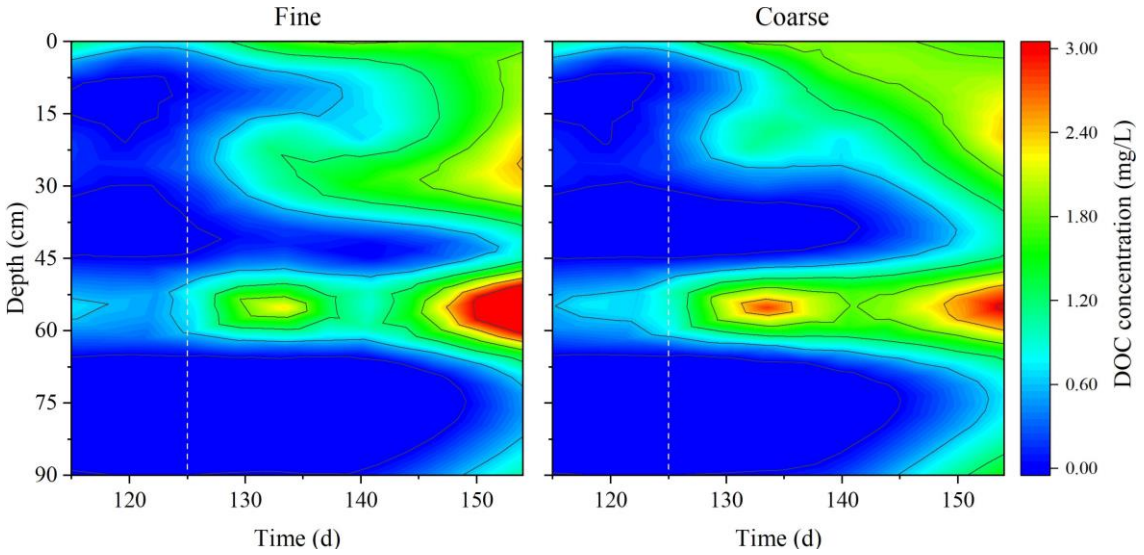

Fig. 15. Depth profiles of DOC in fine and coarse columns operating at 2 m/h during phase II. The DOC measurements were normalized by removing background concentrations of tap water. The dashed line indicates the start of the phase II – increasing loading rate.

As shown in Fig. 15, DOC penetrated into deeper layers with significant difference ($p < 0.05$) compared to loading rate of 0.5 m/h. The removal at 5 cm depth decreased from 74.1%-76.7% to 54.6%-61.9% 7 days after increasing the loading rate. The peak of DOC at 55 cm was still evident and increased with higher loading rate. The maximum concentration at 55 cm on day 132 increased by 2.40 mg/L and 2.75 mg/L in the fine and coarse column, respectively, compared to day 125.

4.9.2 Removal of ammonium

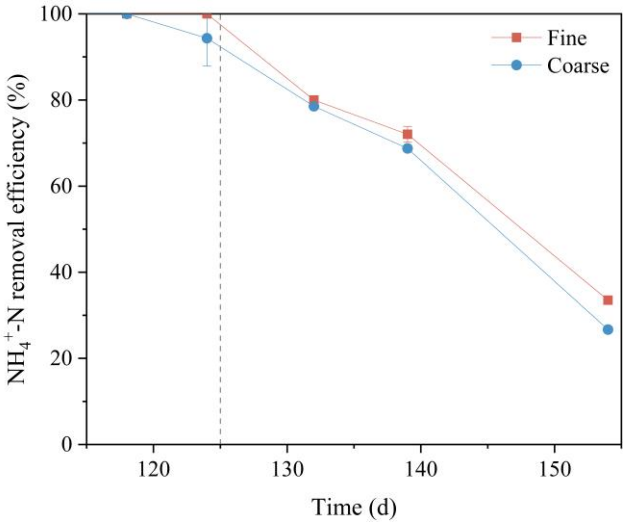

Fig. 16. Temporal changes in NH_4^+-N removal efficiency in fine and coarse columns during phase II. The dashed line indicates the start of the phase II – increasing loading rate.

As shown in Fig. 16, the rise in loading rate exhibited a more pronounced negative impact on NH_4^+ removal compared to DOC. Prior to the onset of clogging, the NH_4^+ removal efficiency in fine and coarse column decreased from 100% to 72.1% ± 1.8% and 68.7% ± 0.7%, respectively. However, compared to day 125, the removal load per unit surface area raised 3.8 times to 0.071 g/h/m^2 and 4.3 times to 0.099 g/h/m^2 for fine and coarse sand, respectively.

After the surface cleaning (day 152), the removal efficiency decreased greatly to only 33.5% ± 0.4% in fine column and 26.7% ± 0.4% in coarse column, indicating that Schmutzdecke and surface sand layer directly or indirectly contributing to a 38.6%-42.0% removal of NH_4^+.

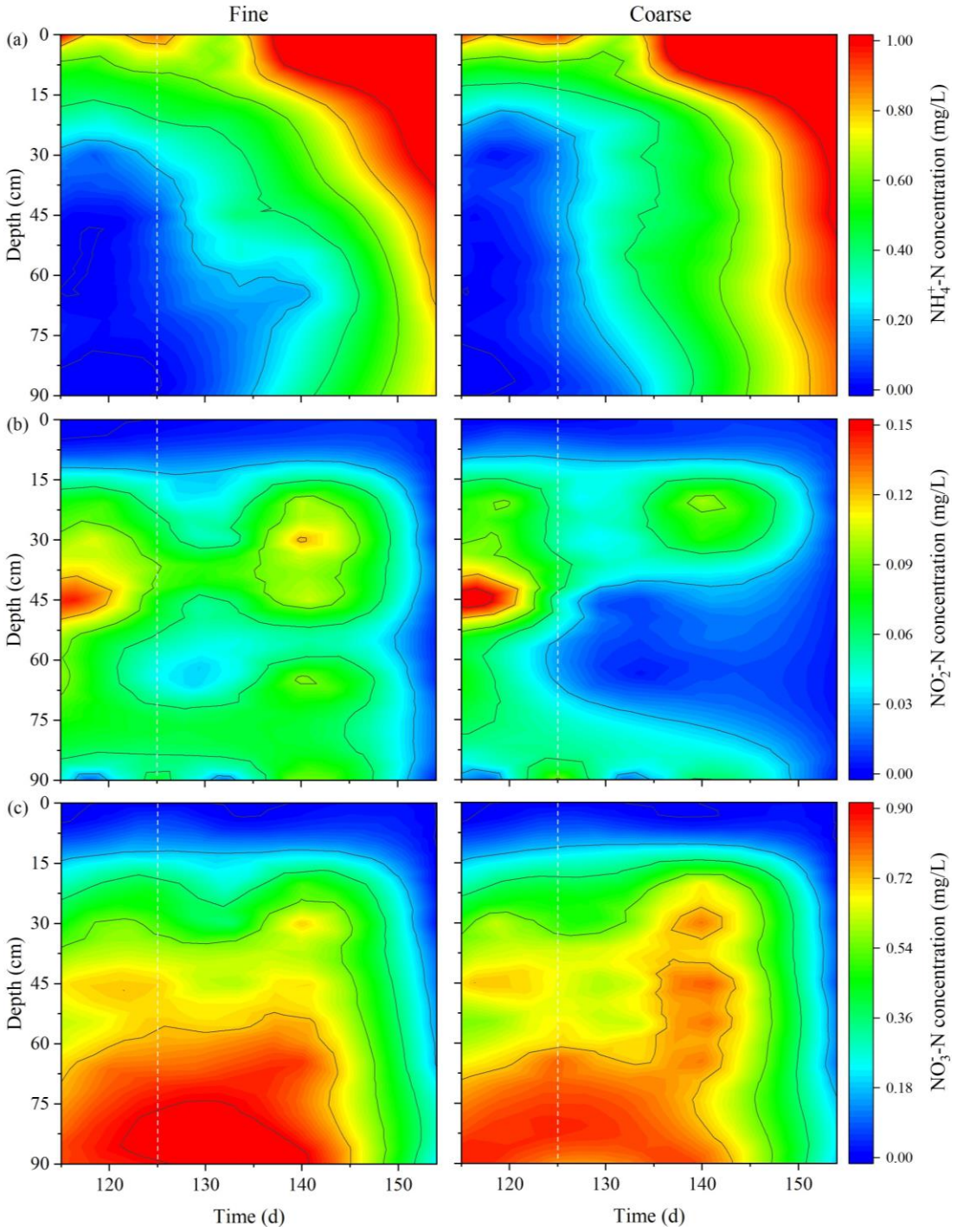

Fig. 17. Depth profiles of NH_4^+-N (a), NO_2^--N (b), and NO_3^--N (c) in fine and coarse columns operating at 2 m/h during phase II. The measurements were normalized by removing background concentrations of tap water. The dashed line indicates the start of the phase II – increasing loading rate.

The NH_4^+ penetrated throughout the entire filter columns upon the increase of loading rate to 2 m/h (Fig. 17). The main removal of ammonium occurred at the depth of 5-20 cm, and the depth below 20 cm contributed less to its removal. The peak of NO_2^- was still observed in the middle sand layer after increasing loading rate, but its depth shifted

upward and the maximum concentration decreased in the coarse column. Despite the noticeable decrease in the overall removal of NH_4^+ due to loading rate variations, the vertical distribution of NH_4^+ within both all columns showed no significant difference under loading rates of 0.5 m/h and 2 m/h ($p > 0.05$) based on *t*-test (Table A2) before surface cleaning.

4.9.3 Microbial water quality

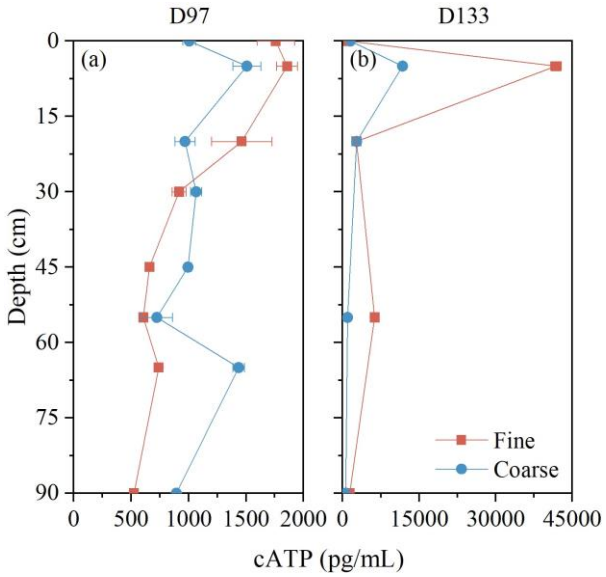

Fig. 18. Depth profile of cATP concentration in water before (a) and 8 days (b) after increasing loading rate.

In Fig. 18, the short-term effect of increasing loading rate on cATP concentration in water is evident. The most significant impact was observed at a depth of 5 cm, where the concentration of cATP in fine column increased by approximately 25.65 times, and in coarse column by 1.87 times. Below 20 cm depth, the change in cATP was not as substantial, with the increase not exceeding one order of magnitude. According to *t*-test results (Table A2), higher loading rate showed a significant influence on cATP concentration in the surface 5 cm layer ($p < 0.05$) of all filter columns. However, there was no significant impact detected below 5 cm depth ($p > 0.05$) in all filter columns.

4.9.4 Biomass development on sand

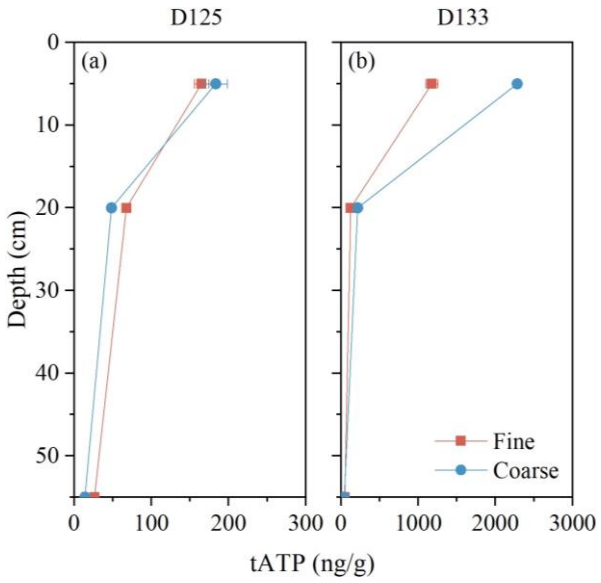

Fig. 19. Depth profile of deposit tATP concentration normalized to the mass of sand before (a) and 8 days (b) after increasing loading rate.

Although the concentration of tATP attached on the sand in the entire filter bed showed a rapid increase within 8 days after the increase of loading rate (Fig. 19). Loading rate showed a significant effect ($p < 0.05$) on the tATP concentration in top 5 cm layer, but no significant difference was observed ($p > 0.05$) in deeper layer (Table A2). The most substantial increase was observed in the surface 5 cm, with a growth factor of approximately 7.44 to 41809.09 ± 1030.53 ng/g in fine column and 13.23 to 11739.52 ± 565.03 ng/g in coarse column. At 20 cm and 55 cm depths, there was a minor increase in attached tATP concentration, and both fine and coarse columns exhibited similar tATP increase at different depths, with a factor of 1.82 and 4.34, respectively.

4.10 Influence of backwashing

The backwashing was conducted to investigate the impact of this cleaning method on stratification of DOC and NH_4^+ removal and biomass in the filter. Backwash was performed using a fluidized bed with 20% expansion for 5 min, based on previous SSF and RSF studies (Crittenden et al. 2012, de Souza et al. 2021a). The coarse column required a higher backwash flow rate to fulfill the expansion criteria.

4.10.1 Removal of DOC

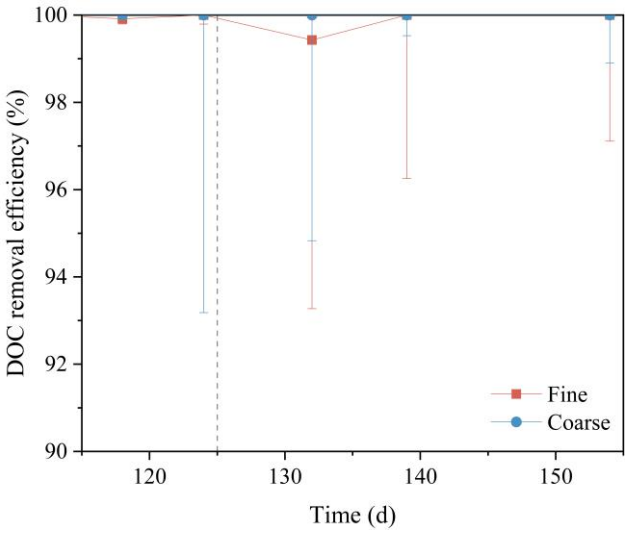

Fig. 20. Temporal changes in DOC removal efficiency in fine and coarse columns during phase II. The dashed line indicates the start of the phase II – backwashing.

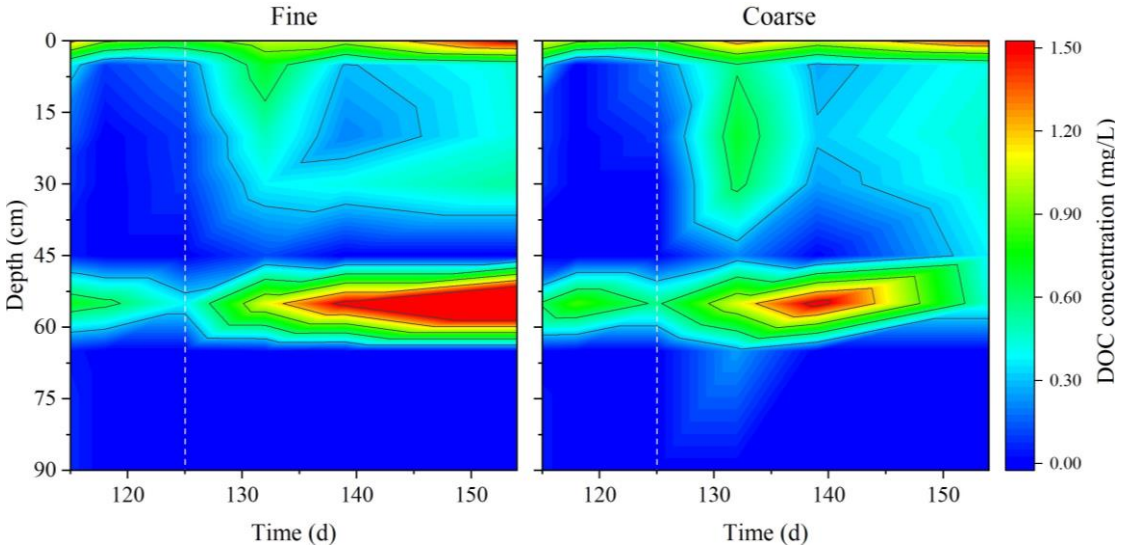

Fig. 21. Depth profiles of DOC in fine and coarse columns operating at 0.5 m/h during phase II. The DOC measurements were normalized by removing background concentrations of tap water. The dashed line indicates the start of phase II - backwashing.

As shown in Fig. 20 and 21, although backwashing showed a slight effect on overall DOC removal efficiency of SSFs, that only fine column slightly decreased to 99.4% ± 6.2% on day 132 but quickly returned to 100% on day 139 (Fig. 20), it reduced the removal capacity in the top 40 cm of both fine and coarse filters. On day 139, the DOC removal ability per unit surface area was 0.020 g/h/m^2 for fine sand and 0.028 g/h/m^2

for coarse sand, similar to pre-backwashing levels. Moreover, the release of DOC at 55 cm was also more prominent. However, the deeper layers below 65 cm showed consistent removal. Overall, there were distinct effects on vertical distribution of DOC observed in fine ($t = -3.352$, $p < 0.05$) and coarse ($t = -4.900$, $p < 0.01$) columns by backwashing.

Firstly, backwashing led to increased DOC concentrations within both fine and coarse columns. By day 132, DOC penetrated to a depth of 65 cm with concentration of 0.02 ± 0.10 mg/L and 0.24 ± 0.03 mg/L in the fine and coarse column, respectively, but the sand layers below 65 cm depth exhibited complete removal of DOC. Moreover, an additional peak of DOC was observed in all columns at 20-30 cm depth, with a higher peak value existed in the coarse column, indicating that the removal process moved deeper in the filter bed from the top layers. Secondly, the backwashing did not change the position of the DOC peak at 55 cm in both fine and coarse columns, but increased the concentration of released DOC. In fine column, the peak value was 2.33 ± 0.56 mg/L (on day 154), which was 1.95 mg/L higher than before backwashing. In coarse column, the value was 1.85 ± 0.04 mg/L (on day 139), 1.28 mg/L higher than before.

4.10.2 Removal of ammonium

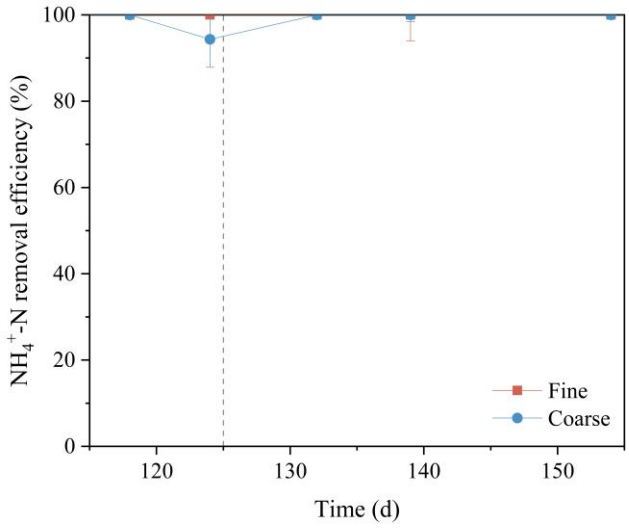

Fig. 22. Temporal changes in NH4+-N removal efficiency in fine and coarse columns during phase II. The dashed line indicates the start of the phase II – backwashing.

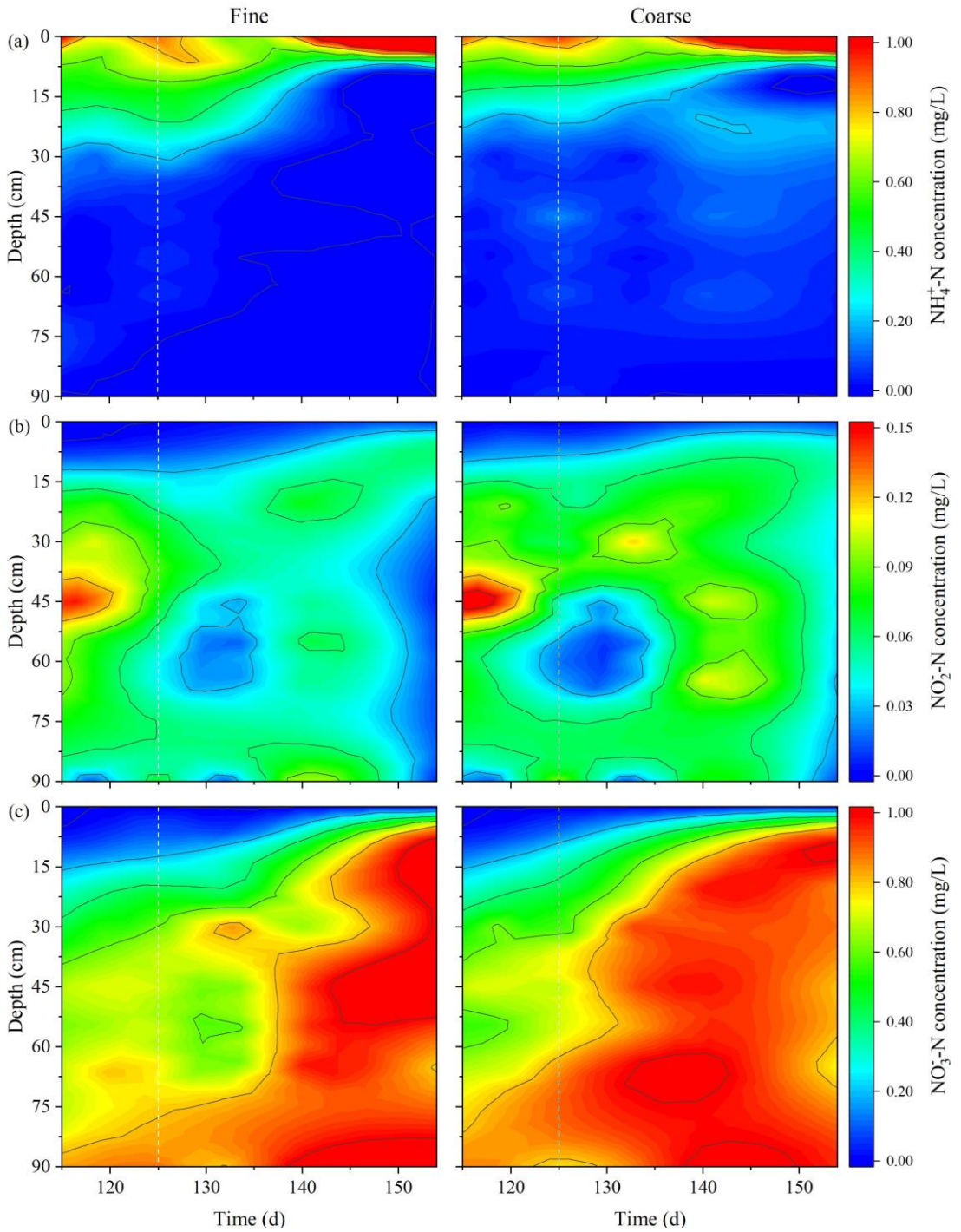

Fig. 23. Depth profiles of NH_4^+-N (a), NO_2^--N (b), and NO_3^--N (c) in fine and coarse columns operating at 0.5 m/h during phase II. The measurements were normalized by removing background concentrations of tap water. The dashed line indicates the start of phase II - backwashing.

As observed in Fig. 22 and 23, similar to the pre-backwashing experiment, the critical surface for the removal and oxidation of ammonium gradually moved upwards. On day 125 before backwashing, 61.9% and 84.8% of NH_4^+ could be removed from the surface 20 cm of the fine and coarse column, respectively. After backwashing, the removal

efficiency by surface 20 cm increased to 100% and 93.0% on day 154, respectively. Additionally, compared to the values on day 125, the NH_4^+-N removal capacity per unit surface area slight increased to 0.026 g/h/m^2 for fine sand and 0.034 g/h/m^2 for coarse sand on day 139, indicating that backwashing in this experiment did not hinder but even promoted the nitrification process in the SSFs. Although backwashing had no impact on the ammonium removal ability of all SSFs that they were able to maintain a 100% removal of the added 1-2 mg/L NH_4^+-N, it showed a significant influence on NH_4^+ vertical distribution within in both fine ($t = 2.986$, $p < 0.05$) and coarse ($t = 4.919$, $p < 0.01$) columns according to *t*-test results (Table A2).

4.10.3 Microbial water quality

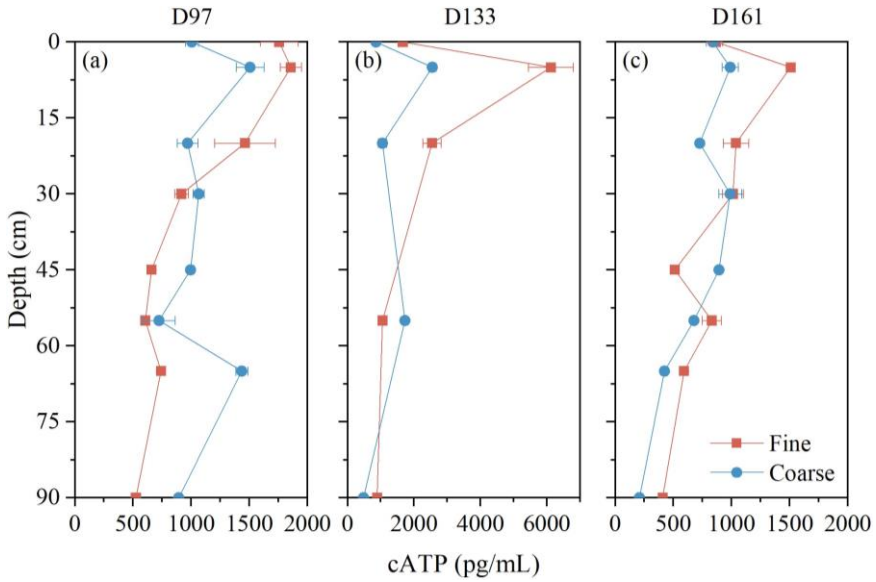

Fig. 24. Depth profile of cATP concentration in water before backwashing (a), 8 days (b), and 36 days (c) after backwashing.

Fig. 24 shows vertical distributions of cATP in the water before and after backwashing. Shortly after backwashing (day 133), there was a significant increase in cATP concentration in the upper 5-20 cm of all columns, particularly at the 5 cm depth. In the fine and coarse columns, concentrations increased from 1857.32 ± 91.26 pg/mL and 1506.85 ± 120.73 pg/mL to 6124.13 ± 676.20 pg/mL and 2550.85 ± 113.99 pg/mL, respectively. However, there were no obvious variations in the cATP concentration below 20 cm in both columns. Overall, backwashing had a minor impact on cATP in all filter columns ($p > 0.05$).

Subsequently, by day 161, the overall cATP concentration in the fine and coarse

columns was lower than before backwashing, especially in the upper 20 cm filter layer, where reductions of 554.50 ± 294.11 pg/mL and 309.18 ± 185.21 pg/mL were observed, respectively. Notably, the peak observed at 65 cm in the coarse column on day 97 was not detected on day 161.

4.10.4 Biomass development on sand

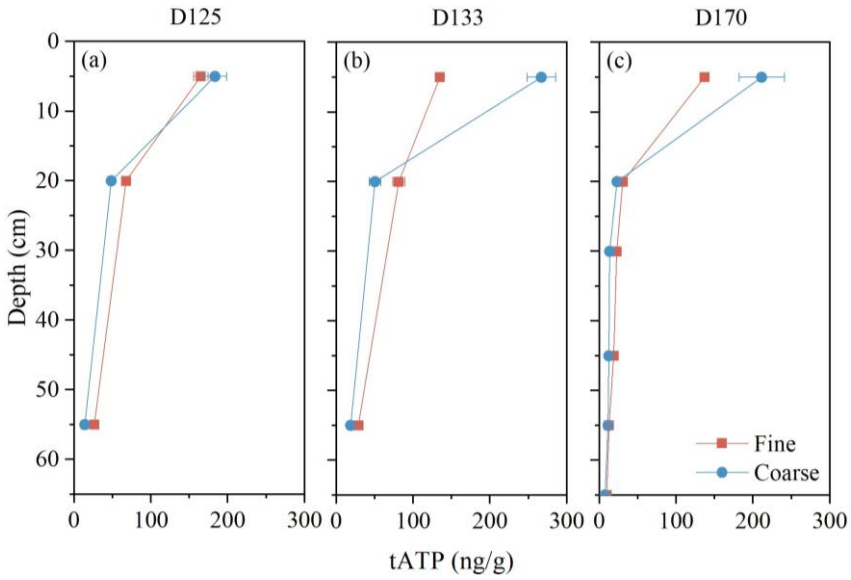

Fig. 25. Depth profile of deposit tATP concentration normalized to the mass of sand before backwashing (a), 8 days (b), and 45 days (c) after backwashing.

According to Fig. 25(a) and (b), on day 133, the tATP concentrations at 20 cm and 55 cm within all filters increased by 2.09-13.55 ng/g and 2.26-4.59 ng/g, respectively. However, a contrasting trend was observed: there was a decrease of 30.00 ng/g at 5 cm in fine column, while an unexpected increase of 83.60 ng/g occurred in coarse column. Additionally, the concentration of tATP attached to sand below 20 cm depth remained nearly unchanged post-backwashing.

Comparing the data on day 170 (after backwashing) (Fig. 25(c)), tATP in the surface 5 cm of the fine column exhibited minimal variation compared to day 125. In the coarse column, although a decrease from 266.87 ± 18.68 ng/g to 211.24 ± 29.60 ng/g was observed in the top 5 cm layer, it remained higher than pre-backwashing levels. Moreover, deeper layers below 20 cm in both fine and coarse columns experienced a reduction of 2.8-37.28 ng/g compared to their pre-backwashing conditions. Considering the *t*-test results, backwashing had minimal impact on the attached tATP concentration attached in all SSFs ($p > 0.05$).

5. Discussion

5.1 Removal processes of DOC and ammonium

5.1.1 DOC

The reduction in DOC began approximately four weeks after the initial start-up (Fig. 6). During the early stages of operation, only small removal in DOC was measured within the filter bed (Fig. A3-A5), consistent with previous founding (Bar-Zeev et al. 2012). At this stage, with only limited bacterial colonization and biofilm development in the filter bed medium (Fig. 12-13), DOC was removed mainly by mechanical exclusion and adsorption in the sand layer. SSFs took about 3 months to establish full biofilm coverage and high bacterial diversity (Bar-Zeev et al. 2012), when DOC showed stable removal efficiencies.

DOC was mainly removed in the first 40 cm, with the highest reduction in the top 5 cm (Fig. 7). The correlation of decreased DO concentration and pH (Fig. A24) imply that the removal of DOC is greatly related to biological processes (Larsen and Harremoës 1994, Zheng et al. 2010). The removal of TOC likely involves a combination of adsorption and respiration of DOC through the activity of microbial extracellular enzymes (Bar-Zeev et al. 2012). Dosed LMW acids and building blocks were significantly reduced, but effluent still contained a substantial amount of LMW compounds (Fig. 8). This indicates that the SSFs had different removal ability on LMW compounds and showed limit removal ability on the original LMW organics in tap water, aligning with previous study (Zheng et al. 2010). However, different from expectation, with the increase of operation time, DOC concentration surged approximately 0.72-0.94 mg/L at 55 cm with continuously increasing peak value (Fig. 7). Chen et al. (2016) reported an increase of approximately 1 mg/L in young biofilters. Perujo et al. (2018) observed an increase ranging from 0.2 to 0.5 mg/L in mono- and bi-layer SSFs. Additionally, Bar-Zeev et al. (2012) noted a DOC increased flux of 0.1-0.4 mg/m^2 in mono- and bi-layer RSFs. However, previous study did not trace the source of the released DOC (Chen et al. 2016, Perujo et al. 2018).

Bar-Zeev et al. (2012) suggested that increased DOC in deeper RSF layers might result from POC degradation or cell lysis, but it is not the case for this experiment, considering the variation of POC (< 50 ug/L) was much lower than DOC increase, and no negative correlation between DOC and POC. Besides, in contrast to mature biofilms, developing

biofilms may have released labile DOC compounds (Bar-Zeev et al. 2012, Luo et al. 2022, Yu et al. 2020). This phenomenon has also been observed in distribution systems, likely due to microbial metabolites released during the growth of heterotrophic bacteria (Li et al. 2022). It may explain the simultaneous rise in DOC peak values as biofilm growth increased with higher loading rate (Fig. 15). Moreover, Table 9 shows the fluxes of DIN and NO_3^- changed to negative at the same depth of the DOC peak (45-55 cm), indicating denitrification. A similar phenomenon of simultaneous DOC increase (ca. 0.5 mg/L) and NO_x^- reduction (ca. 2 mg/L) at the 20 cm within SSFs has been reported (Perujo et al. 2018), suggesting that denitrification in deeper filters may be linked to organic matter released by biofilms, as released DOC by biofilms can be utilized by other microorganisms (Bar-Zeev et al. 2012, Luo et al. 2022). In a batch reactor treating sludge alkaline fermentation liquid, there was an approximately 3 mg/L increase in LMW neutrals corresponding to the onset of denitrification (Cao et al. 2019), indicating that denitrification might produce LMW neutrals from the degradation of HMW substances, such as building blocks and biopolymers. This could explain the increase in DOC at 55 cm depth was mainly composed of LMW compounds (Fig. 8), differing from the released organics often reported contain EPS (classified as biopolymers), soluble microbial products, and other organic matter (Bar-Zeev et al. 2012, Luo et al. 2022). Chen et al. (2016) similarly identified the rise in DOC within the biofilter caused by LMW compounds. However, these explanations remain speculative, and further investigations are needed to pinpoint the exact source of DOC. Furthermore, these theories do not adequately explain why the DOC peak consistently appeared at 55 cm depth, unaffected by influent concentration, grain size, loading rate, and backwashing.

The deeper layer of SSFs reached a DOC consumption flux similar to or even higher than the surface layer (Table 9), even with relative low ATP concentration (Fig. 12-13). This suggests that the degradation of organic material in a mature filter can be higher in the sand bed than on the surface (Chan et al. 2018, Oh et al. 2018). This may be attributed to the DOC produced at 55 cm depth was easily biodegradable organics (Fig. 8). And low ATP concentration may be attributed to predominantly low nucleic acid bacteria containing less ATP pass through the filters (Vital et al. 2012). This phenomenon might lead to potentially underestimating the cell count in deeper layers.

5.1.2 Ammonium

NH_4^+ reduction started about 6 weeks and reached stable complete removal after 3

months (Fig. 10). Most of the NH_4^+ removal occurred in the top layers of the filter (Fig. 11), indicating the critical role played by the Schmutzdecke associated with the upper active layer in ammonium treatment (Zheng et al. 2010). NH_4^+ was used for microbial assimilation above 5 cm, showing a rapid increase in biological activity and no corresponding increase in NO_x^- concentration, while at 5-30 cm approximately 93.0%-93.4% of ammonium was mainly oxidized by nitrifying bacteria (Fig. 9). Others have reported similar stratified nitrification in the RSFs (Lee et al. 2014), granular activated carbon filters (Andersson et al. 2001), and nitrifying trickling filters (van Den Akker et al. 2008). The decrease nitrification with the filter depth may be caused by the low concentrations of ammonium would be available to microbes at lower depths, limiting the growth of nitrifying organisms lower in the filter. Besides, nitrifiers with different metabolic physiologies or different microbial types could be active at different depths, resulting in the stratification of ammonium removal performance (Tatari et al. 2016). Another reason could be nutrient limitations, such as phosphorus, as the majority of any easily available nutrients might be consumed at the top of the filter (Lee et al. 2014). This study ruled out the impact of PO_4^{3-} limitations as its concentration kept above 0.01 mg/L, where nitrification and microbial growth start reducing under this level (De Vet et al. 2012). Additionally, at 45-55 cm, a decrease in NO_3^- and DIN indicated the possibility of aerobic denitrification, in line with previous observations (Gu et al. 2023).

However, the stratification of DOC and NH_4^+ showed different trends that, the maximum reduction rate of NH_4^+ appears at 5-30 cm depth, lower than that of DOC (Fig. 11). Meanwhile, unlike DOC removal (Fig. 7), nitrification first occurred in deeper layers of the filter, and gradually moved upwards and stabilized with operation time. Enrichment of readily biodegradable organic carbon promotes heterotrophic activity, leading to a competitive dynamic between nitrifiers and heterotrophs for oxygen, nutrients and space inside the multispecific biofilms, and ultimately resulting in reduced nitrification rates (De Vet et al. 2012, Michaud et al. 2006). Additionally, previous research found that nitrifiers were covered by heterotrophic bacteria at depths of 100-980 um below the biofilm surface, where DO was limited (van den Akker et al. 2011). Consequently, the presence of more competitive heterotrophic bacteria might bury nitrifiers into a deeper biofilm layer and reduce the nitrification in the environment rich in DOC. Therefore, the higher C/N ratio led to the inhibition of nitrification, aligning with the findings of this study that the depth and timing of the maximum NH_4^+ reduction rate trailed that of DOC (Fig. 7 and 11).

This experiment observed that the concentration of NO_x^- and NH_4^+ exhibited a significant negative correlation (Fig. A24). With the gradually intensified nitrification process, the effluent's NO_3^- concentration in all SSFs started to increase from day 76, following by an increasing NO_2^- occurred on day 83-93 (Fig. 9). As an intermediate product of nitrification, the accumulation of NO_2^- may suggest the relatively higher activity of AOB or AOA compared to NOB (Tatari et al. 2016). However, it is important to be careful about the concentration of nitrite in treated water, which is an undesirable result given the consequences of their ingestion for human health. Several studies have shown that canonical two-step nitrification (ammonia- and nitrite-oxidization) dominates in young filters, but will be outnumbered by comammox after maturation in filters, which are capable of complete ammonia oxidation to NO_3^- (Haukelidsaeter et al. 2023, Tatari et al. 2017), helps to reduce the production of NO_2^-.

5.2 Influence of grain size on slow sand filters

Coarse sand displayed better effectiveness in NH_4^+ removal (Fig. 10), similar to other observations (Liu et al. 2023, Perujo et al. 2017). This phenomenon correlated with lower DO and pH in the upper 30 cm of coarse column compared to fine column after signficant ammonium removal on day 80, indicating that nitrification, as an aerobic acidogenesis process, was stronger in the upper layer of coarse column. However, in contrast to expectations, no significant differences were observed in DOC concentration between fine and coarse treatments (Table A2). Prior research has demonstrated the significant impact of grain size on physical, chemical, and biological parameters. Specifically, fine sand, with its larger specific surface area, exhibits enhanced abilities in adsorption, interception, and straining, leading to more effective bacterial removal (Freitas et al. 2022, Pfannes et al. 2015) and superior phosphorus retention (Nakhla and Farooq 2003). Additionally, smaller particle diameter implies a higher proportion of micropores in the filter medium, which increases the contact of pollutants with adsorption sites on both filter medium and biofilm (Perez-Mercado et al. 2019). While coarse sand, with its higher hydraulic conductivity, facilitates the transfer of nutrients, organic matter, and DO to greater depths. This ability is particularly advantageous for accommodating high nutrient loads, leading to elevated biogeochemical rates (Perujo et al. 2018, Perujo et al. 2017). Moreover, the larger grain size increases water exchange through pores, thereby reducing advection time and accelerating the biogeochemical rates (Perujo et al. 2017).

Fine columns contained a higher cATP concentration in filtrate water at surface 30 cm, but coarse columns showed a more uniform cATP vertical distribution within SSFs (Fig. 12(b)). Except higher straining, previous study suggested that the increased specific surface area encourages a higher microbial oxygen uptake rate, as it provides ample space for biofilm colonization (Higashino 2013). However, the smaller hydraulic conductivity of fine particles limits mass transfer into the deeper sand bed (Nogaro et al. 2010), which theoretically might not be conducive to the optimal functioning of the deep filter material and microbial growth. Moreover, consistent with higher tATP found in the surface of coarse columns (Fig. 13(b)), Perujo et al. (2019) indicated that although both fine and coarse sand exhibited similar biofilm colonization potential resulting in comparable overall biomass densities in the top layer, more live bacteria and higher microbial activity in the coarse system. Pfannes et al. (2015) found that bacterial communities differed more within the vertical layers rather than between different grain sizes.

5.3 Influence of loading rate

Increased loading rate showed no influence on the vertical distributions of DOC and NH_4^+ (Table A2) and even increased their removal load per unit sand surface area in both fine and coarse columns, which could be attributed to the increase in DO transfer (Nakhla and Farooq 2003) and decrease in the external mass transfer resistance resulting from the higher loading rate (Lee et al. 2014, van Den Akker et al. 2008). However, it negatively affected the overall removal efficiencies in DOC and NH_4^+ and nutrients extended to deeper layers within the SSFs (Fig. 14 and 16). As adsorption diminishes with increased flow rate, grain size becomes the most important design parameter for biofilters (Perez-Mercado et al. 2019). Therefore, the slightly greater decrease in nutrient removal ability in coarse columns might be due to their weaker straining and adsorption capacity. Notably, nitrification efficiency displayed a greater decrease, with DOC removal performance showing a lower variation. Indeed, previous studies suggested that ammonium removal is limited by reactions within the biofilm phase and decreased contact times rather than DO concentration and external mass transfer, explaining the reduced ammonium oxidation efficiency at higher loading rates (Lee et al. 2014, Nakhla and Farooq 2003). Additionally, higher DOC caused by higher loading rate inhibits the nitrifying bacteria growth (De Vet et al. 2012, van den Akker et al. 2011), contributing to a more significant impact on NH_4^+ removal compared to DOC (Section 5.1.2).

Following the increased loading rate, ATP concentrations in the upper SSFs layers significantly increased after 8 days (Fig. 18-19), indicating that the higher flow rate did not hinder the biofilm attachment but even promoted its growth. High flow conditions can lead to stronger shear forces, resulting in a denser, cohesive, and more stable biofilm due to better attachment to the EPS matrix (Graba et al. 2013). Furthermore, Perez-Mercado et al. (2019) reported that higher flow rates might make biofilm more active, despite lower flow rates promoting initial biofilm growth through more contact opportunities for organic matter attachment and nutrient provision. Around 14-15 days after the increased loading rate, both fine and coarse columns experienced clogging, in line with previous findings that lower loading rates can slow down the clogging development but might not affect the ultimate clogging extent (Chen et al. 2021). However, it is worth noting that fine column faced clogging issues earlier than the coarse column. This observation corresponded to higher cATP levels detected in the surface layer of fine columns, particularly showing a more significant increase at a depth of 5 cm (Fig. 18), which likely contributed to a faster onset of clogging with less space for biomass growth (Perujo et al. 2019).

5.4 Influence of backwashing

Consistent with previous studies (de Souza et al. 2021b, Liao et al. 2015), backwashing influenced the distribution of the DOC and NH_4^+ within the filters but did not decrease the removal efficiency (Fig. 20-23). In fact, backwashing even accelerated the reduction of NH_4^+. Periodic backwashing did not affect biofilter performance as long as 60%-80% of the biomass was retained (Hozalski et al. 1999). While some studies suggested that biomass concentration was not directly correlated with DOC removal in drinking water biofilters (Boon et al. 2011). Backwashing detached nonbiological particles from the grain surface, renewed the capacity for adsorption (Liao et al. 2015), and reduced biofilm thickness accelerating the diffusion (Simpson 2008), possibly contributing to a positive impact on nutrient removal. As for bioactivity, after backwashing on 8th day, the surface layer of the fine column saw a slight decrease in attached tATP, while the coarse column even showed a slight increase (Fig. 25). However, backwashing alone was not sufficient to significantly remove biomass from the sand surface (de Souza et al. 2021a) and the turbidity in the backwash water was mostly due to the interstitial or non-organic materials (de Souza et al. 2016, Pizzolatti et al. 2015). Additionally, backwashing did not remove the stratification of water quality and biological activity in the filter (Fig. 20-25), aligning with previous findings (Lee et al. 2014). The weak

destratification could be due to the buildup of precipitates over time, leaving the top of the filter with larger, less dense filter material, which remained at the top of the filter after the backwash (Lee et al. 2014) (Fig. A21).

The impact of backwashing was more pronounced on nutrient vertical distributions within the coarse column compared to the fine columns (Table A2), indicating superior cleaning performance of the coarse systems under identical backwashing conditions. Lower backwashing flow rates for fine sand reduced drag tension between water and sand grains after complete fluidization (de Souza et al. 2021a, de Souza et al. 2016, de Souza et al. 2021b). Consequently, larger diameter grains provide more effective cleaning under the same expansion conditions (de Souza et al. 2016). However, it comes at the expense of higher water consumption and less efficient filtering (de Souza et al. 2016).

Microbial activity (Fig. 24-25) and DOC removal efficiency (Fig. 20) returned to pre-backwashing levels after 8 and 14 days after cleaning, respectively, suggesting that the short-term impact of backwashing on SSFs can gradually be restored. Previous studies suggested that performance and attached biomass can almost fully recover within 2 days in SSFs (de Souza et al. 2021b, Liao et al. 2015, Wang et al. 2023) and 2-5 days in granular activated carbon biofilters (Gibert et al. 2013, Hozalski and Bouwer 2001). However, microbial community recovery requires more time for about 15 days (Liao et al. 2015, Wang et al. 2023).

Compared to other cleaning methods like superficial agitation or stirring, backwashing has advantages in ease of operation and minimal biomass loss. Traditional procedures can take several days and disrupt the biological layer, leading to reduced bacterial removal effectiveness (Freitas et al. 2022). Moreover, the duration of post-maintenance recovery can vary depending on the maintenance method, ranging from 8.5 to 23 days by surface agitation or replacement (Singer et al. 2017), which is longer than for backwashing.

5.5 Assessment of optimum design and operation of slow sand filters

When evaluating the suitability of SSFs for drinking water treatment, several key operational criteria must be considered, with the primary objective being the reduction of pollutant concentrations to level that guarantee the hygienically safe and biologically stable drinking water. These operational criteria include factors such as capital and

operating expenses, robustness, and longevity of performance.

Coarse sand within the range of 0.85-1.25 mm appears to be a favorable choice for SSFs in this study. Contrary to expectations, there was no significant difference between fine and coarse columns in the removal of DOC, NH_4^+, and PO_4^{3-} after SSF maturation. This could be attributed to the low dosed pollutant concentrations, making it challenging to discern the maximum treatment load of SSFs. However, the DOC and NH_4^+ concentrations applied in the study were relatively high compared to typical influent levels in Dutch SSFs. This allowed to investigate stratification in removal processes, although it may not fully representative. Coarse columns demonstrated a lower removal efficiency of pollutants when operated at 2 m/h, indicating limited removal capacity at higher flow rates than their fine counterparts. However, the lower risk of clogging in coarse columns translated to an extended operational lifespan. Under identical backwashing conditions, coarse sand exhibited more pronounced cleaning effects, with virtually no impact on pollutant removal efficiency. Although achieving the same fluidization effect as fine sand necessitated a higher backwashing flow rate, potentially resulting in greater wastewater disposal concerns, the infrequent need for cleaning (no clogging observed after 125 days of operation at 0.5 m/h) diminishes the significance of this drawback in the overall assessment.

According to this study, 0.5 m/h was deemed satisfactory that it showed effective DOC and NH_4^+ removal without clogging issues over 125 days, despite this value falling on the higher end of recommended flow rates of 0.1-0.4 m/h for SSFs (Table 1). Notably, the choice of flow rate directly impacts the footprint of SSFs, a substantial component of capital expenditure. In theory, the rate of 0.5 m/h can save ca. 900 m^2 of footprint per Mm^3/year of water production compared to 0.1 m/h. Due to the large gap between the selected loading rates, this study did not pinpoint the precise optimum. While by evaluating the DOC and NH_4^+ removal capacities per unit surface area of sand at 2 m/h, a rough estimation suggests that both fine and coarse columns could attain a 100% overall removal efficiency at a maximum of 1.7 m/h. However, as the loading rate increased, biofilm growth accelerated, resulting in severe clogging within a brief period (2 weeks at 2 m/h) and rendering the treatment performance of SSFs unsustainable. It is worth noting that in full-scale SSFs, influent concentrations of DOC and NH_4^+ are typically very low, around 1.5 mg/L (Hijnen et al. 2007) and < 0.02 mg/L (Ahmad et al. 2020), respectively. Consequently, clogging issues might not be as prominent as observed in this study. Therefore, further research could investigate the impact of

increased flow rates under low influent nutrient loading conditions.

Backwashing proved to be an effective cleaning strategy for lab-scale SSFs, with no significant impact on pollutant removal efficiency. While the implementation of backwashing needs additional construction of water distribution systems compared to scraping methods, it offers notable advantages: simple and fast operation, no need for filter draining, prevention of sand loss, and similar efficiency to regular SSFs. However, because this study did not compare different cleaning strategies and backwashing intensities, it cannot definitively determine the optimal cleaning strategy.

6. Conclusions

1. Coarse sand (0.85-1.25 mm) exhibited similar DOC and NH_4^+ removal efficiency, adaptability to increased loading rate, more effective cleaning by backwashing, and a reduced risk of bioclogging compared to fine sand (0.4-0.6 mm).

2. The increase of loading rate (2 m/h) diminished the effectiveness of DOC and NH_4^+ removal in all SSFs, and led to accelerated microbial proliferation and clogging, thereby diminishing the filter's operational lifespan, and compromising nutrient removal efficiency. The flow rate of 2 m/h resulted in the decrease of DOC and NH_4^+ removal effect in all SSFs.

3. The process of backwashing demonstrated minimal impact on SSFs' efficiency in removing DOC and NH_4^+. The microbial activity and removal efficiency was restored within 7-14 days after backwashing, suggesting that backwashing has the potential to sustain the longevity and performance of SSFs.

4. This study underscores several findings for the optimum design and operation of SSFs: 1) coarse sand (0.85-1.25 mm) is preferred for SSFs, offering better cleaning capabilities and reduced clogging risks; 2) flow rate of 0.5 m/h is favorable for maintaining efficient nutrient removal and longer lifespan, and occupies a relatively small footprint than regular SSFs; 3) backwashing can be an adoptable cleaning strategy to ensuring the continued effectiveness of SSFs.

5. Both fine and coarse SSFs demonstrated their capability to achieve 100% removal of approximately 1.5 mg/L AOC and 1.0 mg/L NH_4^+-N under 0.5 m/h. A stable removal efficiency was achieved after 90-100 days of operation.

6. An unexpected rise in DOC concentration of 0.72-0.94 mg/L occurred at a depth of 55 cm in all SSFs. This increase was potentially linked to the release of microbial metabolites by heterotroph from young, developing filters. The increased DOC was primarily due to higher concentration of LMW compounds, particularly LMW neutrals. This could be attributed to denitrification processes transforming other organic compounds into LMW neutrals. However, release of DOC in the deeper layers of the filters needs further attention.

7. Limitations and suggestions

1. Incomplete mass balance: The study did not include measurements of carbon, nitrogen, and phosphate attached to the sand or biofilm. Furthermore, the absence of data on DON and total nitrogen restricted the ability to calculate closed mass balances. The exclusion of these factors could potentially limit the comprehensiveness of the nutrient removal assessment. Future studies should consider above parameters or apply stable isotope analysis to provide a more complete understanding of the process.

2. Limited microbial community characterization: The research primarily focused on microbial activity and nutrient removal without providing an in-depth characterization of the microbial communities. A deeper exploration of microbial diversity, composition, and their potential impact on the filtration process could offer valuable insights. Including metagenomics could provide a deeper understanding of nutrient transformation pathways and microbial contributions within the filter beds.

3. Inferred mechanisms of DOC peak: The underlying factors contributing to the observed DOC peak at the 55 cm depth in the filter were hypothesized rather than directly measured. Further research, for example applying strong destratification process or raising or lowering the relative position of sand at the current 55 cm, is needed to elucidate the precise mechanisms behind this phenomenon, including its depth-specific occurrence, temporal patterns, and underlying dynamics. Such investigations would facilitate a more accurate interpretation of the observed results and aid in optimizing filter bed design.

4. Limited loading rate range: The study focused on a broad range of flow rates. However, this may have deviated from the practical operational range, potentially impacting the generalizability of findings to real-world scenarios.

5. Short-term recovery assessment: The investigation provided insights into the short-term recovery of SSFs after backwashing. However, due to limitations on the sampling frequency, a comprehensive understanding of the complete recovery process was not attained. Future studies could benefit from a more detailed and extended recovery analysis.

Reference

Adeyemo, F.E., Kamika, I. and Momba, M.N.B. (2015) Comparing the effectiveness of five low-cost home water treatment devices for Cryptosporidium, Giardia and somatic coliphages removal from water sources. Desalination and Water Treatment 56(9), 2351-2367.

Ahmad, A., Heijnen, L., de Waal, L., Battaglia-Brunet, F., Oorthuizen, W., Pieterse, B., Bhattacharya, P. and van der Wal, A. (2020) Mobility and redox transformation of arsenic during treatment of artificially recharged groundwater for drinking water production. Water Research 178, 115826.

Albers, C.N., Ellegaard-Jensen, L., Harder, C.B., Rosendahl, S., Knudsen, B.E., Ekelund, F. and Aamand, J. (2015) Groundwater chemistry determines the prokaryotic community structure of waterworks sand filters. Environmental Science & Technology 49(2), 839-846.

Anderson, W.B., DeLoyde, J.L., Van Dyke, M.I. and Huck, P.M. (2009) Influence of design and operating conditions on the removal of MS2 bacteriophage by pilot-scale multistage slow sand filtration. Journal of Water Supply: Research and Technology-AQUA 58(7), 450-462.

Andersson, A., Laurent, P., Kihn, A., Prévost, M. and Servais, P. (2001) Impact of temperature on nitrification in biological activated carbon (BAC) filters used for drinking water treatment. Water Research 35(12), 2923-2934.

Attinti, R., Wei, J., Kniel, K., Sims, J.T. and Jin, Y. (2010) Virus'(MS2, ϕX174, and Aichi) attachment on sand measured by atomic force microscopy and their transport through sand columns. Environmental Science & Technology 44(7), 2426-2432.

Baghoth, S., Maeng, S., Rodriguez, S.S., Ronteltap, M., Sharma, S., Kennedy, M. and Amy, G. (2008) An urban water cycle perspective of natural organic matter (NOM): NOM in drinking water, wastewater effluent, storm water, and seawater. Water science and technology: Water Supply 8(6), 701-707.

Baig, S.A., Mahmood, Q., Nawab, B., Shafqat, M.N. and Pervez, A. (2011) Improvement of drinking water quality by using plant biomass through household biosand filter – A decentralized approach. Ecological Engineering 37(11), 1842-1848.

Baker, M.A. and Vervier, P. (2004) Hydrological variability, organic matter supply and denitrification in the Garonne River ecosystem. Freshwater Biology 49(2), 181-190.

Baker, M.N. and Taras, M.J. (1948) The quest for pure water: the history of water purification from the earliest records to the twentieth century.

Bar-Zeev, E., Belkin, N., Liberman, B., Berman, T. and Berman-Frank, I. (2012) Rapid sand filtration pretreatment for SWRO: Microbial maturation dynamics and filtration efficiency of organic matter. Desalination 286, 120-130.

Bauer, R., Dizer, H., Graeber, I., Rosenwinkel, K.H. and López-Pila, J.M. (2011) Removal of bacterial fecal indicators, coliphages and enteric adenoviruses from waters with high fecal pollution by slow sand filtration. Water Research 45(2), 439-452.

Boon, N., Pycke, B.F., Marzorati, M. and Hammes, F. (2011) Nutrient gradients in a granular activated carbon biofilter drives bacterial community organization and dynamics. Water Research 45(19), 6355-6361.

Brix, H., Arias, C., A. and del Bubba, M. (2001) Media selection for sustainable phosphorus removal in subsurface flow constructed wetlands. Water Science and Technology 44(11-12), 47-54.

Cao, S., Sun, F., Lu, D. and Zhou, Y. (2019) Characterization of the refractory dissolved organic matters (rDOM) in sludge alkaline fermentation liquid driven denitrification: Effect of HRT on their fate and transformation. Water Research 159, 135-144.

Castro-Castellon, A., Chipps, M.J., Hughes, J. and Hankins, N.P. (2014) 54. Living-Filter: an in-reservoir biofiltration system for phytoplankton reduction at the abstraction point.

Chan, S., Pullerits, K., Riechelmann, J., Persson, K.M., Rådström, P. and Paul, C.J. (2018) Monitoring biofilm function in new and matured full-scale slow sand filters using flow cytometric histogram image comparison (CHIC). Water Research 138, 27-36.

Chen, F., Peldszus, S., Elhadidy, A.M., Legge, R.L., Van Dyke, M.I. and Huck, P.M. (2016) Kinetics of natural organic matter (NOM) removal during drinking water biofiltration using different NOM characterization approaches. Water Research 104, 361-370.

Chen, S., Dougherty, M., Chen, Z., Zuo, X. and He, J. (2021) Managing biofilm growth and clogging to promote sustainability in an intermittent sand filter (ISF). Science of the Total Environment 755, 142477.

Chien, C., Kao, C., Chen, C., Dong, C. and Wu, C. (2008) Application of biofiltration

system on AOC removal: column and field studies. Chemosphere 71(9), 1786-1793.

Chu, C. and Lu, C. (2004) Effects of oxalic acid on the regrowth of heterotrophic bacteria in the distributed drinking water. Chemosphere 57(7), 531-539.

Crittenden, J.C., Trussell, R.R., Hand, D.W., Howe, K.J. and Tchobanoglous, G. (2012) MWH's water treatment: principles and design, John Wiley & Sons.

de Oliveira, F.F. and Schneider, R.P. (2019) Slow sand filtration for biofouling reduction in seawater desalination by reverse osmosis. Water Research 155, 474-486.

de Souza, F., Roecker, P., Silveira, D., Sens, M. and Campos, L. (2021a) Influence of slow sand filter cleaning process type on filter media biomass: backwashing versus scraping. Water Research 189, 116581.

de Souza, F.H., Pizzolatti, B.S., Schöntag, J.M. and Sens, M.L. (2016) Study of slow sand filtration with backwash and the influence of the filter media on the filter recovery and cleaning. Environmental Technology 37(14), 1802-1810.

de Souza, F.H., Pizzolatti, B.S. and Sens, M.L. (2021b) Backwash as a simple operational alternative for small-scale slow sand filters: from conception to the current state of the art. Journal of Water Process Engineering 40, 101864.

De Vet, W., Van Loosdrecht, M. and Rietveld, L. (2012) Phosphorus limitation in nitrifying groundwater filters. Water Research 46(4), 1061-1069.

Dong, L.F., Smith, C.J., Papaspyrou, S., Stott, A., Osborn, A.M. and Nedwell, D.B. (2009) Changes in benthic denitrification, nitrate ammonification, and anammox process rates and nitrate and nitrite reductase gene abundances along an estuarine nutrient gradient (the Colne Estuary, United Kingdom). Applied & Environmental Microbiology 75(10), 3171-3179.

Eisfeld, C., Schijven, J.F., van der Wolf, J.M., Medema, G., Kruisdijk, E. and van Breukelen, B.M. (2022) Removal of bacterial plant pathogens in columns filled with quartz and natural sediments under anoxic and oxygenated conditions. Water research 220, 118724.

Ellis, K.V. and Aydin, M.E. (1995) Penetration of solids and biological activity into slow sand filters. Water Research 29(5), 1333-1341.

Freitas, B., Terin, U.C., Fava, N., Maciel, P., Garcia, L., Medeiros, R.C., Oliveira, M., Fernandez-Ibanez, P., Byrne, J.A. and Sabogal-Paz, L.P. (2022) A critical overview of household slow sand filters for water treatment. Water Research 208, 117870.

Gibert, O., Lefèvre, B., Fernández, M., Bernat, X., Paraira, M., Calderer, M. and Martínez-Lladó, X. (2013) Characterising biofilm development on granular activated carbon used for drinking water production. Water Research 47(3), 1101-1110.

Graba, M., Sauvage, S., Moulin, F.Y., Urrea, G., Sabater, S. and Sanchez-Pérez, J.M. (2013) Interaction between local hydrodynamics and algal community in epilithic biofilm. Water Research 47(7), 2153-2163.

Grace, M.A., Clifford, E. and Healy, M.G. (2016a) Performance of novel media in stratified filters to remove organic carbon from lake water. Water Research 104, 371-380.

Grace, M.A., Healy, M.G. and Clifford, E. (2016b) Performance and surface clogging in intermittently loaded and slow sand filters containing novel media. Journal of Environmental Management 180, 102-110.

Gu, Q., Ma, J., Zhang, J., Guo, W., Wu, H., Sun, M., Wang, J., Wei, X., Zhang, Y. and Chen, M. (2023) Nitrogen-metabolising microorganism analysis in rapid sand filters from drinking water treatment plant. Environmental Science and Pollution Research 30(11), 29458-29475.

Guchi, E. (2015) Review on slow sand filtration in removing microbial contamination and particles from drinking water. American Journal of Food and Nutrition 3(2), 47-55.

Haukelidsaeter, S., Boersma, A.S., Kirwan, L., Corbetta, A., Gorres, I.D., Lenstra, W.K., Schoonenberg, F.K., Borger, K., Vos, L. and van der Wielen, P.W. (2023) Influence of filter age on Fe, Mn and NH_4^+ removal in dual media rapid sand filters used for drinking water production. Water Research, 120184.

Hendricks, D.W., Barrett, J.M., Bryck, J., Collins, M., Janonis, B. and Logsdon, G. (1991) Manual of design for slow sand filtration. Denver: American Water Works Association Research Foundation.

Higashino, M. (2013) Quantifying a significance of sediment particle size to hyporheic sedimentary oxygen demand with a permeable stream bed. Environmental Fluid Mechanics 13(3), 227-241.

Hijnen, W.A., Dullemont, Y.J., Schijven, J.F., Hanzens-Brouwer, A.J., Rosielle, M. and Medema, G. (2007) Removal and fate of Cryptosporidium parvum, Clostridium perfringens and small-sized centric diatoms (Stephanodiscus hantzschii) in slow sand filters. Water Research 41(10), 2151-2162.

Hijnen, W.A., Schijven, J., Bonne, P., Visser, A. and Medema, G.J. (2004) Elimination of viruses, bacteria and protozoan oocysts by slow sand filtration. Water Science and Technology 50(1), 147-154.

Hozalski, R.M. and Bouwer, E.J. (2001) Non-steady state simulation of BOM removal in drinking water biofilters: applications and full-scale validation. Water Research 35(1), 211-223.

Hozalski, R.M., Bouwer, E.J. and Goel, S. (1999) Removal of natural organic matter (NOM) from drinking water supplies by ozone-biofiltration. Water Science and Technology 40(9), 157-163.

Huang, X., Liu, C., Wang, Z., Gao, C., Zhu, G. and Liu, L. (2013) The effects of different substrates on ammonium removal in constructed wetlands: A comparison of their physicochemical characteristics and ammonium-oxidizing prokaryotic communities. Clean: Soil, Air, Water 41(3), 283-290.

Huber, S.A., Balz, A., Abert, M. and Pronk, W. (2011) Characterisation of aquatic humic and non-humic matter with size-exclusion chromatography–organic carbon detection–organic nitrogen detection (LC-OCD-OND). Water Research 45(2), 879-885.

Huisman, L. and Wood, W.E. (1974) Slow sand filtration, World Health Organization.

Hussain, G., Haydar, S., Bari, A.J., Anis, M., Asif, Z. and Aziz, J.A. (2015) Evaluation of plastic household biosand filter (BSF) in combination with solar disinfection (SODIS) for water treatment. Journal of the Chemical Society of Pakistan 37(2).

Jacquin, C., Lesage, G., Traber, J., Pronk, W. and Heran, M. (2017) Three-dimensional excitation and emission matrix fluorescence (3DEEM) for quick and pseudo-quantitative determination of protein-and humic-like substances in full-scale membrane bioreactor (MBR). Water Research 118, 82-92.

Jenkins, M.W., Tiwari, S.K. and Darby, J. (2011) Bacterial, viral and turbidity removal by intermittent slow sand filtration for household use in developing countries: Experimental investigation and modeling. Water Research 45(18), 6227-6239.

Larsen, T.A. and Harremoës, P. (1994) Degradation mechanisms of colloidal organic matter in biofilm reactors. Water Research 28(6), 1443-1452.

Lautenschlager, K., Hwang, C., Ling, F., Liu, W.T., Boon, N., Köster, O., Egli, T. and Hammes, F. (2014) Abundance and composition of indigenous bacterial communities in a multi-step biofiltration-based drinking water treatment plant. Water Research 62, 40-52.

Lee, C.O., Boe-Hansen, R., Musovic, S., Smets, B., Albrechtsen, H.J. and Binning, P. (2014) Effects of dynamic operating conditions on nitrification in biological rapid sand filters for drinking water treatment. Water Research 64, 226-236.

Li, N., Li, X. and Fan, X.Y. (2022) Biofilm development under different pipe materials and water quality conditions in raw water transportation system: Bacterial communities and nitrogen transformation. Journal of Cleaner Production 343, 130952.

Liao, X., Chen, C., Zhang, J., Dai, Y., Zhang, X. and Xie, S. (2015) Operational performance, biomass and microbial community structure: impacts of backwashing on drinking water biofilter. Environmental Science and Pollution Research 22, 546-554.

Liu, H.-L., Li, X. and Li, N. (2023) Application of bio-slow sand filters for drinking water production: Linking purification performance to bacterial community and metabolic functions. Journal of Water Process Engineering 53, 103622.

Lopato, L., Röttgers, N., Binning, P.J. and Arvin, E. (2013) Heterogeneous nitrification in a full-scale rapid sand filter treating groundwater. Journal of Environmental Engineering 139(3), 375-384.

Luo, Y., Liu, C., Li, C., Shan, Y. and Mehmood, T. (2022) Transformation mechanism and fate of dissolved organic nitrogen (DON) in a full-scale drinking water treatment. Journal of Environmental Sciences 121, 122-135.

Lytle, D.A., White, C., Williams, D., Koch, L. and Nauman, E. (2013) Innovative biological water treatment for the removal of elevated ammonia. Journal-American Water Works Association 105(9), 524-539.

Mahlangu, T.O., Mamba, B.B. and Momba, M.N. (2012) A comparative assessment of chemical contaminant removal by three household water treatment filters. Water SA 38(1), 39-48.

Maiyo, J.K., Dasika, S. and Jafvert, C.T. (2023) Slow sand filters for the 21st century: A review. International Journal of Environmental Research and Public Health 20(2), 1019.

Michaud, L., Blancheton, J.P., Bruni, V. and Piedrahita, R. (2006) Effect of particulate organic carbon on heterotrophic bacterial populations and nitrification efficiency in biological filters. Aquacultural Engineering 34(3), 224-233.

Mueller, M., Pander, J., Wild, R., Lueders, T. and Geist, J. (2013) The effects of stream substratum texture on interstitial conditions and bacterial biofilms: Methodological

strategies. Limnologica 43(2), 106-113.

Nakhla, G. and Farooq, S. (2003) Simultaneous nitrification-denitrification in slow sand filters. Journal of Hazardous Materials 96(2-3), 291-303.

Nogaro, G., Datry, T., MERMILLOD-BLONDIN, F., Descloux, S. and Montuelle, B. (2010) Influence of streambed sediment clogging on microbial processes in the hyporheic zone. Freshwater Biology 55(6), 1288-1302.

Oh, S., Hammes, F. and Liu, W.T. (2018) Metagenomic characterization of biofilter microbial communities in a full-scale drinking water treatment plant. Water Research 128, 278-285.

Oudega, T.J., Lindner, G., Derx, J., Farnleitner, A.H., Sommer, R., Blaschke, A.P. and Stevenson, M.E. (2021) Upscaling transport of bacillus subtilis endospores and coliphage phiX174 in heterogeneous porous media from the column to the field scale. Environmental Science & Technology 55(16), 11060-11069.

Perez-Mercado, L.F., Lalander, C., Joel, A., Ottoson, J., Dalahmeh, S. and Vinnerås, B. (2019) Biochar filters as an on-farm treatment to reduce pathogens when irrigating with wastewater-polluted sources. Journal of Environmental Management 248, 109295.

Perujo, N., Romaní, A. and Sánchez-Vila, X. (2018) Bilayer infiltration system combines benefits from both coarse and fine sands promoting nutrient accumulation in sediments and increasing removal rates. Environmental Science & Technology 52, 5734-5743.

Perujo, N., Romani, A.M. and Sanchez-Vila, X. (2019) A bilayer coarse-fine infiltration system minimizes bioclogging: The relevance of depth-dynamics. Science of the Total Environment 669(15), 559-569.

Perujo, N., Sánchez-Vila, X., Proia, L. and Romaní, A.M. (2017) Interaction between physical heterogeneity and microbial processes in subsurface sediments: a laboratory-scale column experiment. Environmental Science & Technology 51(11), 6110-6119.

Pfannes, K.R., Langenbach, K.M., Pilloni, G., Stührmann, T., Euringer, K., Lueders, T., Neu, T.R., Müller, J.A., Kästner, M. and Meckenstock, R.U. (2015) Selective elimination of bacterial faecal indicators in the Schmutzdecke of slow sand filtration columns. Applied Microbiology and Biotechnology 99(23), 10323-10332.

Pizzolatti, B.S., Soares, M., Romero, L. and Luiz Sens, M. (2015) Comparison of backwashing with conventional cleaning methods in slow sand filters for small-

scale communities. Desalination and Water Treatment 54(1), 1-7.

Ranjan, P. and Prem, M. (2018) Schmutzdecke - A Filtration Layer of Slow Sand Filter. International Journal of Current Microbiology and Applied Sciences 7(7), 637-645.

Simpson, D.R. (2008) Biofilm processes in biologically active carbon water purification. Water Research 42(12), 2839-2848.

Singer, S., Skinner, B. and Cantwell, R.E. (2017) Impact of surface maintenance on BioSand filter performance and flow. Journal of Water and Health 15(2), 262-272.

Soliman, M.Y., Medema, G., Bonilla, B.E., Brouns, S.J. and van Halem, D. (2020) Inactivation of RNA and DNA viruses in water by copper and silver ions and their synergistic effect. Water Research X 9, 100077.

Tatari, K., Musovic, S., Gülay, A., Dechesne, A., Albrechtsen, H.J. and Smets, B.F. (2017) Density and distribution of nitrifying guilds in rapid sand filters for drinking water production: Dominance of Nitrospira spp. Water Research 127, 239-248.

Tatari, K., Smets, B.F. and Albrechtsen, H.J. (2013) A novel bench-scale column assay to investigate site-specific nitrification biokinetics in biological rapid sand filters. Water Research 47(16), 6380-6387.

Tatari, K., Smets, B.F. and Albrechtsen, H.J. (2016) Depth investigation of rapid sand filters for drinking water production reveals strong stratification in nitrification biokinetic behavior. Water Research 101, 402-410.

Terin, U.C. and Sabogal-Paz, L. (2019) Microcystis aeruginosa and microcystin-LR removal by household slow sand filters operating in continuous and intermittent flows. Water Research 150, 29-39.

Trikannad, S.A., van Halem, D., Foppen, J.W. and van der Hoek, J.P. (2023) The contribution of deeper layers in slow sand filters to pathogens removal. Water Research 237, 119994.

USEPA (2001) Cryptosporidium: human health criteria document, USEPA, Washington, DC.

van den Akker, B., Holmes, M., Cromar, N. and Fallowfield, H. (2008) Application of high rate nitrifying trickling filters for potable water treatment. Water Research 42(17), 4514-4524.

van den Akker, B., Holmes, M., Pearce, P., Cromar, N.J. and Fallowfield, H.J. (2011) Structure of nitrifying biofilms in a high-rate trickling filter designed for potable

water pre-treatment. Water Research 45(11), 3489-3498.

van der Aa, L.T.J., Kors, L.J., Wind, A.P.M., Hofman, J.A.M.H. and Rietveld, L.C. (2002) Nitrification in rapid sand filter: phosphate limitation at low temperatures. Water science and technology: Water Supply 2(1), 37-46.

Verma, S., Daverey, A. and Sharma, A. (2017) Slow sand filtration for water and wastewater treatment-a review. Environmental Technology Reviews 6(1), 47-58.

Visscher, J.T., Paramasivam, R., Raman, A. and Heijnen, H. (1987) Slow sand filtration for community water supply: planning, design, construction, operation and maintenance, Village Earth.

Vital, M., Dignum, M., Magic-Knezev, A., Ross, P., Rietveld, L. and Hammes, F. (2012) Flow cytometry and adenosine tri-phosphate analysis: alternative possibilities to evaluate major bacteriological changes in drinking water treatment and distribution systems. Water Research 46(15), 4665-4676.

Wang, D., Zhou, J., Lin, H., Chen, J., Qi, J., Bai, Y. and Qu, J. (2023) Impacts of backwashing on micropollutant removal and associated microbial assembly processes in sand filters. Frontiers of Environmental Science & Engineering 17(3), 34.

Wang, H., Narihiro, T., Straub, A.P., Pugh, C.R., Tamaki, H., Moor, J.F., Bradley, I.M., Kamagata, Y., Liu, W.T. and Nguyen, T.H. (2014) MS2 bacteriophage reduction and microbial communities in biosand filters. Environmental Science & Technology 48(12), 6702-6709.

Weber-Shirk, M.L. and Dick, R.I. (1997) Physical-chemical mechanisms in slow sand filters. American Water Works Association. Journal 89(1), 87.

WHO. (2004) Guidelines for drinking-water quality, World Health Organization.

Wielen, P.W.v.d., Senden, W.J. and Medema, G. (2008) Removal of bacteriophages MS2 and ΦX174 during transport in a sandy anoxic aquifer. Environmental Science & Technology 42(12), 4589-4594.

Wilczak, A., Jacangelo, J.G., Marcinko, J.P., Odell, L.H. and Kirmeyer, G.J. (1996) Occurrence of nitrification in chloraminated distribution systems. Journal-American Water Works Association 88(7), 74-85.

Wu, H.M., Zhang, J., Ngo, H.H., Guo, W.S., Hu, Z., Liang, S., Fan, J.L. and Liu, H. (2015) A review on the sustainability of constructed wetlands for wastewater treatment: Design and operation. Bioresource Technology 175, 594-601.

Yan, Z., Liu, C., Liu, Y. and Bailey, V.L. (2017) Multiscale investigation on biofilm distribution and its impact on macroscopic biogeochemical reaction rates. Water Resources Research 53(11), 8698-8714.

Young-Rojanschi, C. and Madramootoo, C. (2014) Intermittent versus continuous operation of biosand filters. Water Research 49, 1-10.

Yu, X., Lin, T., Xu, H., Tao, H. and Chen, W. (2020) Ultrafiltration of up-flow biological activated carbon effluent: Extracellular polymer biofouling mechanism and mitigation using pre-ozonation with H_2O_2 backwashing. Water Research 186, 116391.

Zheng, X., Ernst, M. and Jekel, M. (2010) Pilot-scale investigation on the removal of organic foulants in secondary effluent by slow sand filtration prior to ultrafiltration. Water Research 44(10), 3203-3213.

Zhou, J., Wang, D., Ju, F., Hu, W., Liang, J., Bai, Y., Liu, H. and Qu, J. (2022) Profiling microbial removal of micropollutants in sand filters: biotransformation pathways and associated bacteria. Journal of Hazardous Materials 423, 127167.

Appendix

A1. Tracer test

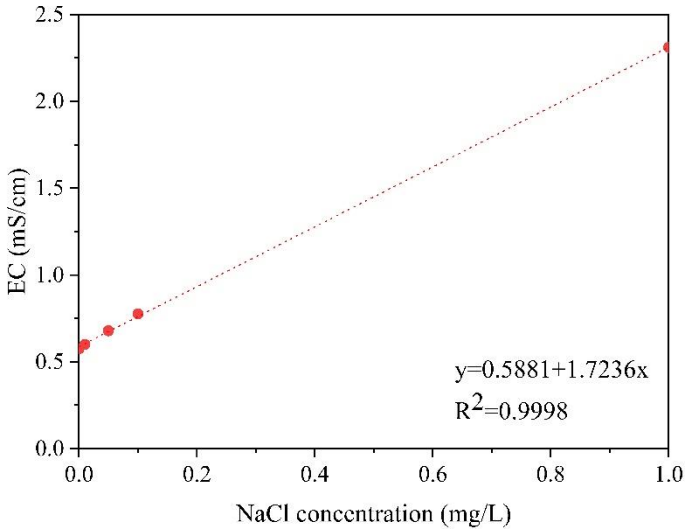

Fig. A1. Calibration curve of NaCl concentration and electric conductivity in tap water at 15 ℃.

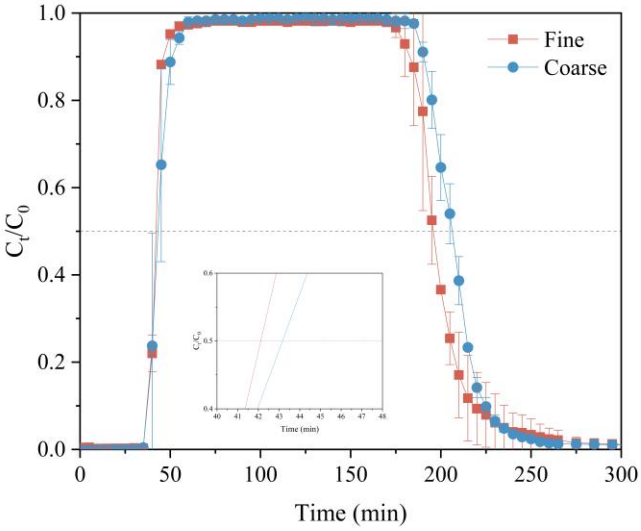

Fig. A2. Tracer test results in SSFs.

A2. Results of Phase I – Unstable stage

A2.1 Removal of DOC, ammonium, and phosphorus

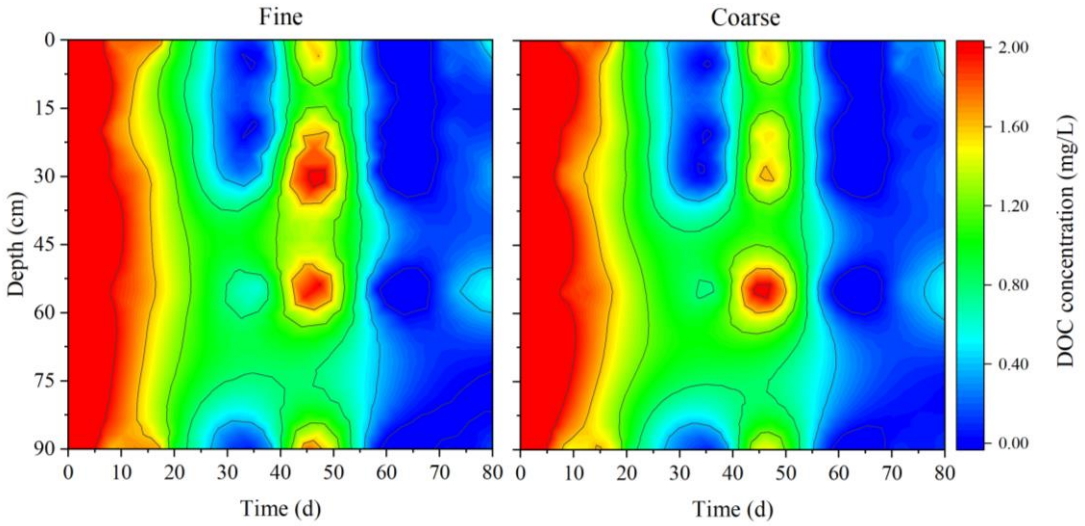

Fig. A3. Depth profiles of DOC in fine and coarse columns operating at 0.5 m/h during immature stage in phase I. The DOC measurements were normalized by removing background concentrations of tap water.

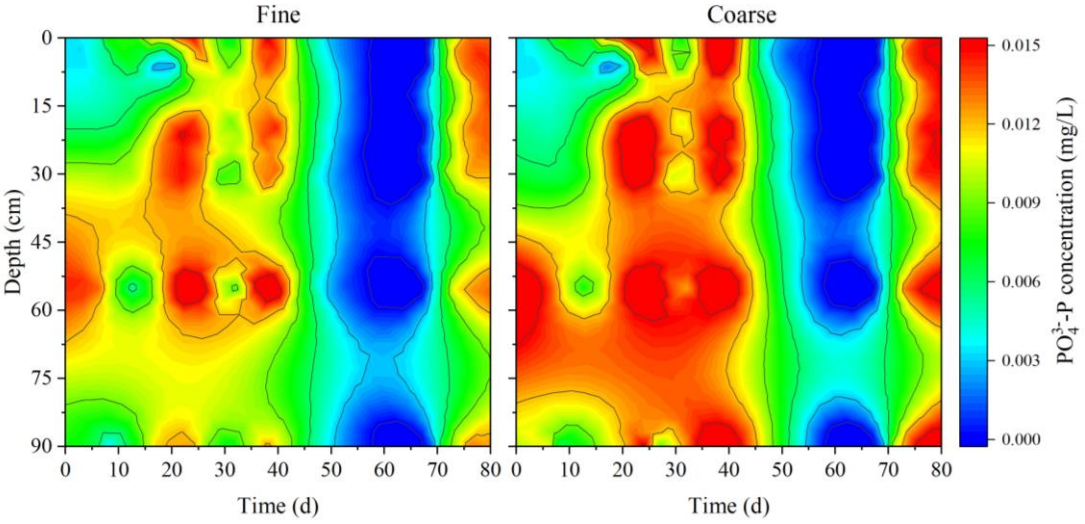

Fig. A4. Depth profiles of PO_4^{3-}-P in fine and coarse columns operating at 0.5 m/h during immature stage in phase I. The DOC measurements were normalized by removing background concentrations of tap water.

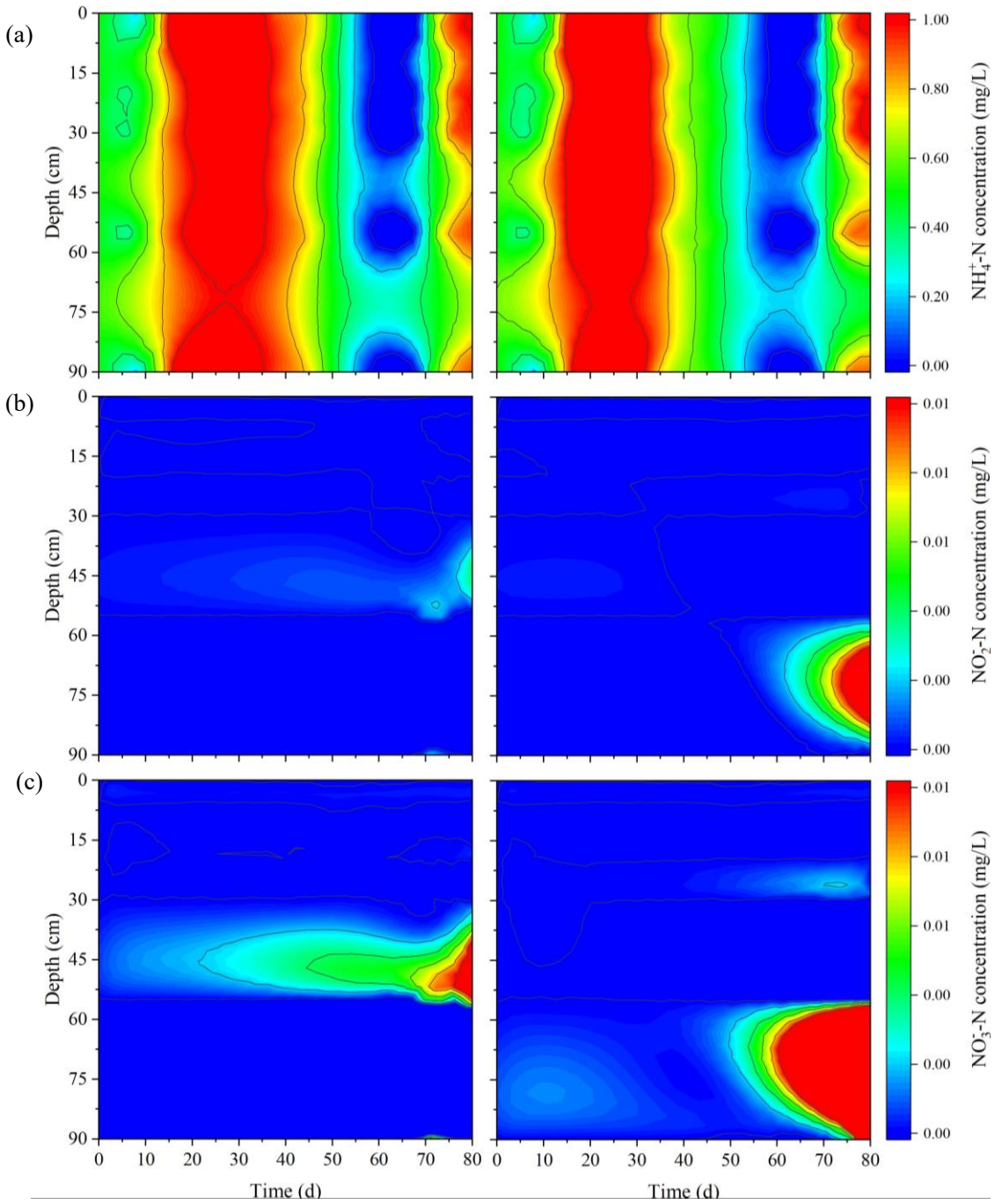

Fig. A5. Depth profiles of NH_4^+-N (a), NO_2^--N (b), and NO_3^--N (c) in fine and coarse columns operating at 0.5 m/h during immature stage in phase I. The DOC measurements were normalized by removing background concentrations of tap water.

A2.2 Breakthrough curves of *E.coli* WR1

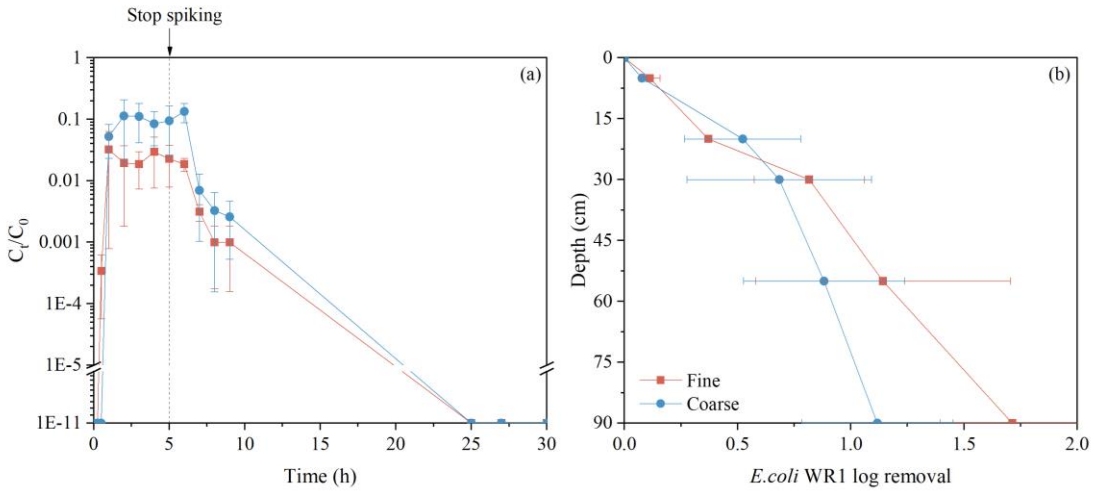

Fig. A6. Breakthrough curve (a) and log removal over the height (b) of *E.coli* WR1 in SSFs.

Spiking experiments were performed during day 34-64 to evaluate bacteria removal capacity. BTCs and depth profile of *E.coli* WR1 in fine and coarse columns are shown in Fig. A6. The BTCs are characterized by a climbing limb, a plateau phase, a decline limb, and finally a gradual declining tail. In the fine columns, a maximum relative concentration (C_t/C_0) of 0.02 ± 0.005 was reached after 1 h operation, indicating a log reduction value (LRV) of 1.64 ± 0.38. A lower C_t/C_0 of 9.97×10^{-4} and *E.coli* concentration of 195-450 cfu/mL was measured in effluent 4 h after stopping the spike, indicating the detachment of attached cells. Upon 20 h after spiking, C_t/C_0 dropped to 0 with the effluent concentration remained below 1 cfu/mL. Similarly, in coarse columns, the maximum relative concentration was 0.10 ± 0.01 with a relatively lower LRV of 1.05 ± 0.26 compared with that of fine columns. Comparing different grain sizes, C_t/C_0 value show significant difference ($p < 0.05$) according to *t*-test, indicating grain size can affect the removal of *E.coli*, and smaller grain size shows better bacterial removal efficiency.

Log_{10} removal of *E.coli* along the height of the filters is shown in Fig. A6(b). The fine and coarse columns depicted an overall LRV of 1.71 ± 0.32 and 1.12 ± 0.33, respectively. In the fine column, maximum removal of 0.82 log_{10} was obtained between 0-30 cm with an average removal efficiency of 0.027 log_{10} per cm. While the deeper layers of 30- 90 cm depth contributed to removal of 0.89 log_{10} and the average LRV per unit depth was 0.015. Similarly, for coarse column, the relatively higher removal rate of 0.026 log_{10}/cm was achieved by the surface 20 cm with the overall LRV of 0.52, then

dropped to 0.008 $\log_{10}$/cm below 20 cm depth.

A2.3 Breakthrough curves of PhiX 174

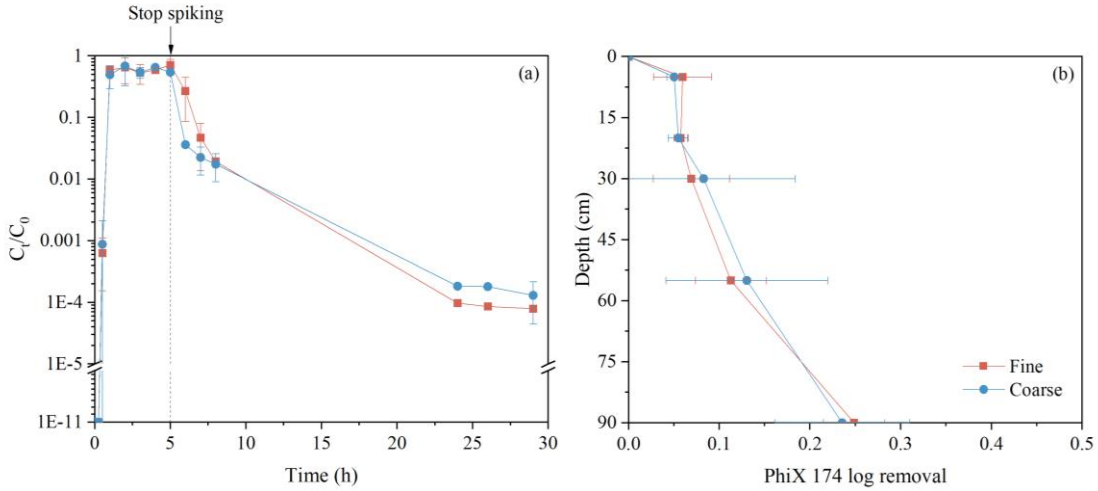

Fig. A7. Breakthrough curve (a) and log removal over the height (b) of PhiX 174 in SSFs.

Spiking experiments were performed on day 36-56 to evaluate virus removal efficiency. Shown as Fig. A7(a), the BTCs of PhiX 174 showed a similar trend with *E.coli* that, comprises a steep ascending limb, a plateau, a declining limb, and a gradually decreased tail. According to *t*-test, the fine and coarse columns exhibited similar performance on PhiX removal ($p > 0.05$) that, a C_t/C_0 ratios were stabilized after 1 h at approximately 0.62 ± 0.08 and 0.61 ± 0.08, respectively, with comparable LRV of 0.26 ± 0.04 and 0.26 ± 0.11. Upon cessation of the spiking, the PhiX concentration in the effluent of both fine and coarse columns promptly declined but still remained above 2.70×10^4 pfu/mL and 2.05×10^4 pfu/mL, respectively. Throughout the observed timeframe, the C_t/C_0 value did not drop to 0, instead stabilizing at levels of 97 pfu/mL and 409 pfu/mL for fine and coarse columns, respectively. This continues release from SSFs following the disappearance of phages in the influent has also been observed in PhiX and MS2 experiments (Anderson et al. 2009, Trikannad et al. 2023). The PhiX concentration of the effluent from the fine column was higher after the spiking was stopped, while was exceeded by that of coarse column at 13 h, implying a faster substantial detachment of attached PhiX in fine columns as compared to coarse columns.

In Fig. A7(b), the PhiX log removal profiles over the height in both fine and coarse sand were comparable with an overall LRV of 0.25 and 0.24, respectively. The surface 5 cm layer displayed the removal efficiency by achieving a reduction of 0.06 $\log_{10}$ and 0.05 $\log_{10}$ for the fine and coarse column, respectively, and the entire filter bed demonstrated

the ability to remove PhiX. A linear removal trend was observed below 20 cm along the fine and coarse filters with the slopes of 0.0027 $\log_{10}$/cm (r^2 = 0.929) and 0.0025 $\log_{10}$/cm (r^2 = 0.986), respectively.

A2.4 Discussion of microorganisms spiking test

Moreover, previous research reported that mature SSFs could achieve the reduction of 3.71 $\log_{10}$ for *E.coli* and 2.25 $\log_{10}$ for MS2 (Young-Rojanschi and Madramootoo 2014). Considering the higher adhesion of PhiX 174 on sand compared to MS2 (Attinti et al. 2010, Wielen et al. 2008), SSF should be able to achieve a higher removal of PhiX than MS2. However, on day 34-64, the filters only achieved the overall LRV of *E.coli* and PhiX at 1.12-1.71 and 0.26, respectively, which was much lower than that of ripened filters (Fig. A6-A7). Studies have shown that household SSF efficiency typically improves after the immature stage, leading to an average bacterial reduction of ≤ 1 $\log_{10}$ before ripening (Freitas et al. 2022, Terin and Sabogal-Paz 2019). The LRV of *E.coli* and PhiX with unit depth above 5 cm layer in this experiment was only 0.02 and 0.01, respectively (Fig. A6-A7), which were far lower than the removal performance of 0.08 and 0.06 of clean sand in a recent study (Trikannad et al. 2023). Although this may be due to the larger grain applied in this experiment, it indicated that the filters during microorganisms spiking test did not show the removal effect of biofilm and active organisms on pathogen, mainly relying on the effect of sand. Therefore, the inefficient Schmutzdecke did not achieve the target removal ability (0.33 -$\log_{10}$/cm for *E.coli* and 0.12 -$\log_{10}$/cm for PhiX)(Trikannad et al. 2023). Furthermore, a linear decline in PhiX was evident below a depth of 20 cm (Fig. A7(b)), aligning with the linear MS2 removal within unripened biosand filter but an exponential removal in mature filters found in previous research (Wang et al. 2014). These findings suggest that rather than being dominated by Schmutzdecke's function, the deeper sand layer likely plays a more important role in the overall pathogen removal during the ripening phase, as the volume of deeper sand is much greater than the Schmutzdecke occupied space. After the development of biofilm, water quality improvements tend to ascend towards the Schmutzdecke and upper sand layer, consistent with previous studies on mature filters (Bauer et al. 2011, de Oliveira and Schneider 2019, Pfannes et al. 2015).

A3. Results of Phase I – Stable stage

A3.1 Water temperature

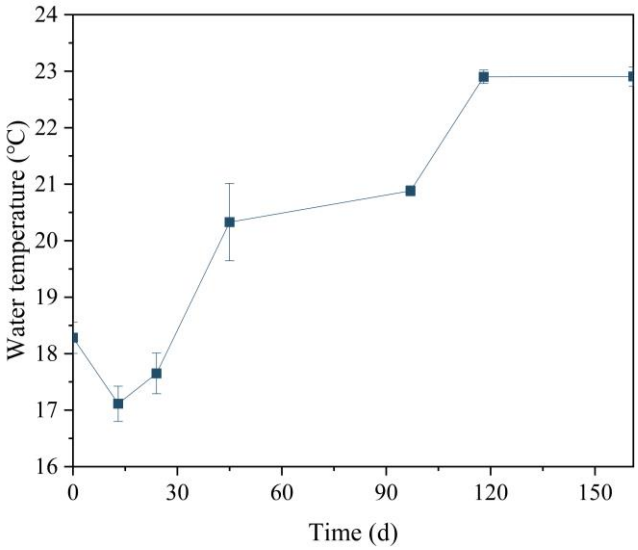

Fig. A8. Temporal changes in water temperature during experiment.

A3.2 Removal of DOC

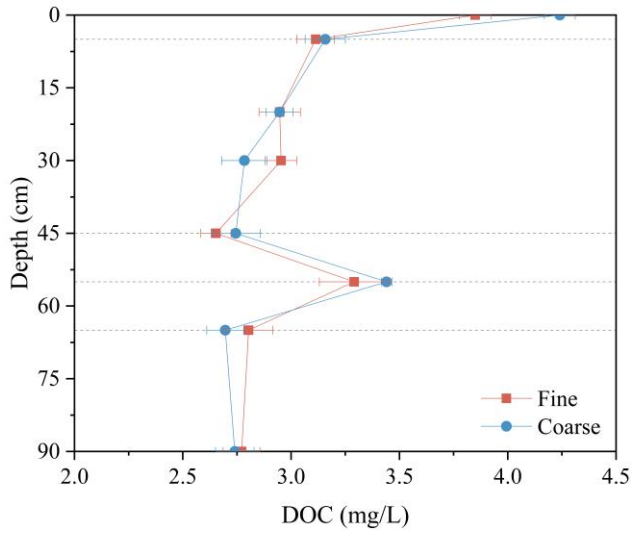

Fig. A9. Depth profile of DOC concentration within the SSFs on day 106.

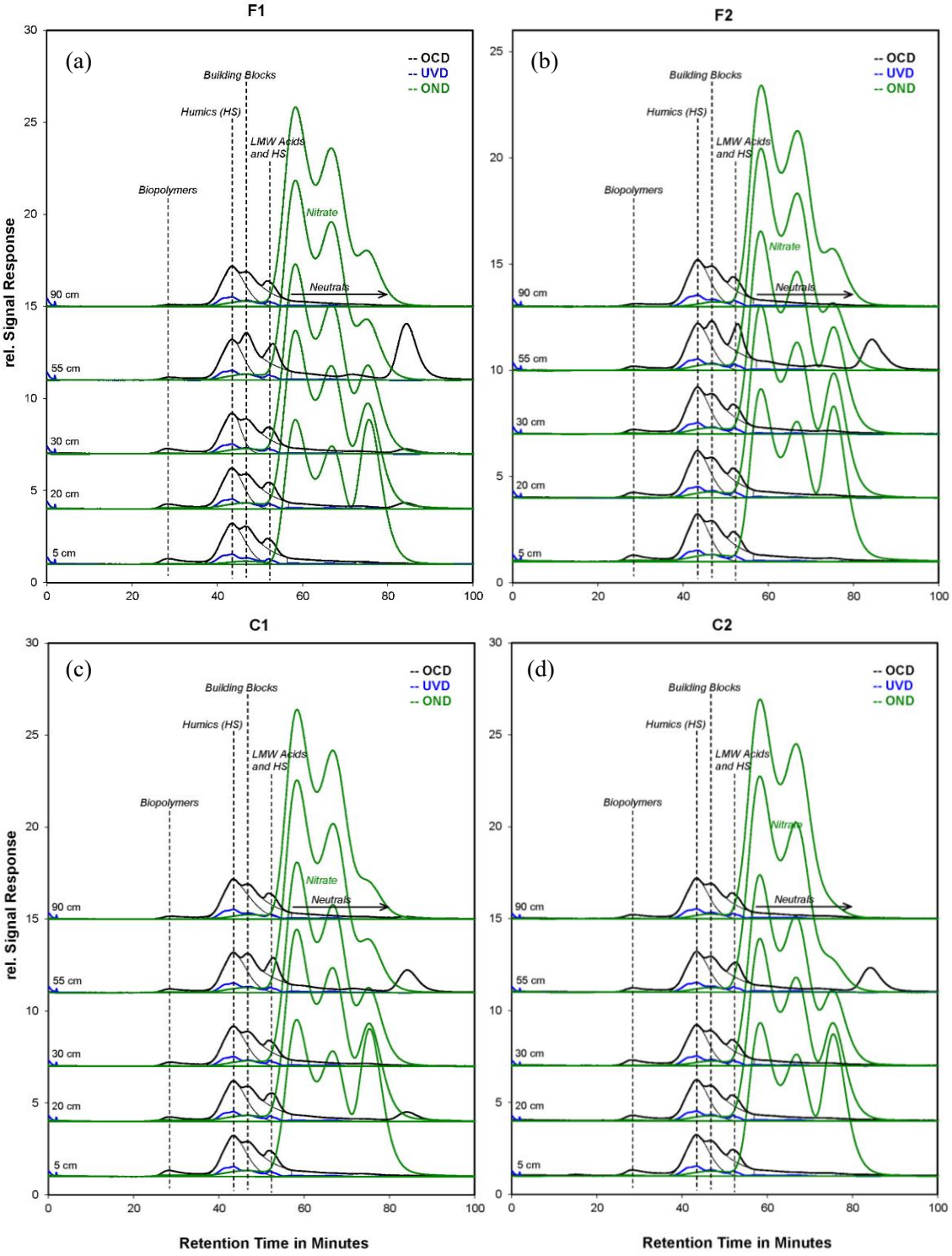

Fig. A10. Chromatograms of water samples within filter columns F1 (a), F2 (b), C1(c), and C2 (d) responses for organic carbon detection (OCD), UV-detection at 254 nm (UVD), and organic nitrogen detection (OND). Ammonium appears as a single peak eluting at 70 min and nitrate appears as a "double peak" due to competitive ionic interactions between nitrate, the mobile phase and the chromatographic column.

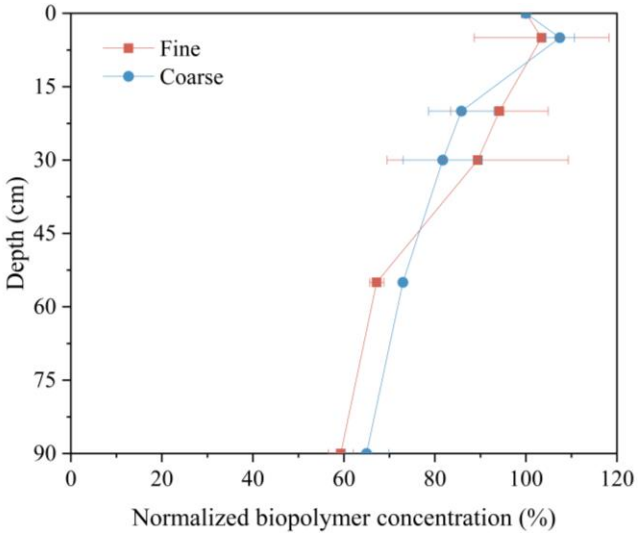

Fig. A11. Biopolymer removal profile in fine and coarse columns on day 106.

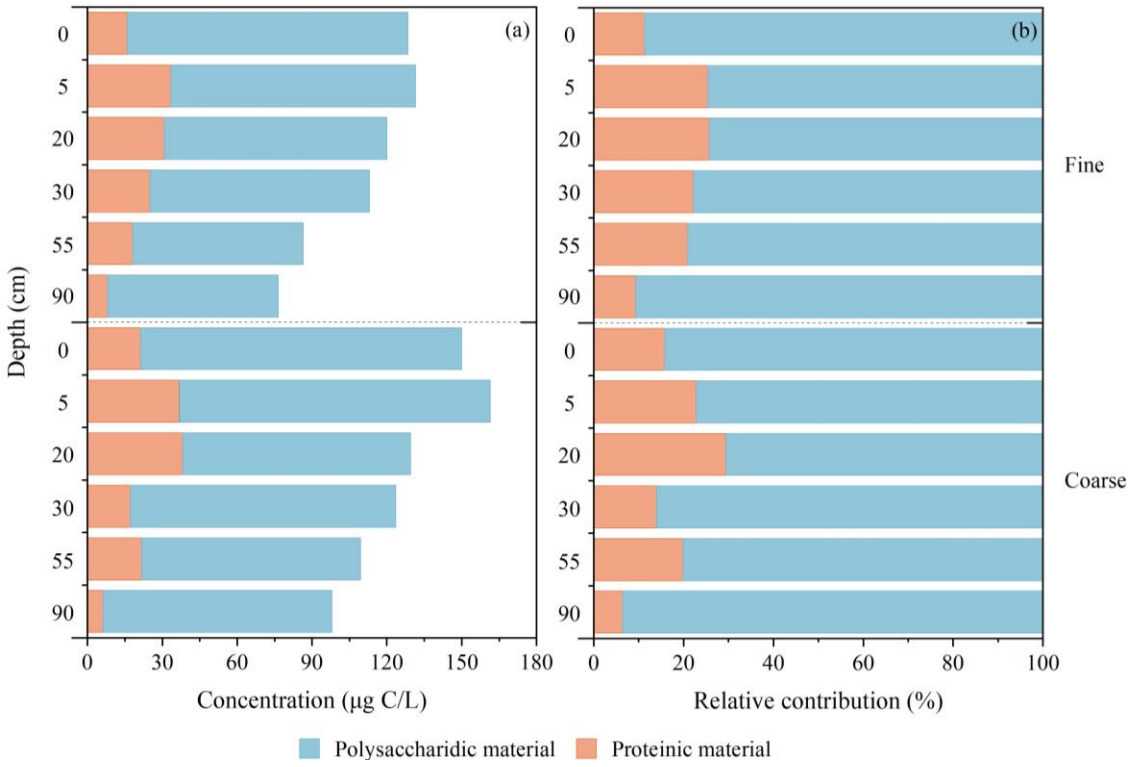

Fig. A12. Vertical concentrations (a) and relative distributions (b) of the polysaccharides and proteins fractions in biopolymers within the SSFs on day 106.

Biopolymers are constituted of polysaccharides and proteins. Indeed, all DON associated with the biopolymers was assumed to be bound in proteins (Jacquin et al. 2017). With an estimated C/N mass ratio of 3 for proteins (Huber et al. 2011), the concentration and relative contributions of polysaccharides and proteins within biopolymers are shown in Fig. A12. The rise of biopolymers at 5 cm was caused by proteins, which increased by 17.36 ± 5.17 ug/L and 15.47 ± 11.08 ug/L in the fine and

coarse column, respectively, and then decreased with depth. The increase of proteins is likely attributed to the desorbed cells or cell fragments, which typically contain a higher proteins than carbohydrates (de Oliveira and Schneider 2019). As for polysaccharides, its concentration gradually decreased by 44.04 ± 9.37 ug/L and 36.92 ± 20.12 ug/L in fine and coarse columns, respectively, showing the similar values as observed in other SSFs (Chen et al. 2016, de Oliveira and Schneider 2019, Lautenschlager et al. 2014).

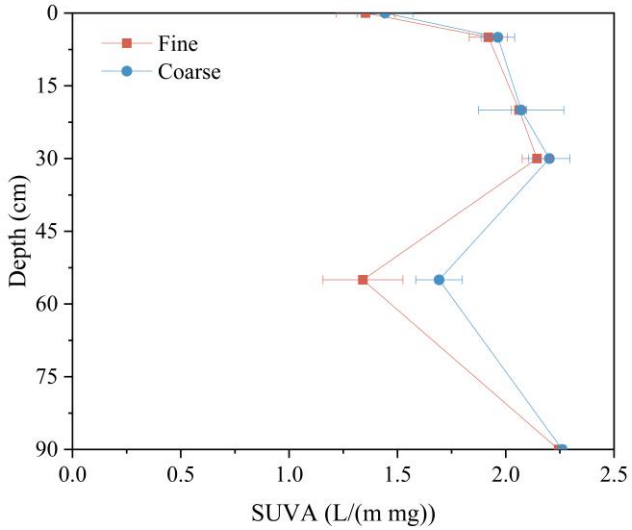

Fig. A13. Depth profile of SUVA in fine and coarse columns on day 106.

A3.3 Removal of nitrogen

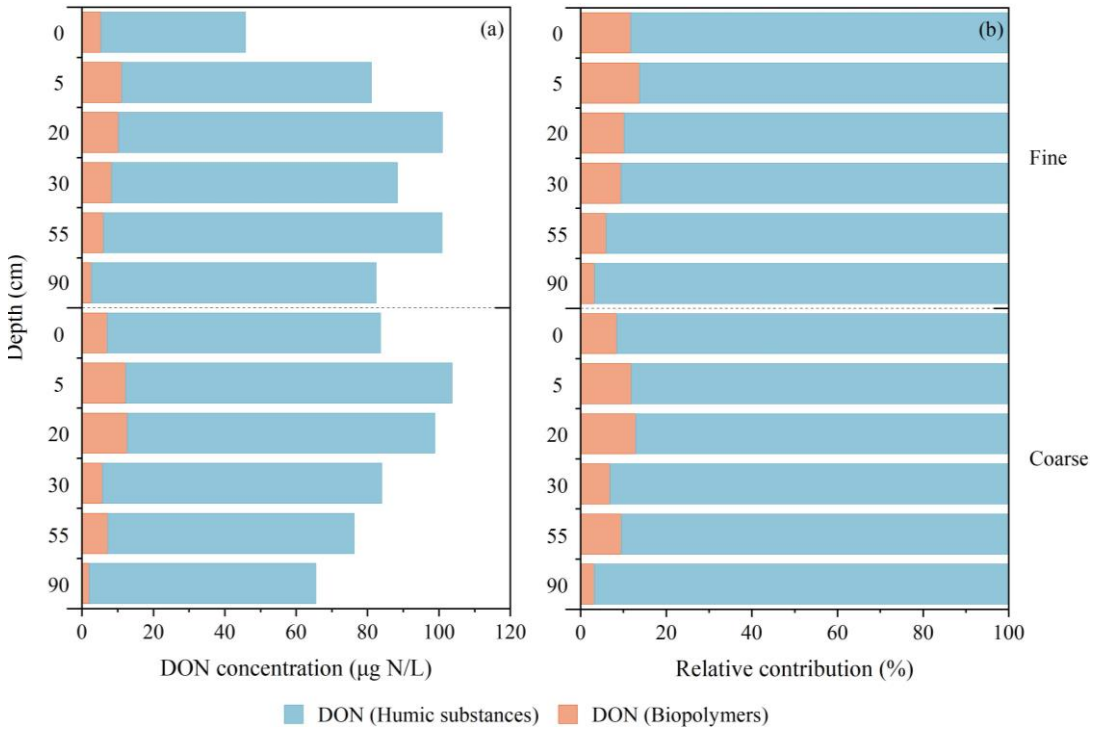

Fig. A14. Vertical concentrations (a) and relative distributions (b) of the DON fractions in biopolymers and humic substances within the SSFs on day 106.

Fig. A14 shows the results of DON linked to biopolymers and humic substances according to LC-OCD measurement on day 106. The concentration of DON in these two fractions increased in the top layer (0-5 cm) of the filter beds of both fine and coarse columns. However, in the fine column, the filter below 5 cm did not exhibit a significant removal effect on DON, with the effluent concentration even higher than that in the influent. However, the coarse column showed a progressive decrease in DON concentration below 5 cm, and overall, demonstrated a removal of 21.7%. Additionally, humus-linked DON showed a more obvious response to the filter column compared to biopolymers-linked DON with higher molecular weight, exhibiting a more pronounced variation among filter depth.

A3.4 Removal of phosphorus

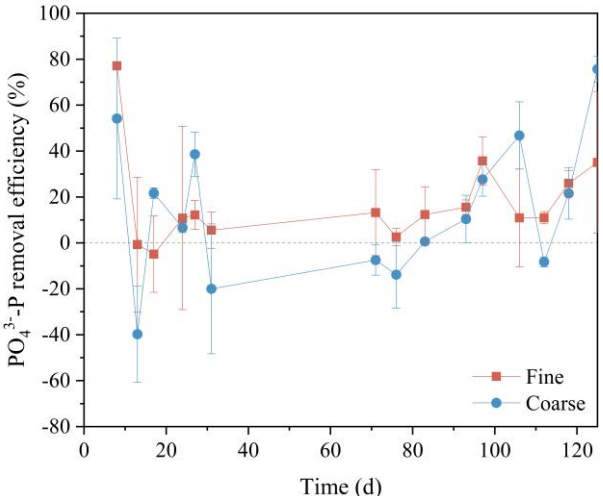

Fig. A15. Temporal changes in PO_4^{3-}-P removal efficiency in fine and coarse columns during phase I.

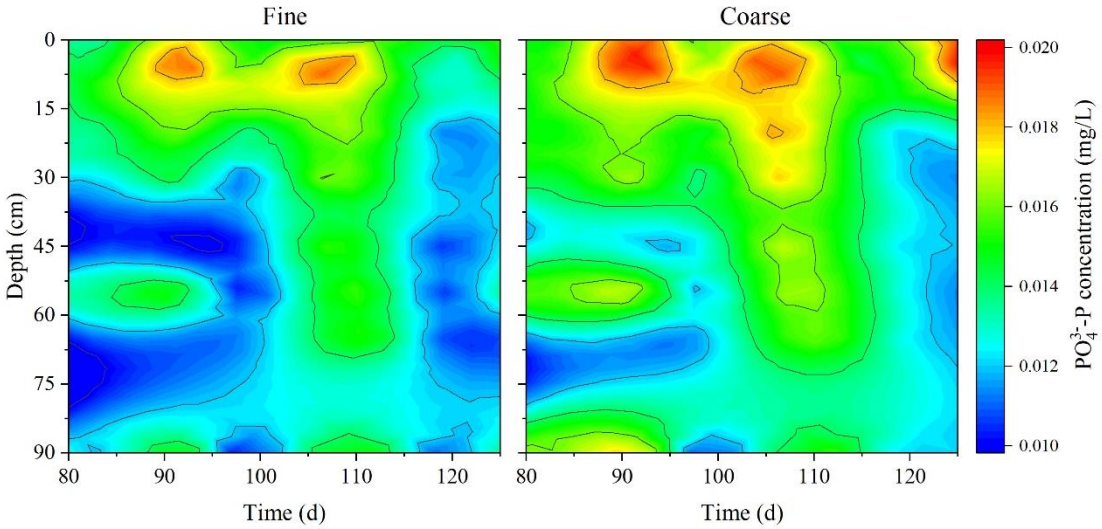

Fig. A16. Depth profiles of PO_4^{3-}-P in fine and coarse columns operating at 0.5 m/h in phase I. The PO_4^{3-}-P measurements were normalized by removing background concentrations of tap water.

Fig. A15 and A16 illustrate the distribution and removal performance of PO_4^{3-}-P. The vertical phosphate concentration gradually decreased after stable operation. However, the removal efficiency showed no clear variation trend at early-stage, that PO_4^{3-}-P concentrations sometimes even increasing within the coarse column. After 80 days, the removal efficiency of phosphate improved, fluctuating at around 20.9 ± 11.1% and 24.9 ± 28.8% in the fine and coarse column, respectively. The distribution of PO_4 concentration along the sand depth was obviously affected by grain size ($p < 0.01$), although there was no significant difference in the removal efficiency ($p > 0.05$).

A3.5 Mass balance

Table A1. The spatial changes in concentrations of DOC, nitrogen, phosphate, and DO within intermediate horizontal layers of the filters. The data is derived from the average values recorded between days 97 and 125. A negative value indicates substance reduction through the layer, while a positive value indicates substance increase.

Depth (cm)	DOC (mg/L)	DIN	NH_4^--N	NO_2^--N	NO_3^--N	PO_4^{3-}-P	DO
Fine column							
0-5	-0.83	-0.31	-0.31	0.00	0.00	0.001	-0.31
5-45	-0.50	0.11	-0.53	0.53	0.11	-0.003	-0.27
45-55	0.92	-0.09	-0.03	-0.04	-0.02	0.000	0.01
55-65	-0.90	0.03	-0.01	0.05	-0.01	0.000	-0.01
65-90	-0.04	0.09	0.01	0.12	-0.04	-0.000	0.00
Overall	-1.31	-0.17	-0.88	0.65	0.05	-0.003	-0.58
Coarse column							
0-5	-0.83	-0.19	-0.19	0.00	0.00	0.000	-0.28
5-45	-0.56	-0.04	-0.67	0.52	0.11	-0.002	-0.35
45-55	0.72	-0.09	-0.01	-0.04	-0.04	0.000	-0.01
55-65	-0.65	0.12	-0.03	0.14	0.00	-0.000	0.01
65-90	-0.04	-0.01	-0.09	0.12	-0.05	-0.001	0.00
Overall	-1.31	-0.21	-0.99	0.75	0.03	-0.003	-0.63

A4. Results of Phase II – Increasing loading rate

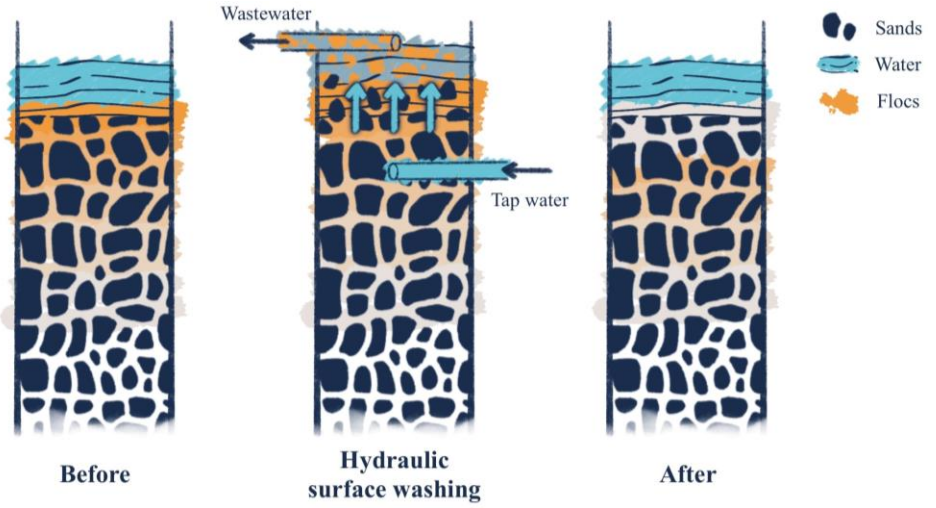

Fig. A17. Schemes of hydraulic surface cleaning.

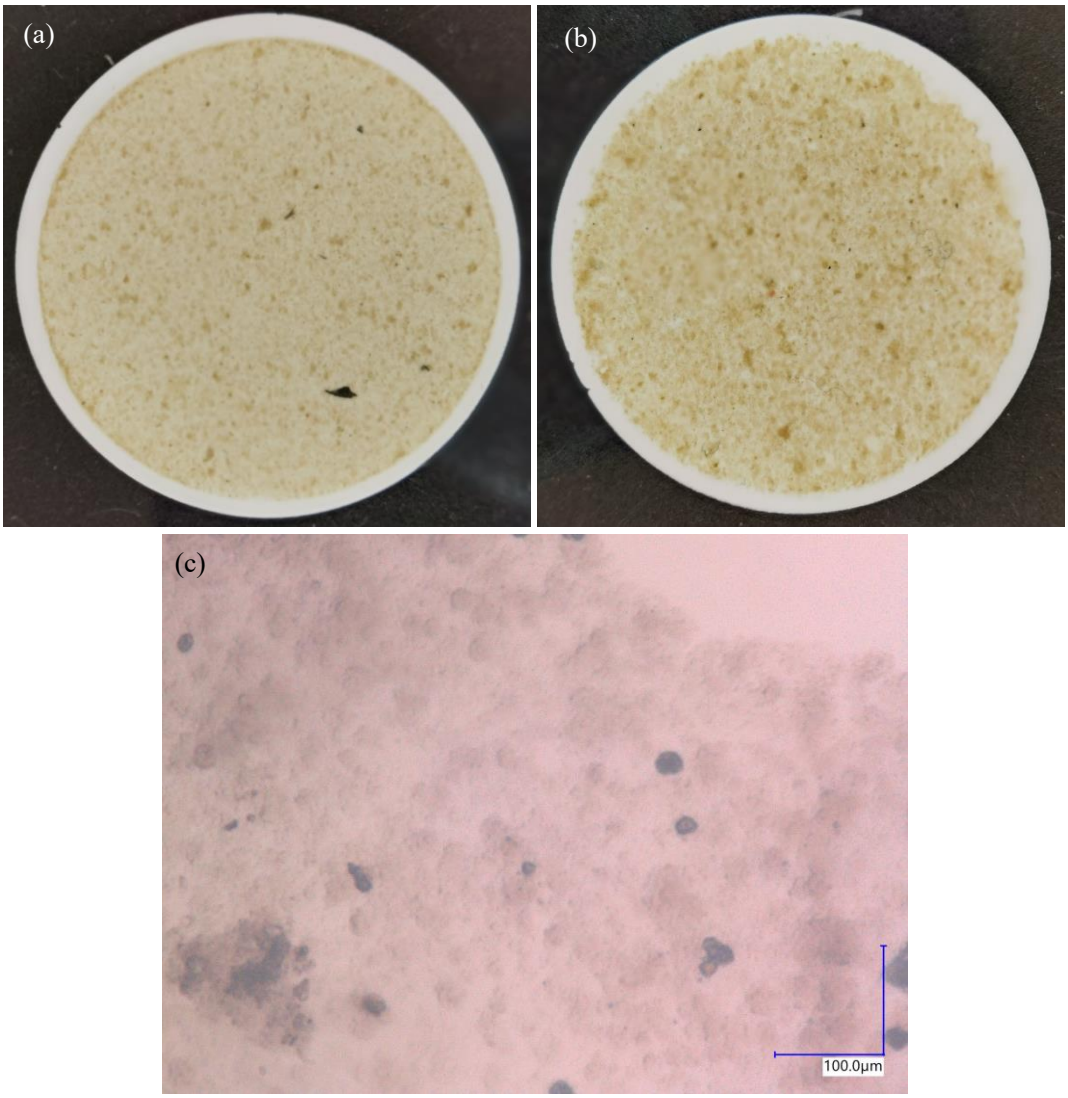

Fig. A18. Photos of the flocs in the wastewater of hydraulic washing from fine (a) and coarse (b) columns on 0.45 um on day 152. And the electron microscope image of floc (c).

A4.1 Removal of phosphorus

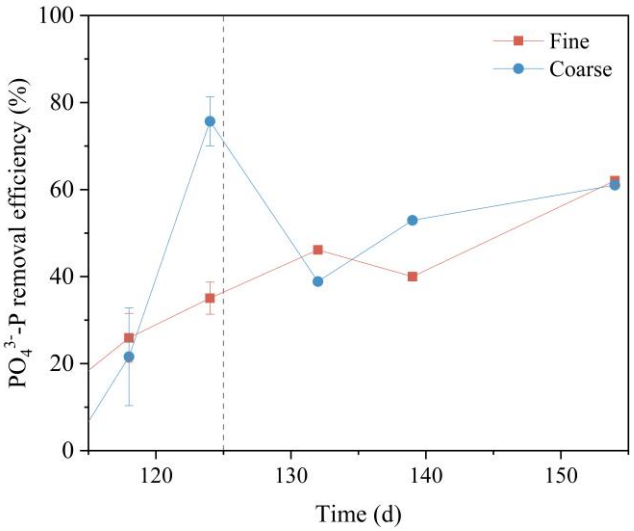

Fig. A19. Temporal changes in PO_4^{3-}-P removal efficiency in fine and coarse columns during phase II. The dashed line indicates the start of the phase II – increasing loading rate.

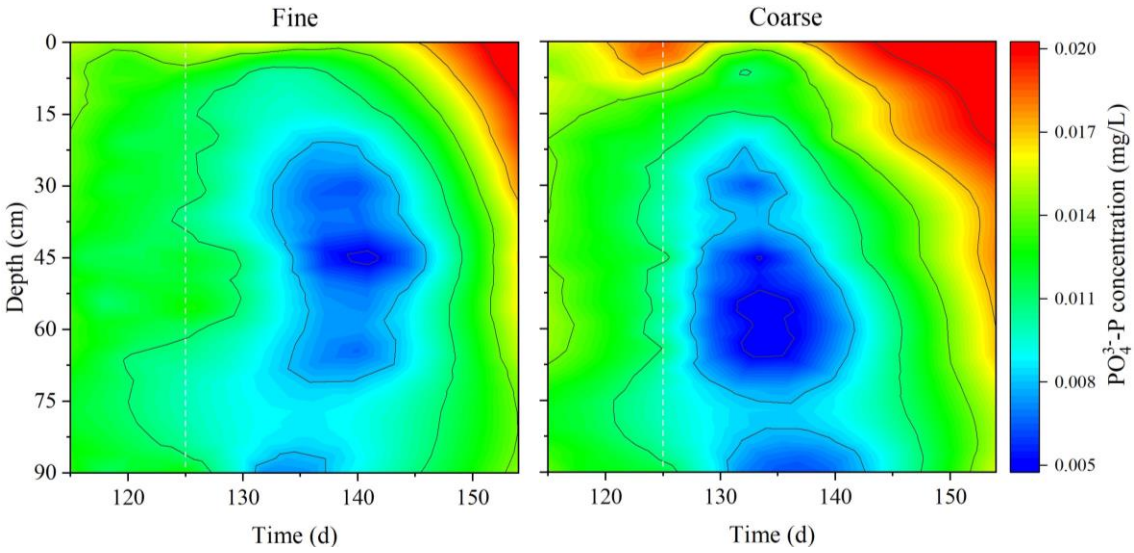

Fig. A20. Depth profiles of PO_4^{3-}-P in fine and coarse columns operating at 2 m/h during phase II. The PO_4^{3-}-P measurements were normalized by removing background concentrations of tap water. The dashed line indicates the start of the phase II – increasing loading rate.

As depicted in Fig. A19 and A20, between days 125-140, the phosphate concentration in the filter column gradually decreased. The removal efficiency for fine and coarse column remained at 49.6% ± 13.5% and 60.0% ± 6.3%, respectively, which were comparable to those observed before the loading rate rising. After day 140 the phosphate removal capacity decreased, but in comparison to the decrease in DOC and ammonium removal efficiencies, the phosphate removal efficiency only decreased to 34.1% and 32.4% in fine and coarse column, respectively. According to *t*-test results,

the increase in loading rate had significant effect on the vertical distribution of PO_4^{3-} within the filter columns ($p < 0.01$).

A5. Results of Phase II – Backwashing

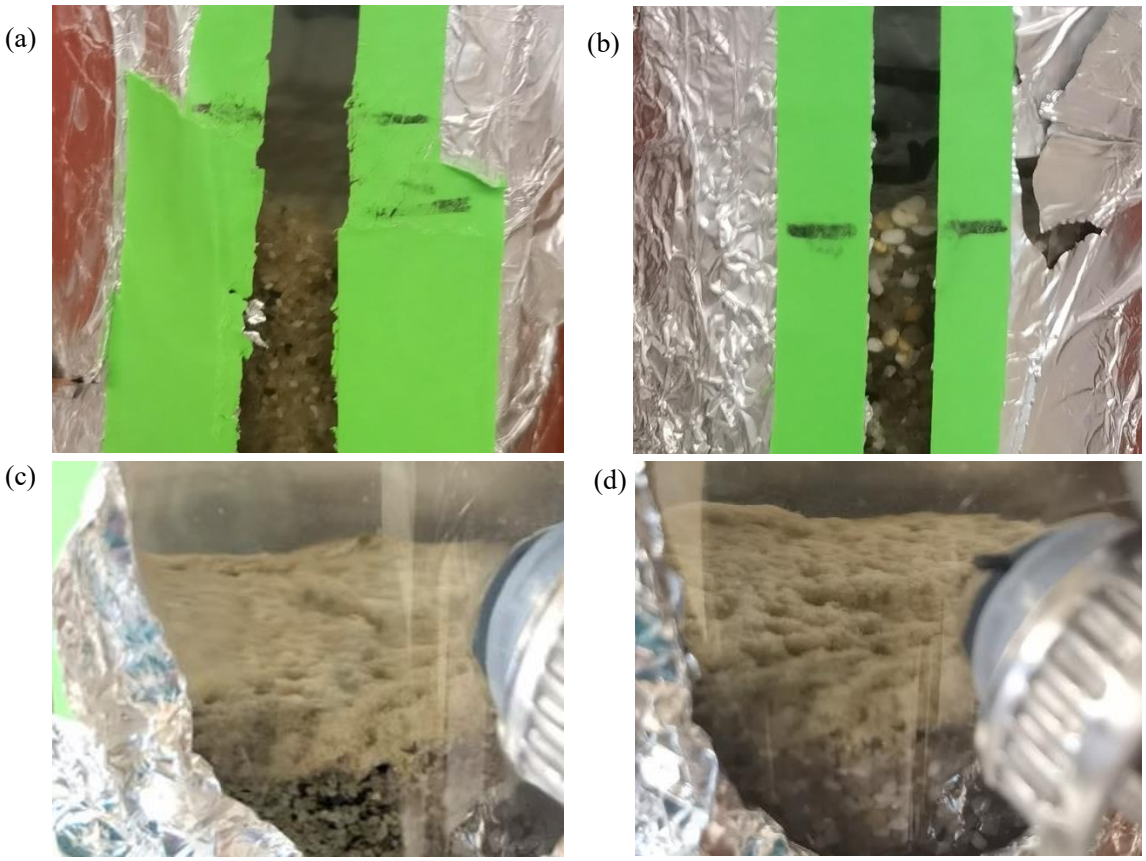

Fig. A21. Photos of the surface of fine and coarse filter columns before (a, b) and after (c, d) backwashing.

A5.1 Removal of phosphorus

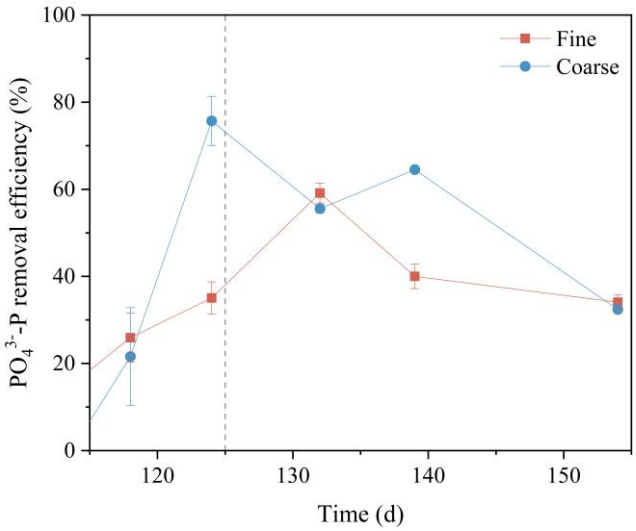

Fig. A22. Temporal changes in PO_4^{3-}-P removal efficiency in fine and coarse columns during phase II. The dashed line indicates the start of the phase II – backwashing.

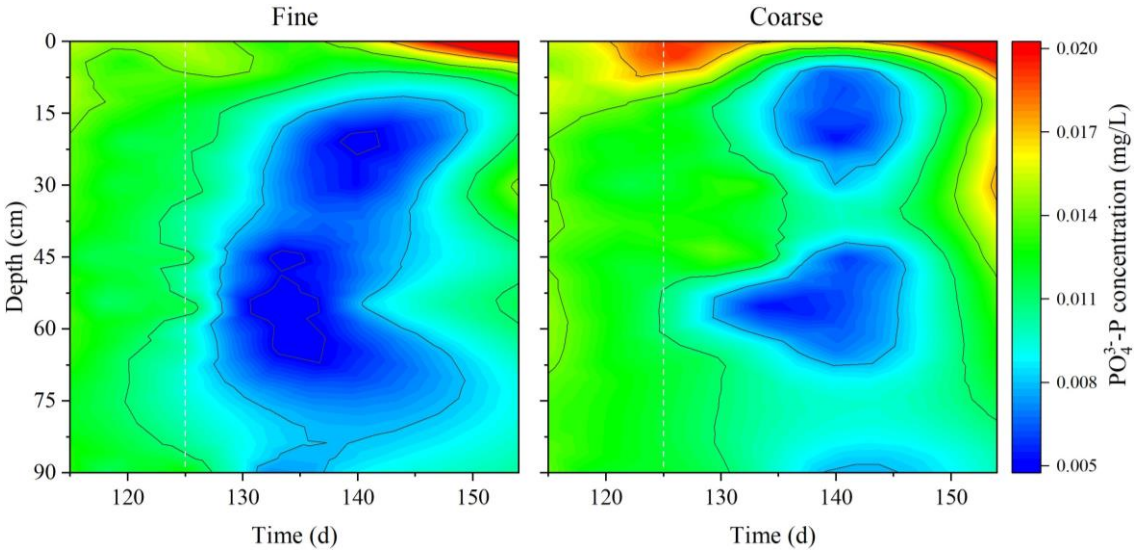

Fig. A23. Depth profiles of PO_4^{3-}-P in fine and coarse columns operating at 0.5 m/h during phase II. The PO_4^{3-}-P measurements were normalized by removing background concentrations of tap water. The dashed line indicates the start of the phase II – backwashing.

Fig. A22 and A23 depict the distribution and removal efficiency of phosphate in the filter columns after backwashing. Backwashing did not diminish the removal efficiency of PO_4^{3-}, instead, the removal efficiency gradually increased to 62.0% and 61.0% over the course of operation. Consistent with the removal performance, the vertical profile showed a more pronounced downward trend than phase I experiment, but this may be attributed to the gradual maturation of the filter columns. According to *t*-test results, backwashing showed significant impact on the PO_4^{3-} vertical distribution within fine columns ($p < 0.01$), but no obvious impact on coarse column ($p > 0.05$).

A6. Data analysis

Table A2. Results of paired samples *t*-test, where df stands for the degrees of freedom, and t stands for the test statistic for the paired *t*-test. *, **, and *** indicate differences are significant at the 0.05, 0.01, and 0.001 levels, respectively.

Parameter	Variable 1	Variable 2	t	df	*p*-value
PhiX concentration	Fine	Coarse	1.384	13	0.190
E.coli concentration	Fine	Coarse	-2.766	14	0.015*
DOC concentration	Fine	Coarse	0.813	51	0.420
DOC removal efficiency	Fine	Coarse	0.709	19	0.487
NH_4^+ concentration	Fine	Coarse	2.849	51	0.006*
NH_4^+ removal efficiency	Fine	Coarse	-1.559	20	0.135
NO_2^- concentration	Fine	Coarse	1.836	51	0.072
NO_3^- concentration	Fine	Coarse	-0.434	51	0.666
PO_4^{3-} concentration	Fine	Coarse	-6.224	51	0***
PO_4^{3-} removal efficiency	Fine	Coarse	0.509	14	0.619
pH	Fine	Coarse	3.137	25	0.004**

DO concentration	Fine	Coarse	-0.962	23	0.346
cATP in water	Fine	Coarse	-3.253	19	0.004**
tATP on sand	Fine	Coarse	0.412	5	0.697
DOC concentration (fine)	0.5 m/h	2 m/h	-3.016	7	0.019*
DOC concentration (coarse)	0.5 m/h	2 m/h	-2.495	7	0.041*
DOC concentration (fine)	Before BW	After BW	-3.352	7	0.012*
DOC concentration (coarse)	Before BW	After BW	-4.900	7	0.002**
NH_4^+ concentration (fine)	0.5 m/h	2 m/h	-0.399	7	0.702
NH_4^+ concentration (coarse)	0.5 m/h	2 m/h	-0.733	7	0.487
NH_4^+ concentration (fine)	Before BW	After BW	2.986	7	0.020*
NH_4^+ concentration (coarse)	Before BW	After BW	4.919	7	0.002**
PO_4^{3-} concentration (fine)	0.5 m/h	2 m/h	3.836	7	0.006**
PO_4^{3-} concentration (coarse)	0.5 m/h	2 m/h	9.131	7	0***
PO_4^{3-} concentration (fine)	Before BW	After BW	4.448	7	0.003**
PO_4^{3-} concentration (coarse)	Before BW	After BW	1.371	7	0.213
cATP above 5 cm (fine)	0.5 m/h	2 m/h	-50.366	1	0.013*
cATP below 5 cm (fine)	0.5 m/h	2 m/h	0.013	5	0.990
cATP above 5 cm (coarse)	0.5 m/h	2 m/h	-32.571	1	0.020*
cATP below 5 cm (coarse)	0.5 m/h	2 m/h	1.920	5	0.113
cATP above 5 cm (fine)	Before BW	After BW	-1.639	3	0.200
cATP below 5 cm (fine)	Before BW	After BW	-3.583	5	0.016
cATP above 5 cm (coarse)	Before BW	After BW	-1.298	3	0.285
cATP below 5 cm (coarse)	Before BW	After BW	2.731	5	0.440
tATP above 5 cm (fine)	0.5 m/h	2 m/h	-19.304	1	0.033*
tATP below 5 cm (fine)	0.5 m/h	2 m/h	-2.128	3	0.123
tATP above 5 cm (coarse)	0.5 m/h	2 m/h	-95.354	1	0.007**
tATP below 5 cm (coarse)	0.5 m/h	2 m/h	-2.549	3	0.084
tATP above 5 cm (fine)	Before BW	After BW	2.731	1	0.223
tATP below 5 cm (fine)	Before BW	After BW	-1.884	3	0.156
tATP above 5 cm (coarse)	Before BW	After BW	-6.220	1	0.101
tATP below 5 cm (coarse)	Before BW	After BW	-0.578	3	0.604

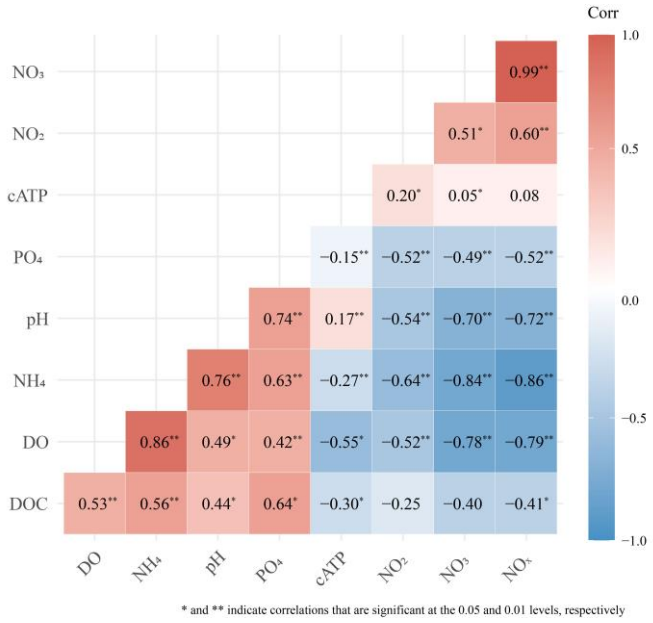

Fig. A24. Average correlation between physicochemical and biological parameters of filtrate water at various depths within both fine and coarse SSFs during phase I. * and ** indicate differences are significant at the 0.05 and 0.01 levels, respectively.